Development of Neodymium Doped Ceria Based Electrolytes for Applications in Intermediate Temperature Solid Oxide Fuel Cells (SOFCs)

By

Muhammad Akmal Rana

Reg. # NUST201260711MCES64112F

Session 2012-14

Supervised by

Dr. Zuhair S. Khan

Associate Professor

A Thesis Submitted to the Centre for Energy Systems in

partial fulfillment of the requirements for the degree of

MASTER of SCIENCE in
ENERGY SYSTEMS ENGINEERING

Center for Energy Systems (CES)
National University of Sciences and Technology (NUST)
H-12, Islamabad 44000, Pakistan
September 2014

Certificate

This is to certify that work in this thesis has been carried out by **Mr. Muhammad Akmal Rana** and completed under my supervision in Advanced Energy Materials and Fuel Cells laboratory, Centre for Energy Systems, National University of Sciences and Technology, H-12, Islamabad, Pakistan.

Supervisor: _____

Dr. Zuhair S. Khan
Centre for Energy Systems
NUST, Islamabad

GEC member # 1:   _____

Dr. Mohammad Bilal Khan
Centre for Energy Systems
NUST, Islamabad

GEC member # 2:   _____

Dr. Iram Mahmood
School of Chemical and Materials
Engineering NUST, Islamabad

GEC member # 3:   _____

Dr. Anis-ur-Rehman
Comsats Institute of Information
Technology, Islamabad

HoD-CES   _____

Dr. Zuhair S. Khan
Centre for Energy Systems
NUST, Islamabad

Principal/ Dean   _____

Dr. Mohammad Bilal Khan
Centre for Energy Systems
NUST, Islamabad

ABSTRACT

Solid oxide fuel cells (SOFCs) are currently attracting tremendous interest because of their huge potential in stationary heat and power generation. Currently SOFCs utilize Yttria stabilized zirconia as electrolyte material that works efficiently from 800-1000°C. The major current impediment of commercializing SOFCs is their high cost that results from high operating temperature. The need at this stage is to develop such materials that can offer better ionic conductivity at low temperature. Pure Ceria is poor ionic conductor but its conduction properties can be greatly enhanced by doping it with some trivalent rare earth atom such as Neodymium (Nd). In literature, there is not enough data available for Neodymium doped Ceria (NDC) electrolytes that can be a substitute for YSZ as they provide higher ionic conductivity at low temperatures. In this dissertation, two compositions $Ce_{0.80}Nd_{0.20}O_{1.90}$ (NDC20) and $Ce_{0.75}Nd_{0.25}O_{1.875}$ (NDC25) were initially selected to investigate the structural and electrical properties of Neodymium doped ceria electrolyte using sol-gel route. X-ray diffraction (XRD) and scanning electron microscope (SEM) results showed that powder particles containing cubic fluorite structure with homogenous and spherical shape with an average size of 1.1 μm were formed at pH10. DC electrical conductivity values for NDC25 and NDC20 were found to be 7.9×10^{-5} S/cm and 3.67×10^{-5} S/cm respectively at 650°C. We further enquired the effect of small amount of Sm, Y and K_2CO_3 to improve the conduction mechanism in NDC25. Conductivity of NDC25 greatly improved by adding small amount of Sm with composition of $Ce_{0.75}Sm_{0.15}Nd_{0.10}O_{1.875}$ (SNDC) and Y with composition of $Ce_{0.75}Y_{0.15}Nd_{0.10}O_{1.875}$ (YNDC) at 700°C . It was also depicted that Sm and Nd are best co-dopants for Ceria. K_2CO_3 was added into NDC25 with 10 and 20% by volume. It was observed carbonates greatly increased the conductivity values of NDC25 from 7.9×10^{-5} S/cm to 1.03×10^{-3} S/cm. The sequence in the conductivity values at 700°C found to be KNDC20>KNDC10>SNDC>YNDC>NDC25>NDC20.

Key words: SOFC, Doped Ceria, Conductivity, Lattice Strain, Co-Doping

ACKNOWLEDGMENT

TABLE OF CONTENTS

LIST OF FIGURES

LIST OF TABLES

LIST OF JOURNALS/CONFERENCE PAPERS

Conference paper: Muhammad Akmal Rana[a], M.N Akbar[a], Mustafa Anwar[a], Kamal Mustafa[a], Sahar shakir[a], Zuhair S. khan[a], "Sol-gel fabrication of novel electrolytes based on Neodymium doped Ceria for application in low temperature solid oxide fuel cells", International conference on solid state physics (ICSSP), Punjab University Lahore December 1-6, 2013. Proceedings Submitted in Springer Verlag

Conference paper: Muhammad Akmal Rana[a], M.N Akbar[a], Mustafa Anwar[a], Kamal Mustafa[a], Sahar shakir[a], Zuhair S. khan[a], "Investigations on doped Ceria electrolytes and their structural and electrical properties for applications in low temperature solid oxide fuel cells"

Published in Conference on Frontiers of Nanoscience and Nanotechnology, PINSTECH Islamabad, June 03-05, 2014.

**Review Article: Muhammad Akmal Rana [(a)], Zuhair S. Khan [(a)*], "Electrical properties of ceramic electrolyte materials based on stabilized zirconia and doped ceria for applications in solid oxide fuel cells (SOFCs): a brief review"

Submitted in Journal of Fuel Cell Science and Technology

***Original research article: Muhammad Akmal Rana[a], M.N Akbar[a], Mustafa Anwar[a], Kamal Mustafa[a], Sahar shakir[a], Zuhair S. khan[a*], Effect of Sm, Y and K_2CO_3 on structural and electrical properties of Neodymium doped Ceria electrolytes for applications in low temperature solid oxide fuel cells.

Submitted in Journal of Electroceramics

*Attached as Annexure I
** Attached as Annexure II
*** Attached as Annexure III

Chapter 1
Introduction

1.1.   Fuel cells

Since long we have been using fossil fuels to get energy. As Industrial revolution progressed, contribution to environmental pollutants increased day by day [1]. We all know that these pollutants play very important role in climate of our planet. Keeping this view in mind different researchers have tried to find such ways of producing power which could result into less hazardous pollutants as well as could provide sufficient power and also it doesn't depend on fossil fuels. Enormous laboratory level experiments were carried out to obtain such routes to get energy with minimum level of pollutants.

 Fuel cell is one such device that fulfills the requirements of such system [2–4]. It is an electrochemical device that converts chemical energy of fuel directly into electrical energy with high power density and higher efficiency[5]. It contains three major components anode, cathode and electrolyte [6]. It provides power as long as fuel is supplied to it. As it needs no mechanical parts involved in power production it works smoothly and doesn't create any noise. It has the capability to replace internal combustion engine and can provide power in portable as well as for stationary purposes [5].

There are various fuel cells types but the most important types of fuel cells are Solid Oxide fuel cell (SOFC) [7–11], Polymer electrolyte membrane fuel cell (PEMFC) [12–18], Phosphoric acid fuel cell (PAFC) [19–23], Alkaline fuel cell (AFC) [24–28] and Molten carbonate fuel cell (MCFC) [29–34]. All these major fuel cell types work on the same electrochemical principle but they all operate at different temperature regimes, incorporate different materials, and often differ in their fuel tolerance. Table 1.1 summarizes a brief overview of main fuel cells types along with their advantages and disadvantages. It is clear from this table that SOFC has more potential for large scale power production applications as it can be stacked up-to 2MW with power production efficiency of 60%. Now we will briefly describe the SOFC.

Table 1.1: Comparison of various fuel cell types

Type	Operating Temperature (^{0}C)	Stack Size	Efficiency	Advantages	Disadvantages
SOFC	1000	1kW-2MW	60%	Fuel flexible Hybrid/ GTL cycle	corrosion Long startup time
PEMFC	50-250	1kW-100kW	35%	Low temperature Quick startup	Expensive membrane and catalyst Low temperature waste heat
AFC	90-100	10-100kW	55%	Low cost components	CO2 sensitivity Excessive water removal problem
MCFC	600-1000	300kW-3MW	45-50%	Highly efficient Fuel flexible	Long startup Low power density
PAFC	175-200	100-400kW	40%	Tolerance to fuels Suitable for CHP	Pt catalyst Long startup Low current & power

1.2 Solid Oxide Fuel Cells (SOFCs)

Solid oxide fuel cells (SOFC), owing to its high operating temperatures, have many advantages over other types of fuel cells. Its commercialization, however, relies greatly on its costs and long term durability. By reducing the operating temperature to the intermediate temperature range, the costs for the balance of plant would be significantly reduced. The greatest contribution to cell over-potential at this temperature range is to develop an electrolyte that is highly efficient oxide ion conductor at low to intermediate temperature range [35]. Fig. 1.1shows the basic principal of a solid oxide fuel cell. Hydrogen fuel enters from anode where is gets oxidized and produces a pair of electrons. These electrons pass through as external circuit and reach at cathode where they reduce the incoming oxygen into oxide ions.
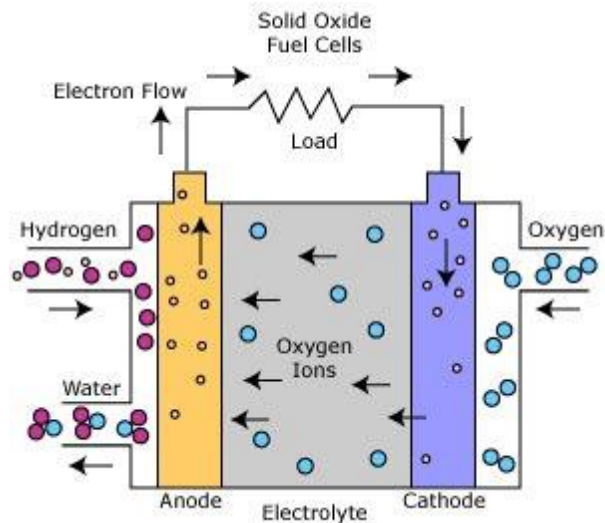
Fig. 1.1 Operating principal of Solid Oxide Fuel Cell

To complete this electrochemical reaction, these oxide ions have to pass through solid electrolyte to react with hydrogen ions to produce water at anode side. As these electrons pass through as external circuit they can be used to get useful power from the fuel cell. When Hydrogen is used as a fuel and Oxygen as oxidant then the reaction at anode and cathode will be:

$$H_2 \longrightarrow 2H^+ + 2e^- \tag{1.1}$$

$$1/2O_2 + 2H^+ + 2e^- \longrightarrow H_2O \tag{1.2}$$

Equations 1.1 and 1.2 show the complete anodic and cathodic reactions [36]. The speed of this electrochemical reaction determines the fuel cell efficiency to generate electric power. The open circuit voltage of a cell can be calculated using Nernst equation for above mentioned electrochemical reaction.

$$E = E_o + RT/4F(\ln P_{O2}) + RT/2F(\ln P_{H2}/P_{H2O}) \tag{1.3}$$

Where,

E = Open circuit voltage

3

E_o = Reversible voltage at standard pressure and operating temperature

R = universal gas constant

F = Faraday constant

E_o can be calculated using the following equation

$$E_{o\,=}\ \Delta G/2F \qquad\qquad (1.4)$$

Where,

ΔG = Gibbs free energy

Since the fuels are normally burnt to release the energy, it would make sense to compare the electrical energy produced with the heat produced by burning the fuel. This is described as the change of enthalpy ΔH. Therefore the efficiency of the fuel cell can be defined as:

$$\textit{Efficiency} = \frac{\textit{electrical energy produced per mole of fuel}}{\Delta H}\ x100 \qquad\qquad (1.5)$$

As the maximum electrical energy available is equal to ΔG, then:

$$\textit{Efficiency} = \Delta G/\Delta H \qquad\qquad (1.6)$$

There are two different values for ΔH. For the burning of hydrogen, value of ΔH is equal to -241.83kJ/mol. H2O is in gas form and -285.84kJ/mol if in liquid form. The difference (44.01kJ/mol) between these two values is the mole enthalpy of vaporization known as the latent heat. The higher value is called the higher heating value (HHV) and lower value is called the lower heating value (LHV). The theoretical cell voltage is dependent on operating conditions such as temperature, pressure and concentration of reactants. The difference between the theoretical cell voltage and the operating voltage is called overpotential and represents the irreversible losses in a fuel cell. In the non-ideal case, the actual operating voltage is less than the theoretical voltage because of the

irreversible losses associated with the fuel cell electrochemistry. The actual voltage output (V) is given by:

$$V = E_0 - IR - \eta_c - \eta_a \qquad (1.7)$$

Where, I is the current through the cell, Ris the cell resistance, and η_c and η_a are the polarization losses associated with the electrodes. There are three primary irreversible losses that result in the degradation of fuel cell performance called activation polarization, ohmic polarization and concentration polarization.

1.3 Current issues in SOFCs

The benefits of solid oxide fuel cells are unambiguous; SOFCs are efficient energy producers that emit smaller amounts of CO_2 than most currently available hydrocarbon-fueled sources. Equally important, they can be adapted to a variety of fuels and might be the missing link to clean energy production. Indeed, a series of technical obstacles to SOFC practicality have fallen in recent years, and large- and small-scale products have begun to be offered. But, SOFCs have a reputation for being finicky divas in the energy world, and progress in pricing and performance has remained incremental. Significant market penetration seemingly always is just a decade away. The challenges for the fuel cell community are to reduce cost and increase reliability. These challenges extend from the cell itself, to the stack interconnect and seals, to the balance of plant. There has been a tremendous effort to lower the operating temperature of SOFCs from ~1000°C to ≤ 800°C, for cost and reliability considerations. Unfortunately, current SOFC technology must operate in the region of ~800°C to avoid unacceptably high polarization losses. These high temperatures demand expensive materials for the fuel cell interconnects and insulation; and significant time and energy to heat up to the operating temperature. Therefore, development of SOFCs to provide reasonable power output at lower temperatures would make SOFCs both more cost competitive with conventional technology, and significantly reduce   start-up times which is critical to transportation and portable power applications.

1.4 Materials for SOFC components

SOFC contains three major components namely anode, cathode and electrolyte. Each part has its own characteristics that are necessary for that particular material to be used in SOFC.

1.4.1 Anode

In early development of SOFC, gold and platinum were used as anode materials but due to their high cost and low instability, new materials were discovered. Currently Ni-YSZ cermet anode is widely used in SOFCs. This type of anode material is fabricated by sintering NiO and YZS powders. In this type of anode, Ni provides electronic conductivity and catalytic activity and YSZ provides a structural framework and improves thermal expansion matching. Both Ni and YSZ are also immiscible and non-reactive over a wide range of temperature. Therefore, this type of anode is chemically stable even in reducing environment. Ni-YSZ anodes also have some drawbacks. During prolonged operation of a cell, they show performance degradation. They also have low tolerance to sulfur impurities present in the fuel. Sulfur poisoning is caused by strong absorption of H_2S on the active sites of Ni, that results reduction in the rate of electrochemical reaction. Due to these reasons, doped ceria materials are being developed for SOFC anode material. The major advantage of doped ceria based anode materials is their ability to deal with carbon deposition, which makes SOFC suitable for hydrocarbon based fuels as well.

1.4.2 Cathode

The cathode must provide high activity for reduction of Oxygen. SOFC cathode must provide electronic, ionic conductivity and electrocatalytic activity. As metal based conductors are not stable in high temperature oxidizing atmosphere, SOFC cathodes are mostly ceramics. There are various cathode materials available like LSM ($LaMnO_3$), LSCF and LSM-YSZ. LSM is considered better due to its good chemical stability, electrical conductivity and catalytic activity. Unfortunately oxide ions conductivity is low in LSM, therefore LSM based cathode cathodes are mixed with YSZ to make LSM-

YSZ composite cathodes because YSZ provides the higher ionic conductivity. LSCF cathodes on the other hand, are suitable for SOFCs in reduced temperature operation. LSCF cathodes contain almost 20% Sr and Fe around 80%.

1.4.3 Electrolyte

Electrolyte plays very significant role by allowing oxide ions to pass through to complete this reaction. Various electrolyte materials have been developed for SOFCs. Some of the major electrolyte materials are Yttria Stabilized Zirconia (YSZ), Doped Ceria, LAMOX family ($La_2Mo_2O_9$) and LSGM (Lanthanum Gallate). Their brief comparison is given in

Table 1.2 [36]. It can be depicted from this table that only YSZ and Doped Ceria are suitable candidates for SOFCs.

Table 1.2: Comparison of electrolytes [36]

Electrolyte	Advantages	Drawbacks	Conductivity
YSZ	Chemically stable Better ionic conductor at high temperature.	Low ionic conductivity at low temperature	0.14 S/cm at 1000°C
Doped Ceria	Shows higher ionic conductivity than YSZ at low temperature	Reduction of Ce^{4+} to Ce^{3+} under the fuel rich conditions of the anode side of the electrolyte.	.01 S/cm at 500°C for $Ce_{0.9}Gd_{0.1}O_{1.95}$
Bismuth Oxides	Highest oxide ion conductor. Doped δ-Bi_2O_3 materials show improved stability compared to pure Bi_2O_3.	Instability in reducing atmospheres. Low mechanical strength.	1 S/cm at 750°C
LAMOX ($La_2Mo_2O_9$)	Suitable in oxidizing conditions and intermediate temperatures	Susceptible to reduction. Electronic conductivity increases with temperature.	0.03 S/cm at ~720°C
LSGM (Lanthanum Gallate)	LSGM does not reduce as easily as GDC. Its thermal expansion is relatively low and well matched to YSZ.	High cost of gallium	0.075 S/cm at 800°C

The cubic fluorite structure of Zirconia makes it good oxide ions conductor but it can't remain stable [37].Zirconia (ZrO_2) exhibits three polymorphs. At room temperature, it has a monoclinic structure and changes to tetragonal at a temperature above 1170 °C,

7

and then to the cubic fluorite structure above 2370 °C. Fig. 1.2 shows the cubic fluorite structure of Zirconia
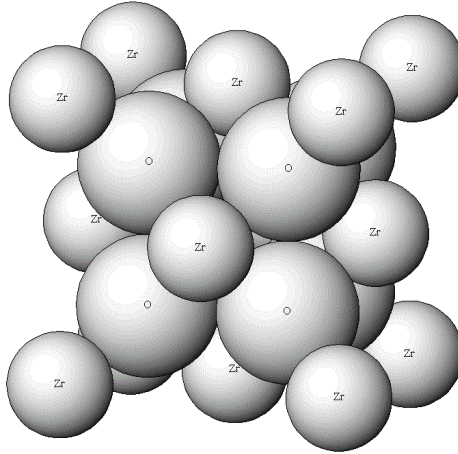
Fig. 1.2 Crystal Structure of ZrO2

Inclusion with Y_2O_3 makes it stable and even more conductive [36]. By the addition of Yttria into Zirconia, oxygen vacancies are created which are caused by charge compensation effects. Yttrium ions disturb the charge balance when they enter into lattice of Zirconia. By the addition of 8 mol% of dopant, 4% of oxide ions sites become vacant. Fig. 1.3 [36] shows the oxide ion conductivity graph with respect to concentration of dopant in $ZrO_2.$ Conductivity value increases up to 8%, but when dopant concentration increase to a certain upper limit, conductivity starts to decrease. By further inclusion of dopant reduces the ionic conduction behavior in the electrolyte as the defects start to interact with each other. Association of defects can also cause traps for vacancies which directly influence ions not to flow easily [37]. Defects ordering can be minimized by selecting dopants with closer ionic sizes to that of host ions. As YSZ provides better ionic conductivity at high temperature that creates many design concerns in SOFC, therefore research is being focused to develop such electrolyte materials that are better ionic conductor than YSZ even at low temperature. The issue with YSZ is that, as the temperature decreases the grain boundary resistance increases and impedes ionic flow which makes YSZ based electrolyte only suitable for high temperature applications.
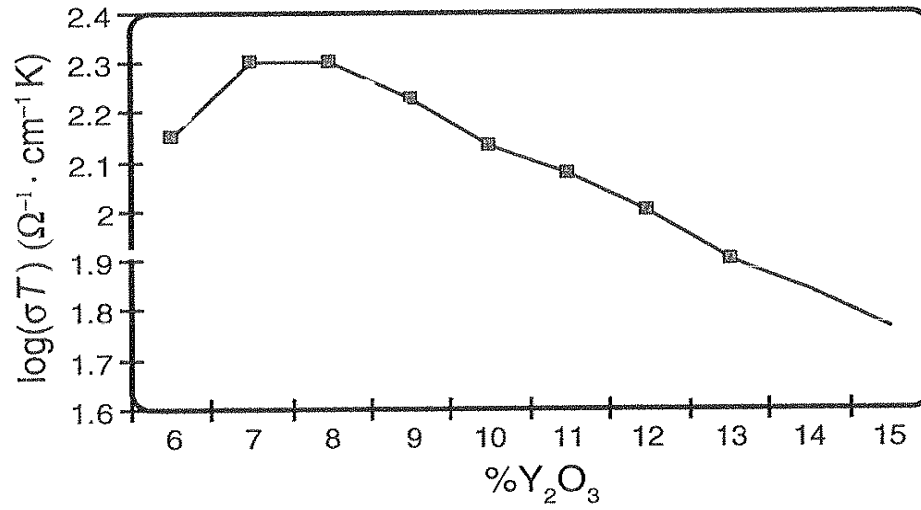
Fig. 1.3 Conductivity of YSZ with respect to concentration of Yttria [36]

Doped Ceria is considered a substitute electrolyte material for YSZ as it is better ionic conductor even at low temperature. In chapter 2, we will briefly describe why Doped Ceria is a better option.

9

Summary

A fuel cell is a device that converts chemical energy of the fuel directly into electrical energy. Solid oxide fuel cells are best among other types of fuel cells as they can be stacked up-to 2MW that makes them suitable candidate for large scale power production applications. The major components of a fuel cell are anode, cathode and electrolyte. Electrochemical system contains two conjugate half reactions: an oxidation reaction and a reduction reaction. Upon oxidation of fuel; a pair of electron is liberated that is consumed at cathode converting oxygen into oxide ions. The open circuit voltage of a cell is calculated by using following equation:

$$E= E_o+ RT/4F(ln\ P_{O2}) +RT/2F(ln\ P_{H2}/P_{H2O})$$

Electrolyte helps to flow oxide ions from cathode to anode. Oxide ions conductivity strongly depends on the electrolyte material. Some of the major electrolyte materials are Yttria Stabilized Zirconia (YSZ), Doped Ceria, LAMOX family ($La_2Mo_2O_9$) and LSGM (Lanthanum Gallate). Among these electrolyte materials, YSZ is widely used but its conductivity is better at high temperature range that is not desirable due to costly components that can withstand at such a high temperature range. Doped ceria electrolytes are considered betters substitute for YSZ because of their better ionic conductivity at low temperature.

References

[1]   C. Withagen, Pollution and exhaustibility of fossil fuels, Resource and Energy Economics, 16 (1994).

[2]   V.V. Lakshmi, R. Bauri, A.S. Gandhi, S. Paul, Synthesis and characterization of nanocrystalline ScSZ electrolyte for SOFCs, Int. J. Hydrogen Energy. 36 (2011) 14936–14942..

[3]   C.F. Cells, Fuel cell facts History of fuel cells, (1992) 1838.

[4]   J.X. Zhu, D.F. Zhou, S.R. Guo, J.F. Ye, X.F. Hao, X.Q. Cao, et al., Grain boundary conductivity of high purity neodymium-doped ceria nanosystem with and without the doping of molybdenum oxide, J. Power Sources. 174 (2007) 114–123.

[5]   J.M. Andújar, F. Segura, Fuel cells: History and updating. A walk along two centuries, Renew. Sustain. Energy Rev. 13 (2009) 2309–2322.

[6]   Y. Xia, Y. Bai, X. Wu, D. Zhou, Z. Wang, X. Liu, et al., Effect of sintering aids on the electrical properties of $Ce_{0.9}Nd_{0.1}O_{2-\delta}$, Solid State Sci. 14 (2012) 805–808.

[7]   K. Sugihara, M. Asamoto, Y. Itagaki, T. Takemasa, S. Yamaguchi, Y. Sadaoka, et al., A quantitative analysis of influence of Ni particle size of SDC-supported anode on SOFC performance: Effect of particle size of SDC support, Solid State Ionics. 262 (2014) 433–437.

[8]   S.A. Taher, S. Mansouri, Optimal PI controller design for active power in grid-connected SOFC DG system, Int. J. Electr. Power Energy Syst. 60 (2014) 268–274.

[9]   D.P. Bakalis, A.G. Stamatis, Optimization methodology of turbomachines for hybrid SOFC–GT applications, Energy. 70 (2014) 86–94.

[10]   T. Horita, M. Nishi, T. Shimonosono, H. Kishimoto, K. Yamaji, M.E. Brito, et al., Visualization of oxide ionic diffusion at SOFC cathode/electrolyte interfaces by isotope labeling techniques, Solid State Ionics. 262 (2014) 398–402.

[11]   J. Patakangas, Y. Ma, Y. Jing, P. Lund, Review and analysis of characterization methods and ionic conductivities for low-temperature solid oxide fuel cells (LT-SOFC), J. Power Sources. 263 (2014) 315–331.

[12]   L. Barelli, G. Bidini, A. Ottaviano, Optimization of a PEMFC/battery pack power system for a bus application, Appl. Energy. 97 (2012) 777–784.

[13]   T. Hordé, P. Achard, R. Metkemeijer, PEMFC application for aviation: Experimental and numerical study of sensitivity to altitude, Int. J. Hydrogen Energy. 37 (2012) 10818–10829.

[14]   K. Oh, P. Chippar, H. Ju, Numerical study of thermal stresses in high-temperature proton exchange membrane fuel cell (HT-PEMFC), Int. J. Hydrogen Energy. 39 (2014) 2785–2794.

[15]   B.H. Kim, O.J. Kwon, J.S. Song, S.H. Cheon, B.S. Oh, The characteristics of regenerative energy for PEMFC hybrid system with additional generator, Int. J. Hydrogen Energy. 39 (2014) 10208–10215.

[16]   P. Jayaraj, P. Karthika, N. Rajalakshmi, K.S. Dhathathreyan, ScienceDirect Mitigation studies of sulfur contaminated electrodes for PEMFC, Int. J. Hydrogen Energy. 39 (2014) 12045–12051.

[17]   P. Jayaraj, P. Karthika, N. Rajalakshmi, K.S. Dhathathreyan, Mitigation studies of sulfur contaminated electrodes for PEMFC, Int. J. Hydrogen Energy. 39 (2014) 12045–12051.

[18]   C.F. Cells, Fuel cell facts What is a fuel cell ? Fuel cell facts How does a fuel cell work.

[19]   M. Ghouse, H. Abaoud, a. Al-Boeiz, Operational experience of a 1 kW PAFC stack, Appl. Energy. 65 (2000) 303–314.

[20]   M. Pareta, S.R. Choudhury, B. Somaiah, J. Rangarajan, N. Matre, J. Palande, Methanol reformer integrated phosphoric acid fuel cell (PAFC) based compact plant for field deployment, Int. J. Hydrogen Energy. 36 (2011) 14771–14778.

[21]   H. Hirata, T. Aoki, K. Nakajima, Numerical study on the evaporative and condensational dissipation of phosphoric acid in PAFC, J. Power Sources. 196 (2011) 8004–8011.

[22]   G. Bizzarri, On the size effect in PAFC grid-connected plant, Appl. Therm. Eng. 26 (2006) 1001–1007.

[23]   L.L.C. Greer, S. Carolina, NREL issues stationary MCFC, PAFC analysis, Fuel Cells Bull. 2010 (2010) 1.

[24] H. Deng, J. Chen, K. Jiao, X. Huang, An analytical model for alkaline membrane direct methanol fuel cell, Int. J. Heat Mass Transf. 74 (2014) 376–390.

[25] M. Hao, X. Liu, M. Feng, P. Zhang, G. Wang, Generating power from cellulose in an alkaline fuel cell enhanced by methyl viologen as an electron-transfer catalyst, J. Power Sources. 251 (2014) 222–228.

[26] T. Ishimoto, H. Kazuno, T. Kishida, M. Koyama, Theoretical study on oxidation reaction mechanism on Au catalyst in direct alkaline fuel cell, Solid State Ionics. 262 (2014) 328–331.

[27] X. Lin, X. Liang, S.D. Poynton, J.R. Varcoe, A.L. Ong, J. Ran, et al., Novel alkaline anion exchange membranes containing pendant benzimidazolium groups for alkaline fuel cells, J. Memb. Sci. 443 (2013) 193–200.

[28] P. Yang, Y. Zhu, P. Zhang, H. Zhang, Z. Hu, J. Zhang, Performance evaluation of an alkaline fuel cell/thermoelectric generator hybrid system, Int. J. Hydrogen Energy. 39 (2014) 11756–11762.

[29] S. Kim, J.Y. Jung, H.H. Song, S.J. Song, K.Y. Ahn, S.M. Lee, et al., Optimization of molten carbonate fuel cell (MCFC) and homogeneous charge compression ignition (HCCI) engine hybrid system for distributed power generation, Int. J. Hydrogen Energy. 39 (2014) 1826–1840.

[30] G. Falcucci, E. Jannelli, M. Minutillo, S. Ubertini, J. Han, S.P. Yoon, et al., Integrated numerical and experimental study of a MCFC-plasma gasifier energy system, Appl. Energy. 97 (2012) 734–742.

[31] S. Campanari, G. Manzolini, P. Chiesa, Using MCFC for high efficiency CO2 capture from natural gas combined cycles: Comparison of internal and external reforming, Appl. Energy. 112 (2013) 772–783.

[32] I. Rexed, C. Lagergren, G. Lindbergh, Effect of sulfur contaminants on MCFC performance, Int. J. Hydrogen Energy. 39 (2014) 12242–12250.

[33] R. Carapellucci, R. Saia, L. Giordano, Study of Gas-steam Combined Cycle Power Plants Integrated with MCFC for Carbon Dioxide Capture, Energy Procedia. 45 (2014) 1155–1164.

[34] U. Desideri, S. Proietti, G. Cinti, P. Sdringola, C. Rossi, Analysis of pollutant emissions from cogeneration and district heating systems aimed to a feasibility

study of MCFC technology for carbon dioxide separation as retrofitting of existing plants, Int. J. Greenh. Gas Control. 5 (2011) 1663–1673.

[35]   S. Omar, E. Wachsman, J. Nino, Higher conductivity Sm3+ and Nd3+ co-doped ceria-based electrolyte materials, Solid State Ionics. 178 (2008) 1890–1897.

[36]   Ryan P. O Hyre, Fuel Cell Fundamentals, John Willey & Sons, INC, 2009.

Figurative Flow Chart of Thesis

```
          ┌─────────────────────┐
          │    Introduction     │
          └──────────┬──────────┘
                     │
                     ▼
          ┌─────────────────────┐
          │   Why Doped Ceria   │
          └──────────┬──────────┘
                     │
                     ▼
          ┌─────────────────────┐
          │ Review on Synthesis │
          │   and               │
          │  Characterization   │
          │    Techniques       │
          └──────────┬──────────┘
                     │
                     ▼
          ┌─────────────────────┐
          │   Experimentation   │
          └──────────┬──────────┘
                     │
                     ▼
          ┌─────────────────────┐
          │     Results and     │
          │    Discussions      │
          └──────────┬──────────┘
                     │
                     ▼
          ┌─────────────────────┐
          │ Conclusions and     │
          │ Future              │
          │ Recommendations     │
          └─────────────────────┘
```
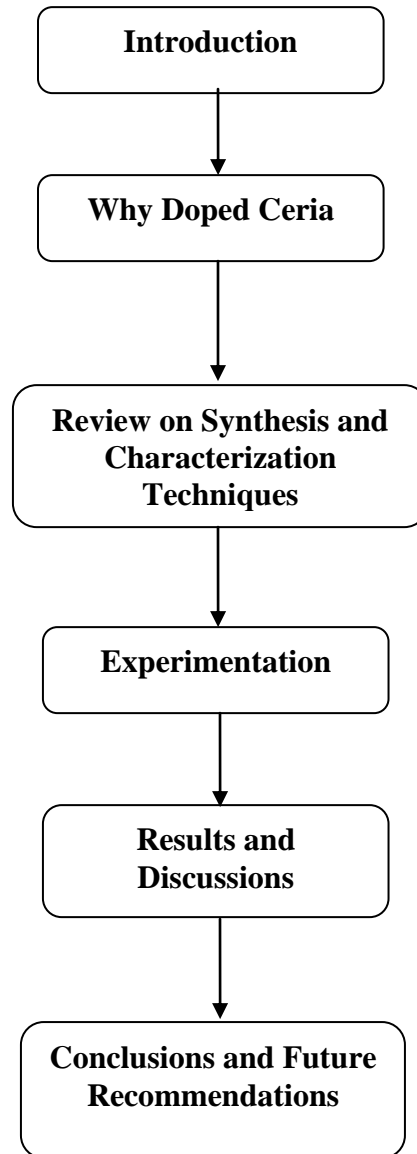
Chapter 2
Why Doped Ceria Electrolytes for SOFC

2.1 Pure Ceria

Cerium dioxide (Ceria) takes the fluorite crystal structure. The lattice is a face centred cubic cation sublattice with oxygen ions filling all the tetrahedral interstices. Pure ceria has a density of 7.22 g/cm^3 with the melting point of approximately 2477°C and its specific heat and thermal conductivity is 460 J/kg °C and 0.12 W/cm°C respectively. Fig. 2.1 shows the crystal structure of ceria. Ceria is able to accommodate significant non-stoichiometry in the form of oxygen deficiency that gives rise to oxygen vacancies. As a result the material allows for ionic conduction via oxygen vacancy migration, an effect which can be enhanced through the addition of trivalent dopants. Section 2.2 describes the oxide ions vacancy creation mechanism in doped ceria by addition of trivalent dopant ions.
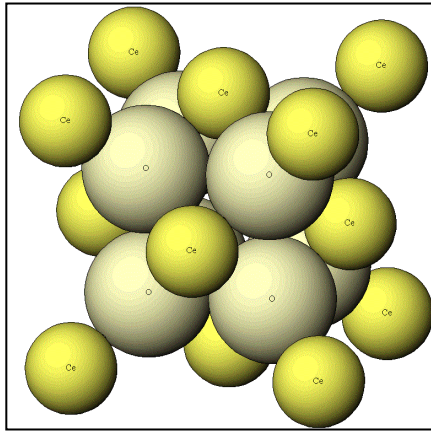
Fig. 2.1 Crystal structure of Ceria

2.2 Vacancy creation mechanism in doped ceria

Pure ceria is a poor ion conductor, for this reason it is doped with some trivalent ion which introduces charge compensation and enhances the oxide ions conduction [1]. Doped ceria electrolytes have been successfully synthesized and proven electrolyte materials for SOFCs applications with general formula of $Ce_{1-x}M_xO_{2-x/2}$ (where M= Gd, Sm and Nd, and Y etc.) and x represents the dopant concentration. The following reaction shows the vacancy creation in ceria when it is doped with trivalent atom.

$$Nd_2O_3 + CeO_2 \rightarrow 2Nd'_{Ce} + V_o^{\bullet\bullet} + 3O_o \qquad (2.1)$$
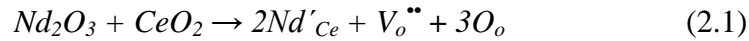
Where, Nd'_{Ce} represents the Neodymium (Nd) atoms that replace the Ce atoms during doping and $V_o^{\bullet\bullet}$ shows the oxide ions vacancy created due to charge compensation.

2.3 Ceria based electrolyte materials

As described in section 2.2, there are various trivalent atoms studied for ceria system. The purpose of every trivalent rare earth dopant is to increase the conductivity of that particular electrolyte. The extensively studied equation for oxide ions conductivity is given by:

$$\sigma T = \sigma_0 \, exp(-E_a/T) \qquad (2.2)$$

Where,

σ = ionic conductivity

σ_0 = pre-exponential term
E_a = Activation energy
T = Temperature
It can be concluded from equation 2.1 that concentration of free vacancies is the function of temperature. It is very difficult to select optimum dopant concentration. Where E_a can be defined by:

$$E_a = H_a + H_m \qquad (2.3)$$

Where,

H_a= Association enthalpy between defects and vacancies

H_m= Migration enthalpy

For low to intermediate temperature range the value of association enthalpy should be small to achieve better conductivity. Association enthalpy can be minimized by selecting dopant ionic radii close to the host ion [2]. Now we will briefly describe the suitable candidates for doped ceria electrolytes.

2.3.1 Gadolinium doped ceria (GDC)

Gadolinium has been extensively studied to improve the conductivity of ceria [3–8]. For this purpose different concentrations of Gd have been widely studied. GDC offers higher ionic conductivity with maximum dopant concentration of 10-20mol% often abbreviated as GDC10 and GDC20 respectively. Fig. 2.2 [9] shows the ionic conduction of various GDC compositions, i. e., 10-25mol%.
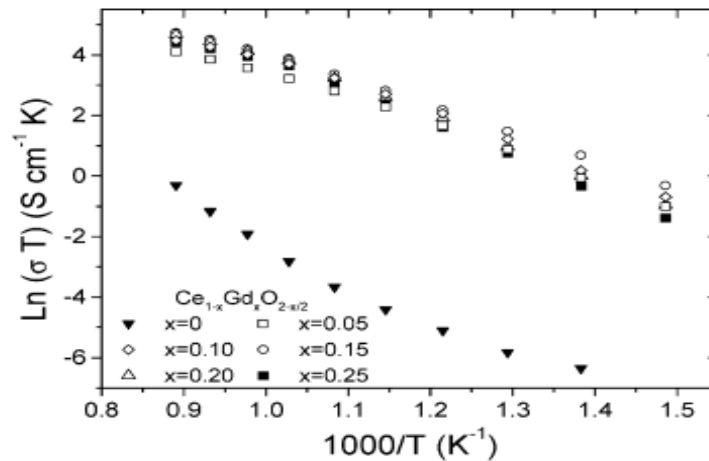
Fig. 2.2 Conductivity of GDC at various concentrations [9]

Ionic conduction mechanism depends on many factors in which grain and grain boundaries are also important parameters. Less resistance offered by grains and grain boundaries make electrolyte more suitable for ionic conduction. GDC10 has more lattice

ionic conductivity with the value of 0.01S/cm at 500 °C [10] but GDC20 offers more total conductivity [11].

2.3.2 Samarium doped ceria (SDC)

The second candidate for doped ceria is samarium which is also considered good ionic conductor with promising results for SDC20(20mol% dopant) [12]. SDC20 is considered for its highest conductivity among other doped ceria electrolytes [13]. Fig. 2.3 [13] shows the conduction properties of SDC with various concentrations of samarium.
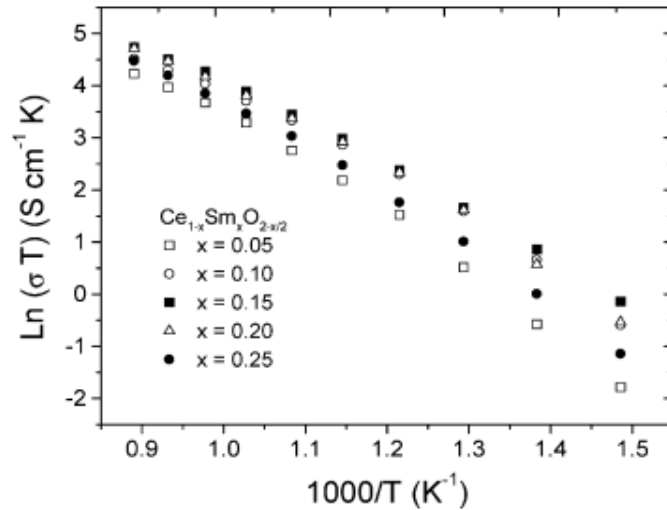
Fig. 2.3 Conductivity of SDC at various concentrations [13]

The optimal dopant concentration for SDC is 20 mole% i.e. $Ce_{0.8}Sm_{0.2}O_{1.9}$ after which conductivity starts to decrease with the increase in dopant concentration because of the increase interaction between the dopant ions and the oxygen vacancies [10]. The ionic conductivity of $Ce_{0.8}Sm_{0.2}O_{1.9}$ (SDC20) reported at 800 °C is 0.02 S/cm. This is due to the relative sizes of dopants ions as compared to primary ions they replace. With the increasing amount of Samarium, the conductivity decreases as the defects association between dopants ions and oxygen vacancies [10].

2.3.3 Neodymium doped ceria (NDC)

The next potential candidate for doped ceria based SOFC electrolyte materials is considered Neodymium (Nd). Neodymium fulfills the requirements upon which a dopant is selected for ceria lattice. Ionic conductivity in doped ceria is highly dependent on the following factors:

- The defect association enthalpy
- Type of the dopant ion
- Concentration of the dopant ion

The defect association enthalpy can be minimized if the difference between the radii of dopant ion and the host ion is not so large. The ionic radius value for Nd is 0.983Å while that of Ce^{+4} is 0.97Å that makes Nd suitable dopant for ceria [14]. For this purpose, effect of Nd content on the conduction properties of ceria has been studied [15–18]. Fig. 2.4 shows the conductivity curves for various Nd concnetrations [19]. The same case can be observed for Nd. The conductivity of NDC electrolyte increases with increasing the Nd content till 25mol% and then starts to decrease. This decrease is due to the increasing association of defects and oxide ions vacancies that forms traps for oxide ions and reduces the conduction.
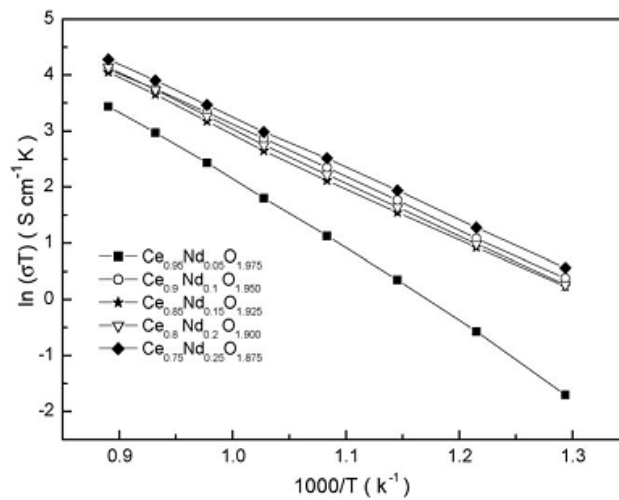
Fig. 2.4 Conductivity of Neodymium doped ceria [19]

The vacancy creation mechanism is already described in equation 2.1. Hikmet et al [15] improved the conduction properties of NDC15 by implying ultrasound assisted co-precipitation method which are in good agreement with already reported NDC15(15mol% dopant) with slightly better results but for NDC system higher ionic conductivity is reported for NDC25 (25mol% Nd) with activation energy of 0.794 ev [19]. They prepared NDC based electrolytes using nitrate based precursors by co-precipitation route. We synthesized the NDC with sol-gel route in which we have studied the effects of pH on the particle size, structure and phase of NDC. We have also studied the effects of co-doping and carbonates on DC electrical conductivity of NDC based electrolytes. Studies based on these parameters have not been reported for NDC electrolyte system. Moreover ND is second most abundantly available rare earth element after Ce in earth's crust. Fig. 2.5 shows a comparison of major rare earth elements present in earth's crust. It is evident from this chart that Ce is the most abundant element and also Nd is present in higher amount as compared to Gd and Sm. This makes Nd a favorable element to be used for doped ceria electrolyte materials [21].
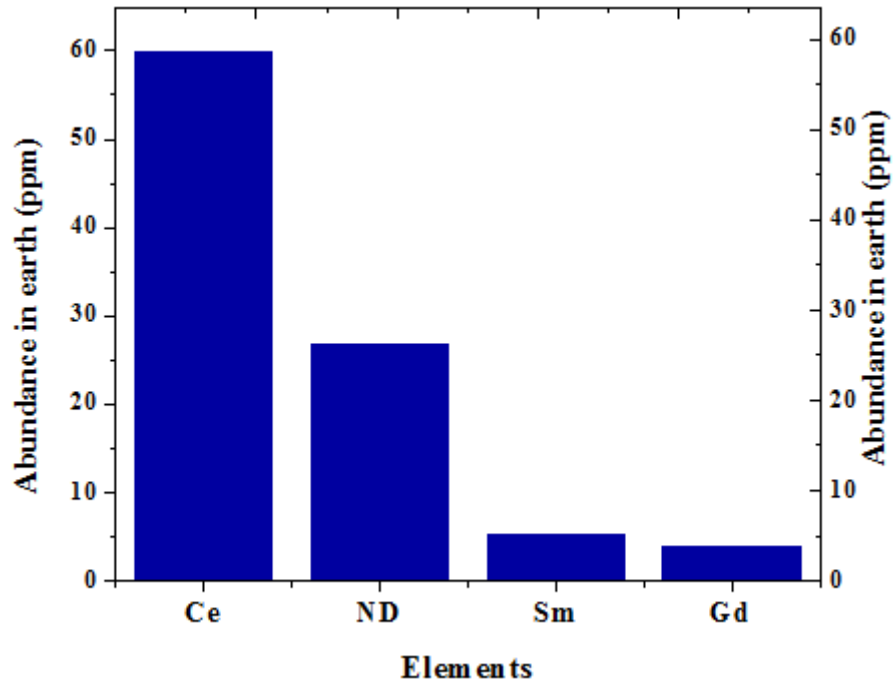
Fig. 2.5 Abundance of Rare Earth Elements in Earth [21]

Summary

Ceria has fluorite crystal structure. The lattice is a face centered cubic cation sublattice with oxygen ions filling all the tetrahedral interstices. Ceria accommodates significant non-stoichiometry in the form of oxygen deficiency that gives rise to oxygen vacancies. Pure ceria is poor ionic conductor but when it is doped with trivalent ions, the oxide ions conductivity increases dramatically. Addition of trivalent ions creates defects in the lattice and due to charge compensation oxygen vacancies are created. As a result the material allows for ionic conduction via oxygen vacancy migration. Ceria is also favorable as the doped ceria provides better ionic conductivity than YSZ at low temperature. For this purpose, ceria has been widely studies using Gd and Sm with various concentrations. GDC10 exhibits higher ionic conductivity with value of 0.01S/cm at 500 °C. 20 mol% of Samarium doped ceria also provide conductivity of 0.02 S/cmat 800 °C. The selection of dopant for ceria depends on the various factors, like defect association enthalpy, type of the dopant ion and concentration of the dopant ion. The value for association enthalpy should be small for selected dopant. To obtain better ionic conductivity, the difference between dopant and host ions radius should be small. Neodymium fulfills all such requirements for dopant for ceria lattice. Moreover, Nd is second most abundantly available rare earth element in earth's crust. This makes Nd most favorable dopant for ceria. NDC have been synthesized using co-precipitation route but no one has studied effects of pH on structure, phase and particle size. Data based on co-doping using Sm and Y for NDC lattice and effects of carbonates on NDC is insufficient that is the main reason to work in this respective area.

References

[1]   D. Bucevac, A. Radojkovic, M. Miljkovic, B. Babic, B. Matovic, Effect of preparation route on the microstructure and electrical conductivity of co-doped ceria, Ceram. Int. 39 (2013) 3603–3611.

[2]   S. Omar, E. Wachsman, J. Nino, Higher conductivity Sm3+ and Nd3+ co-doped ceria-based electrolyte materials, Solid State Ionics. 178 (2008) 1890–1897.

[3]   T.H. Hsieh, D.T. Ray, Y.P. Fu, Co-precipitation synthesis and AC conductivity behavior of gadolinium-doped ceria, Ceram. Int. 39 (2013) 7967–7973.

[4]   A. Atkinson, SOLID ioN # a Chemically-induced stresses in gadolinium-doped ceria solid oxide fuel cell electrolytes, 95 (1997) 249–258.

[5]   P.P. Dholabhai, S. Anwar, J.B. Adams, P. a Crozier, R. Sharma, Predicting the optimal dopant concentration in gadolinium doped ceria: a kinetic lattice Monte Carlo approach, Model. Simul. Mater. Sci. Eng. 20 (2012) 015004.

[6]   A.B. Stambouli, E. Traversa, Solid oxide fuel cells (SOFCs): a review of an environmentally clean and efficient source of energy, Renew. Sustain. Energy Rev. 6 (2002) 433–455.

[7]   G. Kim, N. Lee, K. Kim, B. Kim, H. Chang, S. Song, et al., Various synthesis methods of aliovalent-doped ceria and their electrical properties for intermediate temperature solid oxide electrolytes, Int. J. Hydrogen Energy. 38 (2012) 1571–1587.

[8]   W. Zając, J. Molenda, Electrical conductivity of doubly doped ceria, 179 (2008) 154–158.

[9]   S. Zha, C. Xia, G. Meng, Effect of Gd (Sm) doping on properties of ceria electrolyte for solid oxide fuel cells, 115 (2003) 44–48.

[10] Ryan P. O Hyre, Fuel Cell Fundamentals, John Willey & Sons, INC, 2009.

[11] Z. Tianshu, P. Hing, H. Huang, J. Kilner, Ionic conductivity in the CeO 2 – Gd 2 O 3 system (0 . 05 V Gd / Ce V 0 . 4) prepared by oxalate coprecipitation, 148 (2002) 567–573.

[12] M. Dokiya, T. Horita, T. Kawada, N. Sakai, H. Yokokawa, Low temperature, 2738 (1996) 0–3.

[13] S. Le, S. Zhu, X. Zhu, K. Sun, Densification of Sm0.2Ce0.8O1.9 with the addition of lithium oxide as sintering aid, J. Power Sources. 222 (2013) 367–372.

[14] S. (Rob) Hui, J. Roller, S. Yick, X. Zhang, C. Decès-Petit, Y. Xie, et al., A brief review of the ionic conductivity enhancement for selected oxide electrolytes, J. Power Sources. 172 (2007) 493–502.

[15] G. Zhao, D. Zhou, J. Zhu, M. Yang, J. Meng, Effect of MoO3 concentration on sintering and electrical properties of SiO2-containing neodymium-doped ceria electrolytes, Solid State Sci. 13 (2011) 1072–1075.

[16] İ. Uslu, A. Aytimur, M.K. Öztürk, S. Koçyiğit, Synthesis and characterization of neodymium doped ceria nanocrystalline ceramic structures, Ceram. Int. 38 (2012) 4943–4951.

[17] J.X. Zhu, D.F. Zhou, S.R. Guo, J.F. Ye, X.F. Hao, X.Q. Cao, et al., Grain boundary conductivity of high purity neodymium-doped ceria nanosystem with and without the doping of molybdenum oxide, J. Power Sources. 174 (2007) 114–123.

[18] V. Gil, J. Tartaj, C. Moure, Chemical and thermomechanical compatibility between neodymium manganites and electrolytes based on ceria, J. Eur. Ceram. Soc. 29 (2009) 1763–1770.

[19] Y.-P. Fu, S.-H. Chen, Preparation and characterization of neodymium-doped ceria electrolyte materials for solid oxide fuel cells, Ceram. Int. 36 (2010) 483–490.

[20] H. Okkay, M. Bayramoğlu, M.F. Öksüzömer, Ultrasound assisted synthesis of Gd and Nd doped ceria electrolyte for solid oxide fuel cells, Ceram. Int. 39 (2013) 5219–5225.

[21] W. Permission, Rare Earth Elements : A Review of Production , Processing , Recycling , and Associated Environmental Issues Rare Earth Elements : A Review of Production , Processing , Recycling , and Associated Environmental Issues, (2012).

Chapter 3
Synthesis Methods and Characterization Techniques

3.1 Wet Chemistry Routes

Various routes have been incorporated to synthesize ceria based electrolyte materials. Here we will only focus on wet chemistry routes like sol-gel and co-precipitation.

3.1.1 Sol-gel

Sol-gel method is widely used to synthesize nano-particles. Sol is a dispersion of colloidal particles and gel is a rigid complex network of polymeric chains [1]. In this method metal alkoxides are mixed in organic solvents. The second approach involves utilization of metal salts like nitrates and chlorides etc. in which they are dissolved in water. Metal-inorganic approach for synthesis of particles is much cheaper than organic approach[1]. The general formula for metal alkoxides is $M(OR)_x$ where M is a metal, mostly Si, Ce, Nd, Sm, Gd, Y and Zr etc. and OR is an alkoxy group attached to metal atom and x represents the oxidation state of metal. The main reactions involved in sol-gel technique are hydrolysis and condensation which lead to polymerization. The first step is the hydrolysis of alkoxy group. The next step is polycondensation reaction. The result of this reaction is the formation of polymers. After polycondensation, macromolecular network is formed. A sol is formed in which macroscopic size has not been achieved by the polymerized structures. A gel is formed when the bushy structures are formed due to recombination of polymers. The structure of these polymers are dependent on temperature, hydrolysis ratio, nature of solvents and that of catalysts, use of nucleophilic reagents and complexing ligands etc.

Advantages of Sol-gel

- Low temperature processing and consolidation is possible.
- Smaller particle size and morphological control in powder synthesis.
- Sintering at low temperature also possible.
- Better homogeneity and phase purity compared to traditional ceramic method.

Disadvantages of Sol-Gel Process

- Raw materials for this process are expensive (in the case of metal alkoxides) as compared to mineral based metal ion sources.
- Products would contain high carbon content when organic reagents are used in preparative steps and this would inhibit densification during sintering.
- Since several steps are involved, close monitoring of the process is needed.

3.1.2 Co-precipitation

In this method precursors of salts are mixed in a solvent, mostly water. After mixing of the precursor, rapid precipitation starts by addition of small amount of pH controller. The resulting reactive mixtures are formed after mixing them for some time [2]. The solvent used in this technique may be removed by oven drying. For achieving high homogeneity, the solubility products of the precipitate of metal cations must be closer [3]. Also, co-precipitation process required to control the concentration of the solution, pH, temperature and stirring speed of the mixture in order to obtain the final product with required properties [4]. The calculation of solution equilibria of precipitates needs special knowledge of the solubility and solubility product of the compound. The solubility product requires information on the stoichiometry and composition of the compound. Particle size and ageing processes also significantly affect the solubility of a precipitate. The particle size of a precipitate is formed by the relative rates of nucleation and growth as well as on the concentration of the precursors. Nuclei are the smallest particles of precipitate which can grow spontaneously. Their formation is named nucleation that is a necessary step in the precipitation process.

Advantages of Co-Precipitation Process

- Homogeneous mixing of reactant precipitates reduces the reaction temperature.
- Simple direct process for the synthesis of fine metal oxide powders, which are highly reactive in low temperature sintering.

Disadvantages of Co-Precipitation Process

- This process is not suitable for the preparation of high pure, accurate stoichiometric phase.

- This method does not work well, if the reactants have very different solubility as well as different precipitate rate.
- It is not having universal experimental condition for the synthesis of various types of metal oxides.

3.2 Structural Analysis

In this thesis, to investigate structural properties of the fabricated powders various techniques were used like X-ray diffraction, Scanning electron microscope and particle size analyzers.

3.2.1 X-Ray Diffraction (XRD)

XRD is an analytical tool for identification of phases and orientations in crystalline compounds. XRD is a non-destructive technique that provides crystallographic information of the specimen. It is useful in determining structural properties like crystal size, lattice parameters, lattice strain etc.

Working principle

When crystalline materials are irradiated by X-rays, they interact with atoms of the material and refract X-rays of characteristic energy. An individual pattern is generated by each material. In a mixture of materials, each substance gives its own pattern independently [5]. XRD works on the principal of constructive interference of refracted X-rays. Fig.3.1 shows working of XRD machine. When X-rays interact with matter, three phenomena may occur, Ionization, fluorescence and diffraction. In XRD, when X-rays hit atoms, the electrons in atoms start vibrating with frequency same as the frequency of striking X-rays. Bragg's law is used to describe the working of XRD.

$$n * \lambda = 2d * sin\theta \qquad (3.1)$$

Where:

Θ = Incidentangle

d = Spacing between the planes and

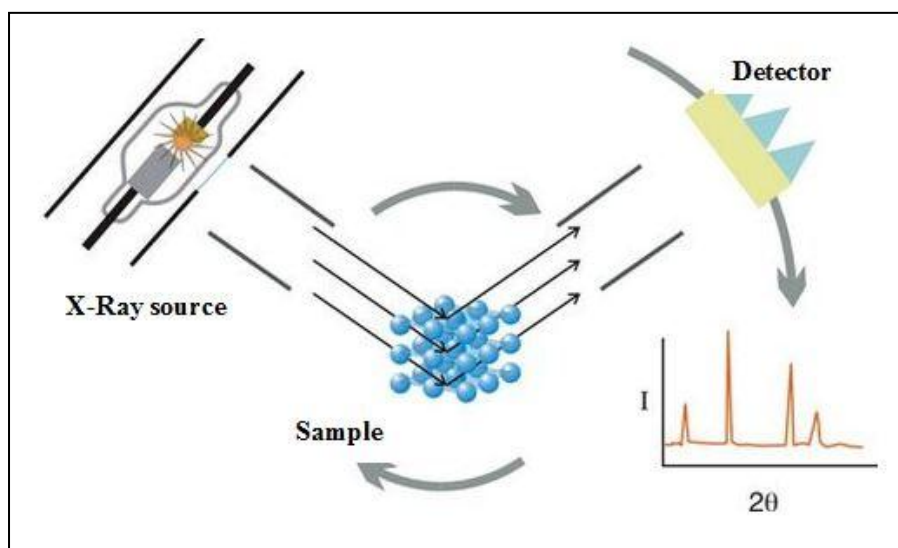λ = wavelength of the X-rays

28

Fig.3.1 Working of XRD

After striking on the sample, these X-rays are detected by a detector that makes a diffractogram. A diffractogram is a graph which is plotted between 2θ on x-axis and intensity on y-axis. The detector records intensities of the diffracted beams and angles. This pattern is a fingerprint of the material. Miller indices define the inter-planar spacing and orientation. Number and position of peaks (2θ values) enable to determine lattice type, cell parameters and crystal class. Intensity of peaks gives information about position and types of atoms in the specimen [6].

3.2.2 Scanning Electron Microscopy (SEM)

SEM is an imaging tool that is used to study surface morphology of the samples. The surface of the prepared substrate is analyzed in three dimensions with high resolution and magnification. SEM provides magnification up-to 300,000X and has an effective probing depth of 10 nm to 1 μm.

Working principal

A focused electron beam is kept over the sample that results excitation of electrons present in the sample. An Image is produced on the display of computer connected to the machine. The magnification depends on the relationship of size between the display and the area of the surface being scanned. Samples being scanned in SEM may face damage problems but it rarely happens. During high magnification some

polymers plastic based materials may be transformed. This damage can be prevented using the machine at low voltage [6].
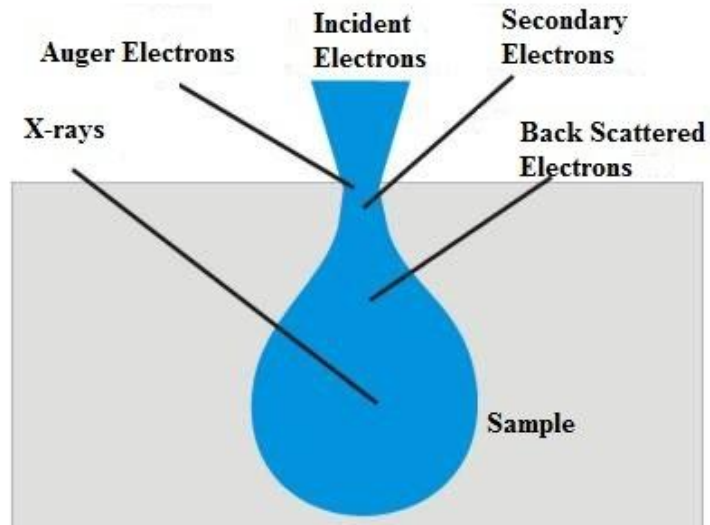

Fig. 3.2 Working principal of SEM

3.2.3 Particle Size Analyzer

Particle size analyzer is a tool to identify the range of particle sizes present in the sample. This technique also gives information about average particle size along-with percentage of particular sizes formed in the powder sample.

Working Principal

Particle size analyzer contains two chambers. First chamber is a conical type that is connected to an electric motor and the second chamber is a transparent box. Sonication is done before feeding the liquid suspension of powder sample into the conical chamber. After inserting the sample into conical section, the suspension is mixed again with motor and then it goes to the transparent section. Here the particles are in suspended form and a laser beam passes through the transparent section and strikes the particles. A detector is placed on the other side of the laser source that measures the size of percent amount present in the sample [7].

3.3 Electrical Conductivity Measurement

DC electrical conductivity is measured using LCR meter. The conductivity of an electrolyte is an important parameter, as it tells us about the internal behavior of

electrolyte material to conduct ions. It also gives information, how efficiently the material allows flowing oxide ions.

Working Principal

Pellets are formed with suitable dimensions to measure the DC electrical conductivity of the material. LCR meter actually tells the DC resistance of synthesized electrolyte material and finally the conductivity of the sample is calculated using the following relation:

$$\rho = (R_{avg} * A)/L \qquad\qquad (3.2)$$

$$\sigma = 1/\rho \qquad\qquad (3.3)$$

where:

ρ = Resistivity of pellet

σ = Conductivity of pellet

R_{avg}= Average resistance of pellet

A = Area of the pellet and,

L= thickness of pellet

Summary

Various routes have been used to synthesize solid electrolyte materials. Wet chemistry routes are better as compared to solid state method. Sol-gel and co-precipitation are widely used methods that give atomic level mixing with better particle size control. For structural analysis of synthesized powders XRD, SEM and particle size analysis were used. XRD is used to identify the structure, phases, lattice strain, crystallite sizes and SEM is used to study surface morphology of the samples. XRD works on Bragg's law. X-Rays are produced using X-Ray source and after striking on the sample, these X-Rays are detected by detector. A diffractogram is a graph that gives information of XRD analysis. I SEM, a focused electron beam is kept over the sample that results excitation of electrons present in the sample. An Image is produced on the display of computer connected to the machine. Particle size analysis is used to identify a range of powder particles actually formed. It also gives information about average particle size with their percentage present in a sample. To measure the electrical conductivity of electrolyte materials DC electrical conductivity is used. This is done using LCR meter that actually measures the DC resistance of electrolyte at various temperature ranges.

References

[1]   L.L. Hench, J.K. West, The sol-gel process, Chemical Reviews. 90 (1990) 33–72.

[2]   I.I.E. Techniques, W.C. Processes, N.O. Powders, S. Process, H. Process, P. Process, et al.

[3]   H.N. T. H. Cho, Y. Shiosaki, Preparation and characterization of layered LiMn 1/3Ni 1/3Co 1/3O 2 as a cathode material by an oxalate co-precipitation method, J. Power Sources. 159 (2006) 1322–1327.

[4]   R.I.B. G. Xu, X. Zhang, W. He, H. Liu, H. Li, No Title, Materials Letters. 60 (2006) 962–965.

[5]   S.S. B. D. Cullity, S. R. Stock, Elements of X-Ray Diffraction, 3rd Edition, 2001.

[6]   C.A. Evans, S. Wilson, Materials characterization, 1999

[7]   https://cma.tcd.ie/misc/particle_size.pdf.

Chapter 4
Experimentation

As fabrication of Neodymium Doped Ceria (NDC) solid electrolyte is the main theme of this thesis. For this reason, we performed several experiments that are listed below.

- First experiment was to synthesize NDC electrolyte with two major compositions of $Ce_{0.80}Nd_{0.20}O_{1.90}$ (NDC20) and $Ce_{0.75}Nd_{0.25}O_{1.875}$ (NDC25) using Cerium Nitrate Hexahydrate and Neodymium Nitrate Hexahydrate.
- Effects of pH on structure, phase formation and powder particle size were studied using two different values of pH i.e., 3 and 10.
- Co-doping also improves the conduction properties of Doped Ceria. Keeping in view this fact, two co-dopants, Sm and Y were doped into NDC lattice.
- K_2CO_3 was added into NDC, by 10 and 20% by volume to study the effects of carbonates on electrical conductivity.
- As it is very necessary for SOFC electrolyte material to remain chemically stable with the other parts of the cell. To investigate the chemical stability of NDC with NiO-SDC anode, we fabricated a composite of these two materials and sintered it at 800°C. The results will be discussed in Chapter-5

4.1 Synthesis of Neodymium Doped Ceria (NDC)

Sol-gel method was applied to fabricate Neodymium Doped Ceria solid electrolyte with two main compositions $Ce_{0.80}Nd_{0.20}O_{1.90}$ (NDC20) and $Ce_{0.75}Nd_{0.25}O_{1.875}$(NDC25) using $Ce(NO_3)_3.6H_2O$(Purity 99.99%) and $Nd(NO_3)_3.6H_2O$ (Purity 99.99%) as starting materials. 1M solutions of both precursors were prepared in separate beakers using distilled water as solvent and then dopant sol was added drop-wise with continuous stirring. Ammonia solution was used as a complexing agent as well as to control the pH. Prepared gels were dried in an oven at 110°C for several hours. Fig. 4.1 shows a complete block flow diagram of steps involved during synthesis and characterization of NDC20 and NDC25.
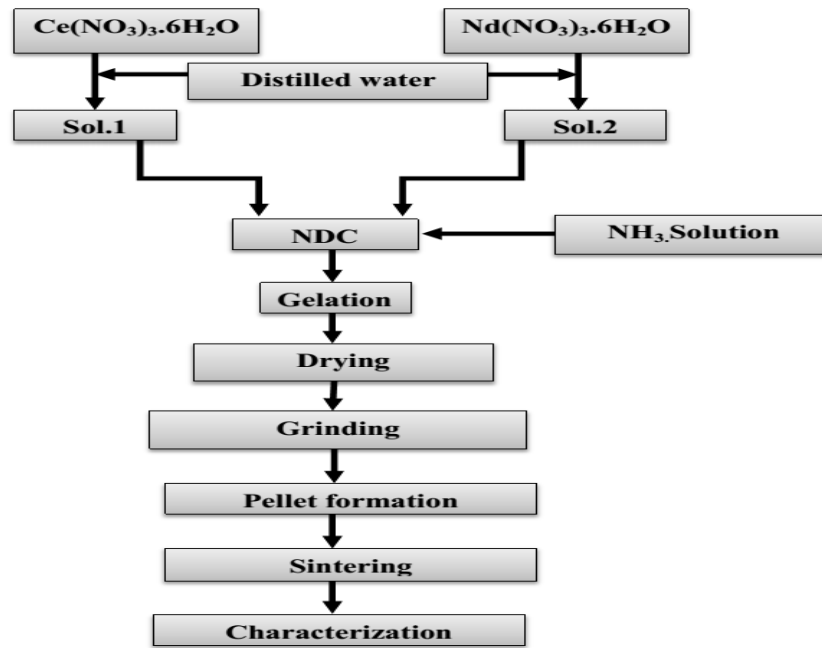
Fig. 4.1 Flow diagram of sol-gel fabrication of NDC

4.2 Effect of pH

The structure of the sol–gel fabricated ceramic powders depends on the relative rates of the hydrolysis and condensation reactions, as well as on the reverse reactions. For this reason, initially pH3 and 10 were selected to fabricate NDC electrolyte. All the synthesis was carried out using sol-gel route. When both sols of precursors were added into each other the pH value reached to 4. 0.5ml solution of citric acid was used to lower the pH value and make it stable up-to 3. To synthesize the NDC in basic medium, Ammonium hydroxide solution was used to control the pH and complexing agent as well.

4.3 Co-doping of NDC using Yttrium and Samarium

To investigate the effects of Yttrium and Samarium as co-dopants, we prepared further two compositions $Ce_{0.75}Y_{0.15}Nd0_{.10}O_{1.875}$ (NYDC) and $Ce_{0.75}Sm_{0.15}Nd_{0.10}O_{1.875}$ (SNDC). Same molar ratios were used as mentioned above. $Y(NO_3)_3.6H_2O$ (Purity 99.99%) and $Sm(NO_3)_3.6H_2O$ (Purity 99.99%) were used as precursors in co-doping experiment. Drying of gels was done in an oven at same temperature as kept during synthesis of NDC20 and NDC25.

4.4 Synthesis of NDC-carbonate composite electrolyte
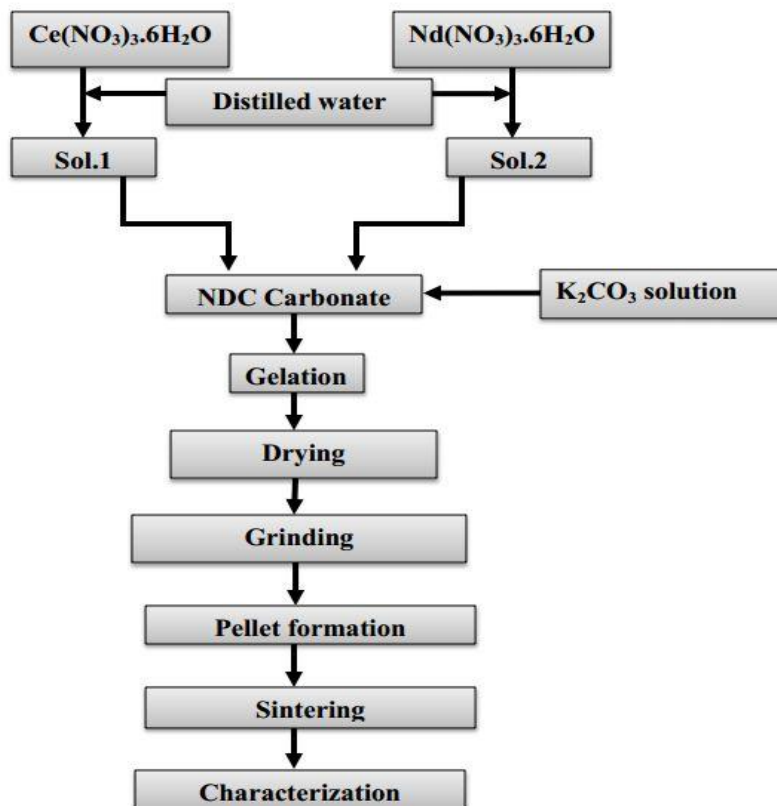
Fig. 4.2 Flow Diagram of NDC Carbonate

Powders with K_2CO_3 inclusion were also prepared via already described sol-gel route. For this purpose 1M solution of K_2CO_3 was prepared and drop-wise added into NDC25 solution with 10 and 20% by volume and finally obtained compounds were names as KNDC10 and KNDC20. Pellets with carbonates inclusion were sintered at 700°C for 3 hours keeping in view the melting point of potassium carbonate. Fig. 4.2 shows a block flow diagram of NDC Carbonate composite electrolyte.

4.5 Chemical compatibility of NDC electrolyte

To investigate the chemical stability of prepared electrolyte material with Nicked Oxide Samarium doped ceria (NiO-SDC) anode material, we carried out a separate experiment. The compositions of NDC and NiO-SDC were 60mol% and 40mol% respectively. The prepared powder was sintered at 800°C and to confirm whether

both the materials remained in separate phases or reacted with each other at such a high temperature. The XRD result will be discussed in chapter 5.

4.6 Characterization

In order to study the properties of synthesized electrolyte materials, we used the following techniques. The name of techniques and their parameters are given as under:

- **XRD**

In order to study the structure, phase, lattice strain, theoretical density and crystallite size, X-ray powder diffractometer (STOE Germany) with computer interface having Cu Kα at λ =1.5418 Å was used by keeping scan angle ranging from 10°- 80°with step size 0.04/sec.Lattice parameters were calculated using six main reflections (111), (200) (220), (311), (222) and (400).

- **SEM**

To study the surface morphology of synthesized materials, Scanning Electron Microscope (HITACHI SU-1500) with 50 μm magnification and voltage was kept up-to 5kV.

- **Particle size analyzer**

Particle size analyzer (HORIBA LA-950) was used to measure the size of powder particles.

- **Pellets formation**

Prepared powders were ground utilizing pestle with mortar in acetone environment to make fine powders. Pellets with 10mm diameter and 2mm thickness were formed using uniaxial hydraulic press under pressure of 4.88kg/cm^2 for 10 minutes.

- **DC Electrical Conductivity**

DC electrical conductivity of pellets was measured using two probe method with the help of Wayne Kerr 6440B LCR meter. For this purpose, a special type of ceramic rod was designed that not only provided the facility to hold the pellets but also helped to make electrical contacts with the pellets. Pellets were hold by using Copper circular sheets. The setup can be seen in Fig. 4.3 that shows a ceramic rod which is used to hold the pellet and helps to provide electrical connections to the pellet.

Fig. 4.3 Pellet Holder

Fig. 4.4 shows a schematic diagram of LCR meter along-with Tube furnace. DC electrical conductivity of the pellet is measured by switching the LCR meter on DC resistance mode. The high temperature environment is provided by Tube furnace. At particular temperature, DC resistance of the pellet was measured three times and then their average value was selected to calculate the DC conductivity of the pellet using equations 3.1 and 3.2.
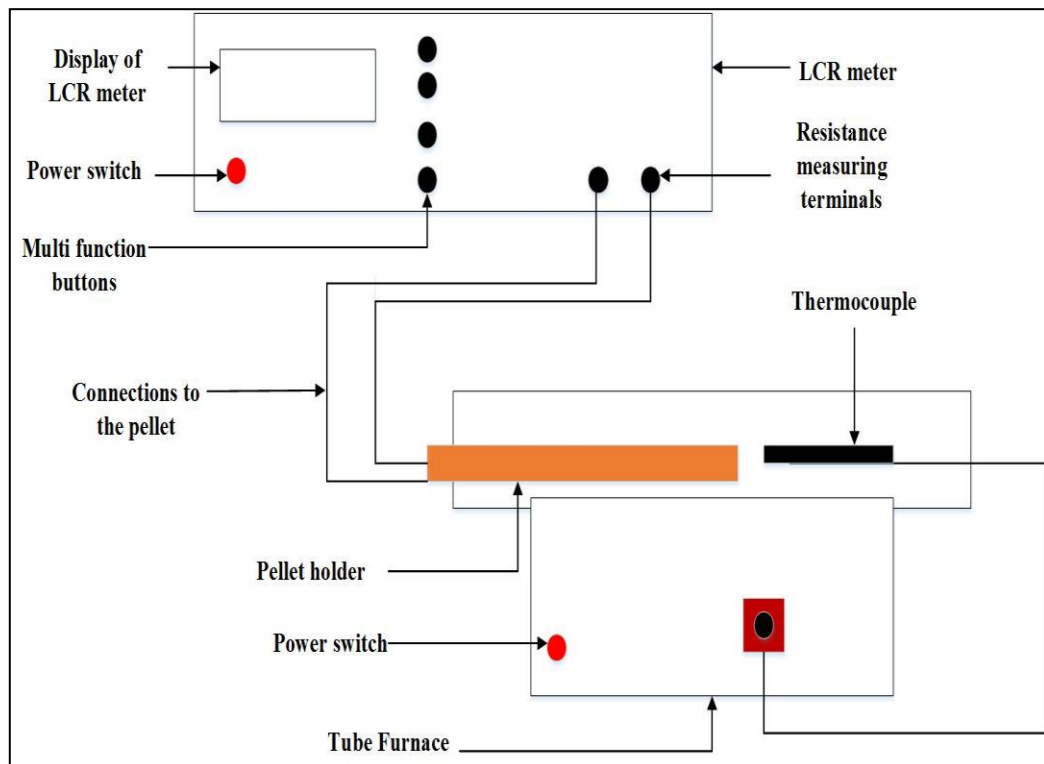

Fig. 4.4 Schematic Diagram of LCR meter

Summary

Sol-gel method was applied to fabricate neodymium doped ceria solid electrolytes. Two compositions $Ce_{0.80}Nd_{0.20}O_{1.90}$ (NDC20) and $Ce_{0.75}Nd_{0.25}O_{1.875}$ (NDC25) using cerium nitrate hexahydrate and neodymium nitrate hexahydrate as precursors. Effect of pH on phase formation and particle size was carried out at three different pH values. Effect of co-doping was also investigated using Sm and Y as co-dopants. Inclusion of K_2CO_3 was made to improve the conductivity of NDC25. For an SOFC electrolyte material, it is strictly desired that it should be chemically and thermally stable with anode material as well. For this purpose, NDC based electrolyte was tested with NiO-SDC anode to investigate whether both the compounds remain stable at high temperature or not. XRD (STOE Germany), Scanning Electron Microscope (HITACHI SU-1500) and HORIBA LA-950 particle size analyzer were used to study the structural properties of synthesized materials. Wayne Kerr 6440B LCR meter was used to calculate DC electrical conductivity of the pellets. Their results will be discussed in Chapter -5.

Chapter 5
Results and Discussions

5.1 Structural Analysis of NDC20 and NDC25

Initially two compositions $Ce_{0.80}Nd_{0.20}O_{1.90}$ (NDC20) and $Ce_{0.75}Nd_{0.25}O_{1.875}$ (NDC25) were selected to synthesize Neodymium Doped Ceria electrolyte. Their precursors are already described in Chapter 4. This initial comparison was done to confirm which one of them is better ionic conductor. Fig. 5.1 shows the XRD patterns of NDC20 and NDC25.It can be seen clearly that synthesized powders were free from impurities. Both the samples exhibited cubic fluorite structure [1]. It can also be noticed that the peaks shifted towards the lower value of 2θ when dopant concentration increased from 0.2 to 0.25. This effect of dopant concentration was later confirmed by analyzing the larger value of inter-planar spacing "d" that resulted into increase of lattice parameters as well for NDC25 as compared to NDC20. Table 5.1 shows the lattice parameters, volumetric strain and crystallite sizes of NDC20 and NDC25. It can be seen that with increase in dopant concentration the lattice parameters were also increased that follows the Vegard's rule [2–4]. Theoretical density was also increased by increasing the concentration of neodymium from 0.2 to 0.25 showing that the grain density increases with addition of small amount of Neodymium.

5.2 DC Conductivity comparison of NDC20 and NDC25

To further confirm whether the increase in Neodymium content actually increased the conductivity or not so, DC electrical conductivity of both the samples were performed ranging from 200-650°C. The equations 4.1 and 4.2 were used to calculate the DC electrical conductivity. Fig. 5.2 shows the comparison chart for DC electrical conductivity of NDC20 and NDC25. It can be noticed from the graph that the value of conductivity for NDC20 is less as compared to NDC25. This result is in good agreement with literature [5]. The value of DC conductivity for NDC20 reached 3.67×10^{-5} S/cm while for NDC25 it was found to be 7.9×10^{-5} S/cm. this shows that NDC25 is better ionic conductor than NDC20 So, NDC25 was selected for further experiments and improvements in conductivity.
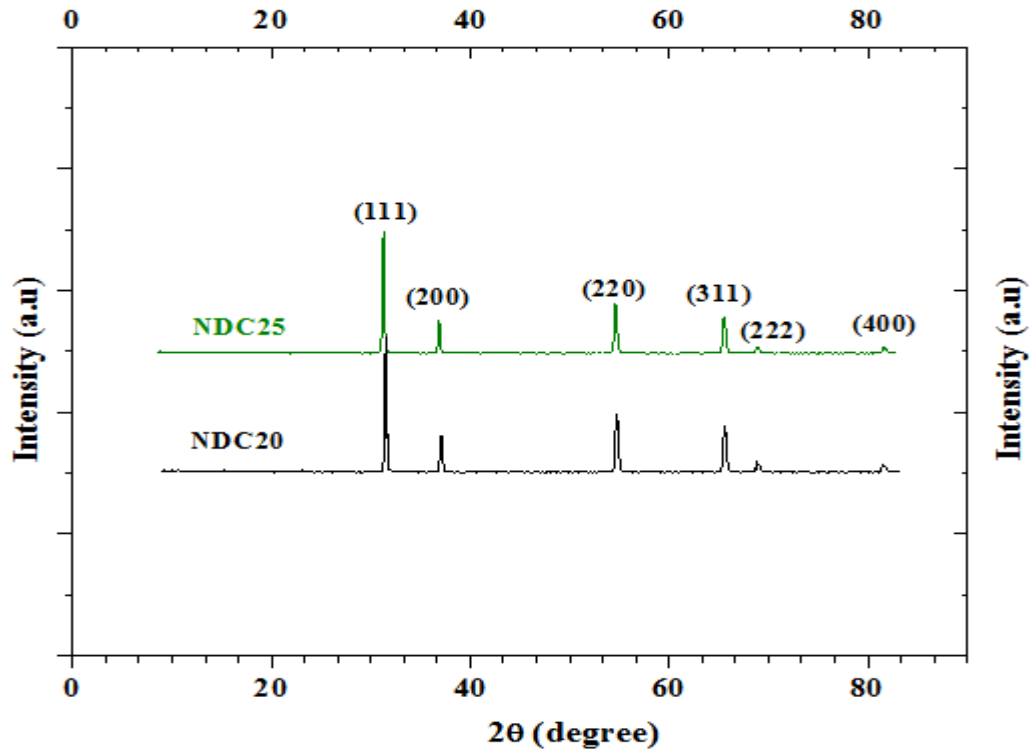
Fig. 5.1 XRD patterns of NDC20 and NDC25

Table 5.1: XRD results of NDC20 and NDC25

Composition	Lattice Parameter(Å)	Lattice Strain (%)	Crystallite size(nm)
NDC20	5.44	0.05	53
NDC25	5.47	0.06	41

5.3 Effect of pH on NDC25

To further optimize the NDC25, synthesis was carried out using three pH values such as 3, 7 and 10. We selected these pH values to investigate the effects of acidic and basic medium on structure and phase of NDC25. The structure of the sol–gel fabricated ceramic powders depends on the relative rates of the hydrolysis and condensation reactions, as well as on the reverse reactions [6]. The influence of the reaction conditions on the mechanism and kinetics of the reactions forms a key issue in understanding the structural evolution. The condensation rate is sufficiently small

that reaction-limited aggregation is assumed to occur under both acid and base catalysis [1].
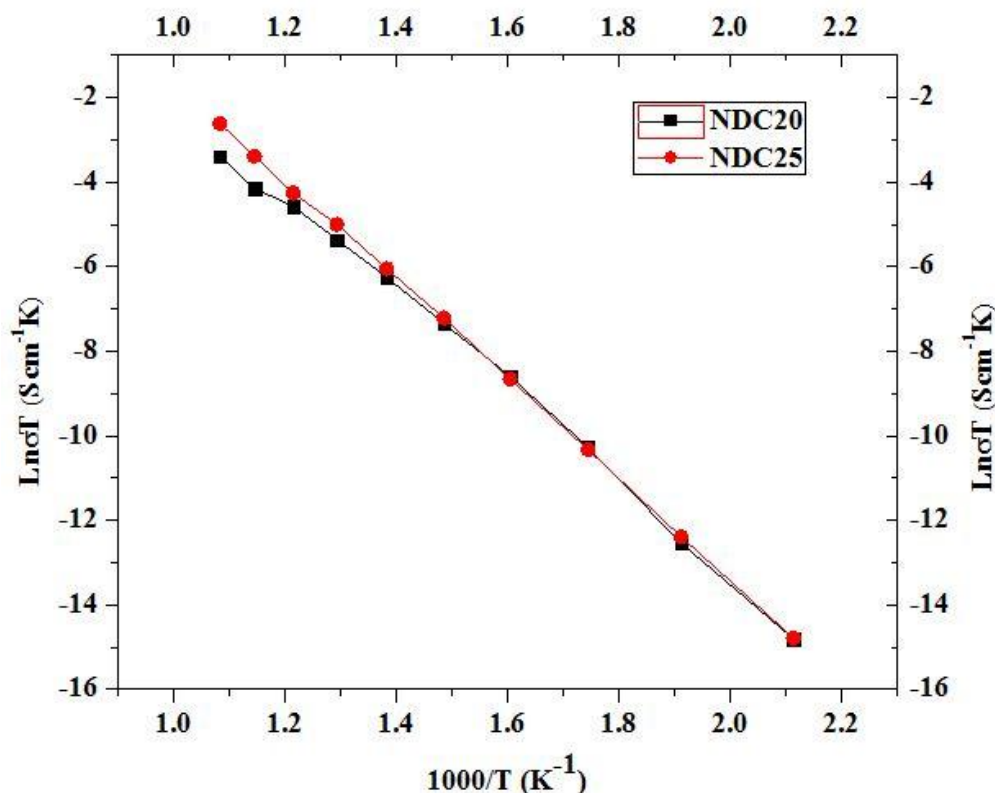
Fig. 5.2 DC Conductivity comparison of NDC20 and NDC25

The cross-linking between the polymer chains is much higher at high pH and high H_2O : Ce ratio (w) so that highly branched clusters are formed under these conditions, whereas more weakly branched clusters are formed at low pH. Now we will consider some reactions based on acidic and basic pH. It is generally assumed that at the isoelectric point (IEP) the gelation rate is proportional to hydroxal group. The base-catalyzed polymerization occurs by a nucleophilic mechanism according to the following reaction sequence.

$$\equiv Ce-OH + OH^- \longrightarrow Ce\text{-}O^- + H_2O \qquad (5.1)$$

$$\equiv Nd-OH + OH^- \longrightarrow Nd\text{-}O^- + H_2O \qquad (5.2)$$

$$Ce\text{-}O^- + \equiv Nd-OH \longrightarrow \equiv Ce-O-Nd \equiv + OH^- \quad (5.3)$$
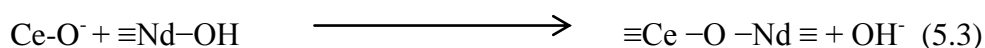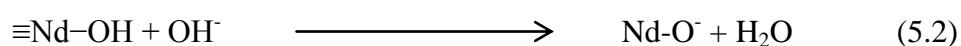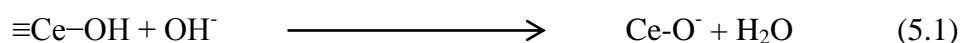
Here the polymerization rate is proportional to $[H^+]$. The following reactions take place under acidic conditions.

$$\equiv Ce-OH + H_3O^+ \longrightarrow \equiv Ce^+ + H_2O \qquad (5.4)$$

$$\equiv Nd-OH + H_3O^+ \longrightarrow \equiv Nd^+ + H_2O \qquad (5.5)$$

$$\equiv Ce^+ + \equiv Nd-OH \longrightarrow \equiv Ce -O -Nd \equiv + H^+ \qquad (5.6)$$
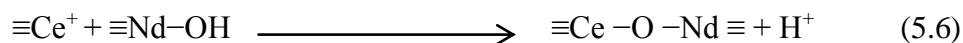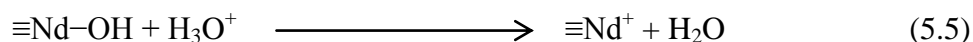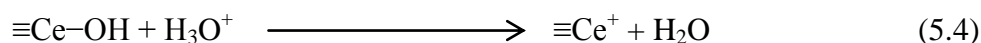
Further growth occurs by continued addition of lower molecular weight species to more highly condensed species (by conventional polymerization or by Ostwald ripening) and by aggregation of the condensed species to form chains and networks. Near the isoelectric point (IEP), where there is no electrostatic repulsion, growth and aggregation occur together and may be indistinguishable. However, particle growth becomes negligible when the particles reach a size of 2–4 nm because of low solubility in this pH range and the greatly reduced size-dependent solubility. The gels consist of chains and networks of very fine particles.

5.3.1 Effect of pH on NDC25 structure

XRD analysis was done to investigate whether the pH medium affected the composition, phase or structure of NDC25. Fig. 5.3 shows the XRD plots of NDC25 drawn for pH3, 7 and 10. It can be concluded from the XRD patterns that there are no other phases formed by changing the pH and XRD results also confirmed that all the three samples prepared at these three different pH values exhibited cubic fluorite structure. Table 5.2 summarizes the results of NDC25 prepared at various pH values.

Table 5.2: Results of NDC25 at different pH values

pH	Calcination temperature (^{0}C)	Time (hrs)	Particle size after calcination (μm)
3	600	5	0.97
10	600	5	1.11
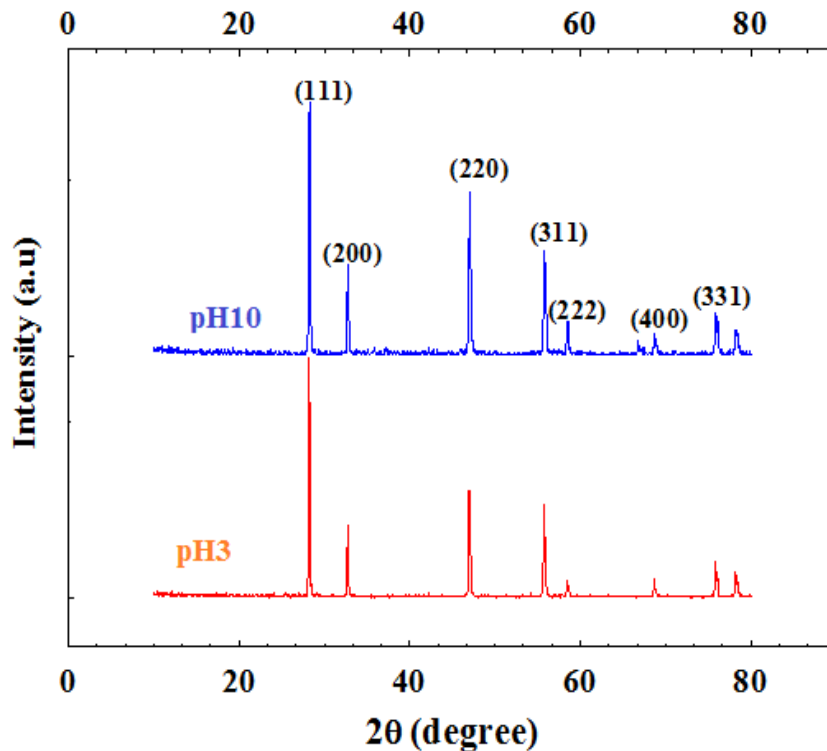
Fig. 5.3 XRD patterns of NDC25 at various pH

These results show that with increasing the pH values particle size slightly increased. Fig. 5.4 and Fig. 5.5 show the particle size distribution before and after calcinations at pH3. For pH3 it can be seen that particles with maximum particle size distribution of 11.08% with particle size of 0.389 μm and the average particle size obtained before calcination was 2.58 μm. When this powder was calcined at elevated temperature, the average particle size reduced from 2.58 μm to 0.97 μm. Fig. 5.6 and 5.7 show the powder paticle size distribution before and after calcinations at pH10. As for pH10 it can be seen that particles with maximum particle size distribution of 14.53 % with particle size of 3.905 μm and the average particle size obtained before calcination was found to be 4.214μm. When this powder was calcined at elevated temperature, the average particle size reduced from 4.214 μm to 1.1 μm.

Fig. 5.4 Particle Size distribution before calcination at pH3
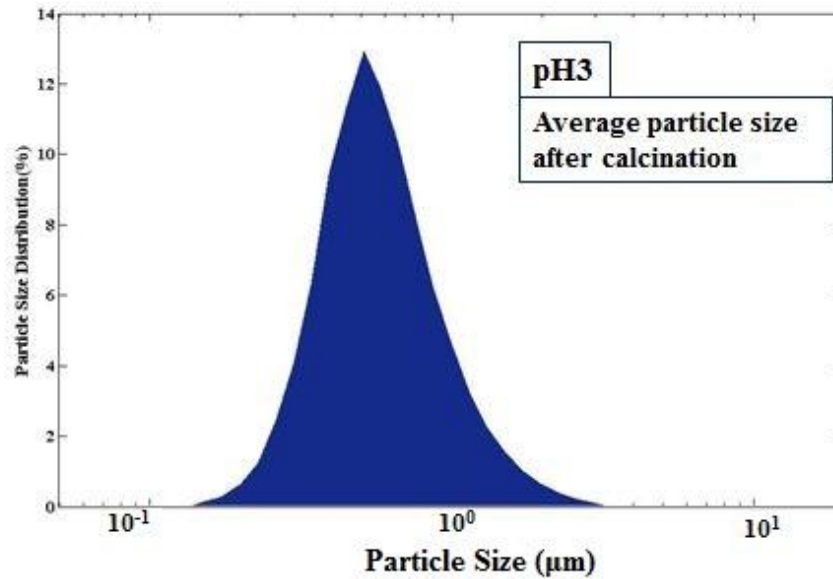
Fig. 5.5 Particle size distribution after calcination at pH3
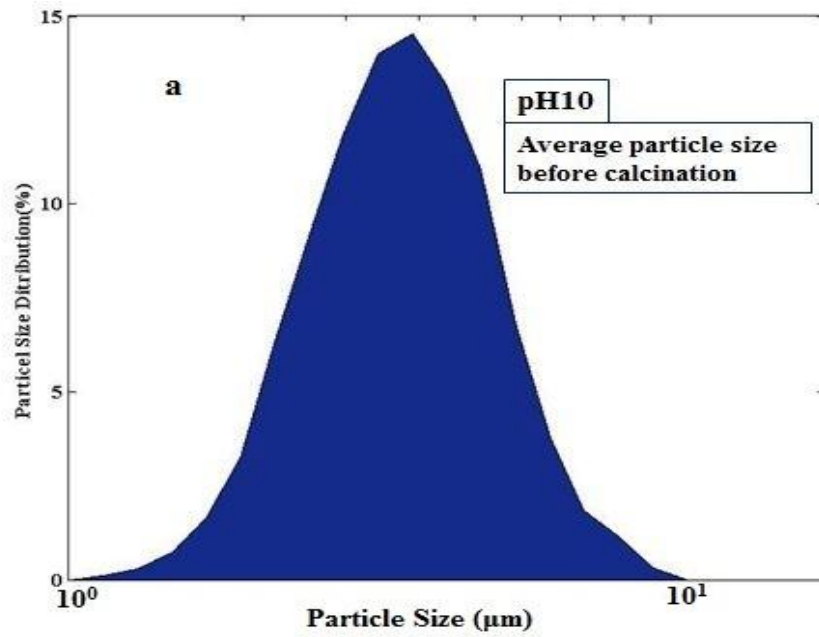
Fig. 5.6 Particle size distribution before calcination
at pH10
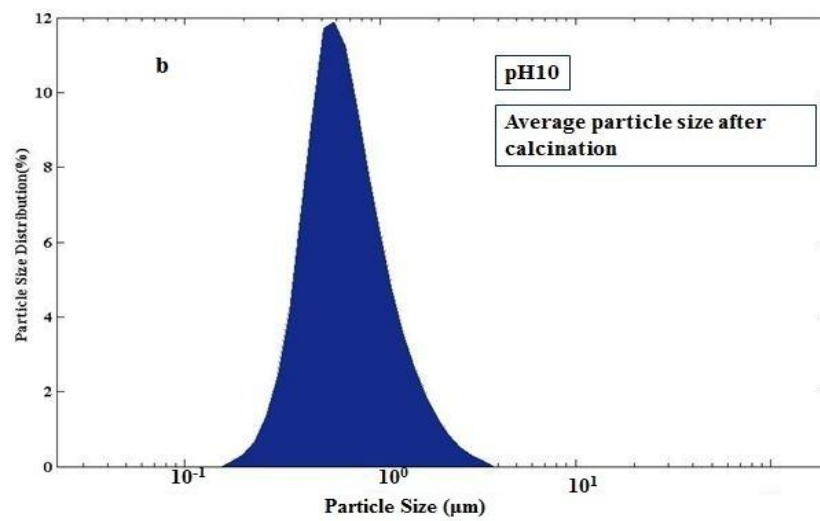
Fig. 5.7 Particle size distribution after calcination at pH10

5.4 Effects of Co-Doping

5.4.1 XRD analysis of NDC25, NYDC and SNDC

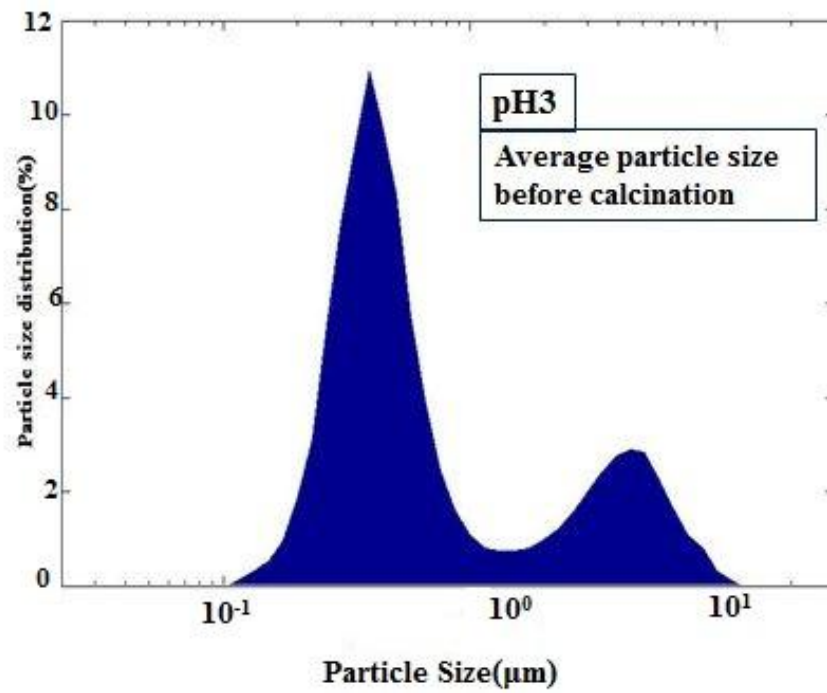Fig. 5.8 shows the XRD patterns of NDC25, NYDC and SNDC respectively. It is evident from these patterns that all the samples are free from impurities. It was also noticed that addition of Y and Sm did not affect the cubic fluorite structure of NDC. However, Co-doping reduced the crystallite size. This could have happened due to the heterogeneous nucleation due to the addition of co-dopants. Change in lattice parameter and lattice strain was found to be 0.01. All these results are summarized in Table 5.3. Broader peaks obtained for NYDC and SNDC which is an indication that the crystallites formed using Yttrium and Samarium were smaller in size [11]. This was also confirmed by analyzing these X-ray diffraction peaks using FWHM values of corresponding higher intensity peaks of all the samples.

Fig. 5.8 XRD patterns of NDC25, NYDC and SNDC

Table 5.3: Combined XRD results of NDC25, NYDC and SNDC

Composition	Lattice Parameter(Å)	Lattice Strain (%)	Crystallite size(nm)
NDC25	5.47	0.06	41
NYDC	5.47	0.06	13
SNDC	5.46	0.05	15

5.4.2 Effect of Co-Doping on Conductivity

Fig. 5.9 shows the Dc conductivity curves of NDC25, NYDC and SNDC respectively ranging from 200 to 700^0C. At low temperature the value of NYDC was found to be low as compared to pure NDC25. One of the reasons for this low conductivity can be related to higher association enthalpy that results into high activation energy for NYDC. But as the temperature increased from 550^0C, the conductivity of NYDC also increased and finally the value reached to 1.26×10^{-4} S/cm at 700^0C and for SNDC, the conductivity value reached up-to 1.69×10^{-4} S/cm. These results proved that Sm is better co-dopant as compared to Y for NDC based electrolytes [13,14]. Increase in the mobility of ions is caused by smaller mismatch in host and dopant ionic radius and smaller value of lattice strain [15].
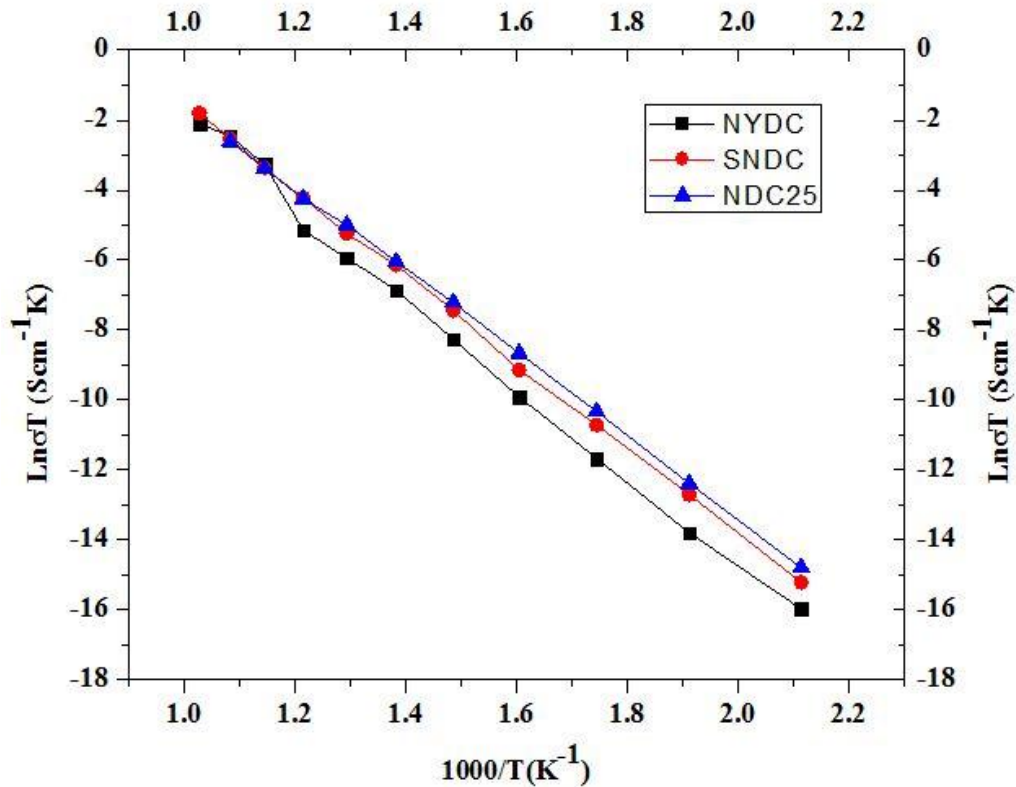
Fig. 5.9 DC conductivity graph of NDC25, NYDC and SNDC

5.5 Effects of Carbonates

5.5.1 XRD Results of NDC25, KNDC10 and KNDC20

In order to study the effects of carbonates addition on structure of NDC25, XRD analysis were carried out. Fig. 5.10 shows the results obtained from XRD analysis.

These diffractograms showed that carbonates did not alter the structure of NDC25. No new phases were observed during XRD analysis however, the peaks were broad as compared to pure NDC25. Heterogeneous nucleation occurred with the addition of carbonates and in the result, the crystallite size was also reduced making the peaks more broad. It is evident from Table 5.4, that increasing the carbonates from 0.1 to 0.2 the crystallite size also reduced. The change in lattice strain was not so much that means that carbonates did not bring any specific change in the structure of NDC25. Here the inclusion with carbonates did not appear in XRD peaks because of the amorphous nature of K_2CO_3 [7–10]. To confirm the presence of carbonates, SEM/EDS analysis was carried out.
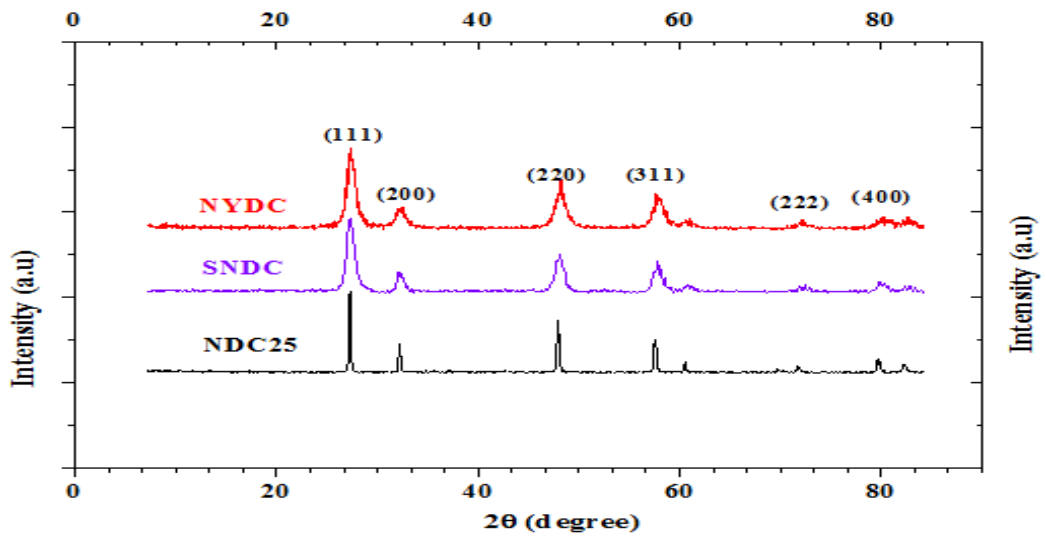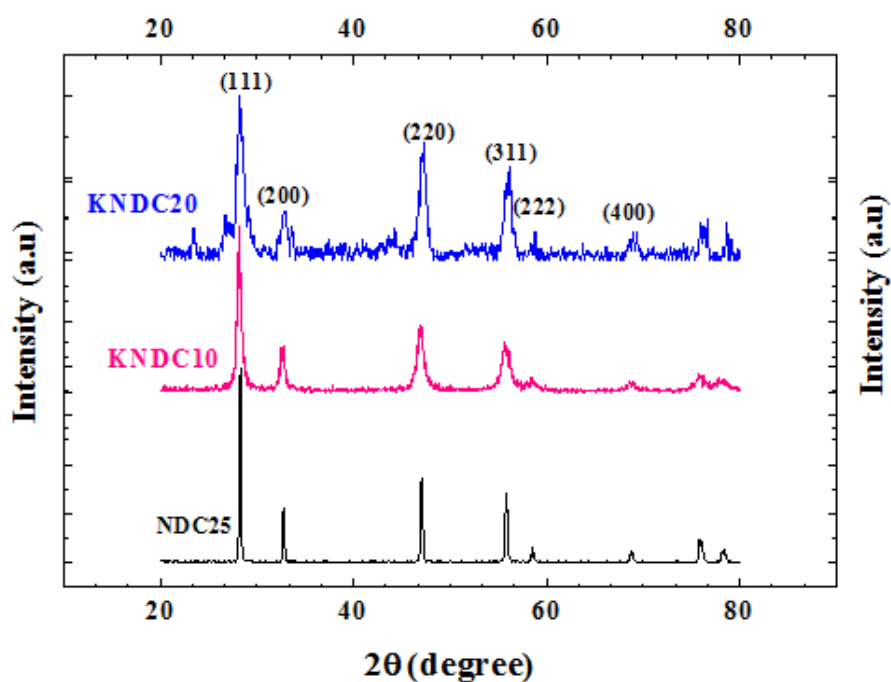

Fig. 5.10 XRD patters of NDC25, KNDC10 and KNDC20

Table 5.4: Combined XRD results of NDC25, KNDC10 and KNDC20

Composition	Lattice Parameter(Å)	Lattice Strain (%)	Crystallite size(nm)
NDC25	5.47	0.06	41
KNDC10	5.48	0.06	15
KNDC20	5.46	0.05	13

5.5.2 SEM and EDS results of KNDC10 and KNDC20

Scanning electron microscope was used to further analyze the morphology of prepared carbonate composite electrolyte materials.

Fig. 5.11 and 5.12 show clearly that the particles are well dispersed and homogeneous. Both the powders have homogeneous phase with uniform grain sizes that contributed into better ionic conductivity. It can also be observed that the addition of carbonates have also improved the densification. The small grains may have contributed into better densification and lowering the sintering temperature of NDC25. Therefore, if the desired microstructure can be formed, the maximum value of conductivity can be achieved. As the carbonates did not appear in the XRD patterns therefore, energy dispersive spectroscopy (EDS) was performed to confirm the presence of carbonates in the sample of KNDC10 and KNDC20. EDS analysis of KNDC10 and KNDC20 was performed to ensure the presence of carbonates as they were not detected in XRD peaks because it is clear from the literature that they remain in amorphous phase. Fig. 5.13 and 5.14 show the EDS analysis of KNDC10 and KNDC20 respectively. EDS results revealed that carbonates were present in the sample in reasonable quantity. Their atomic percentages are given in Table 5.5. It is clear from this table that KNDC20 has more oxygen content as compared to KNDC10. This excess of 7.75% oxygen resulted into better conductivity for KNDC20. The results will be covered in section 5.6.

Fig. 5.11 SEM image of KNDC10

Fig. 5.12 SEM image of KNDC20

Fig. 5.13 EDS graph of KNDC10
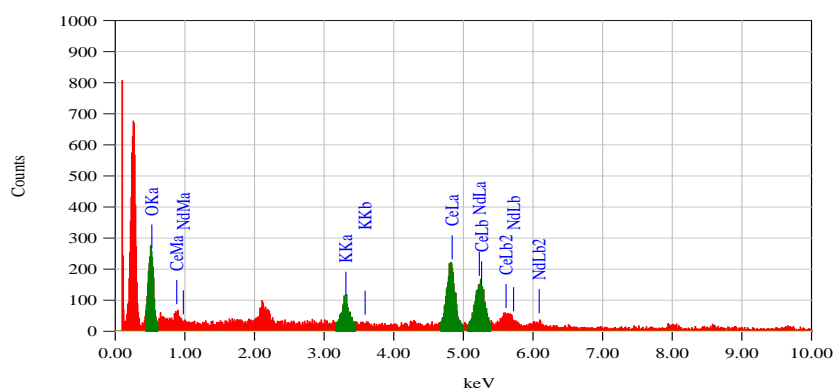
Fig. 5.14 EDS graph of KNDC20

Table 5.5: EDS results of KNDC10 and KNDC20
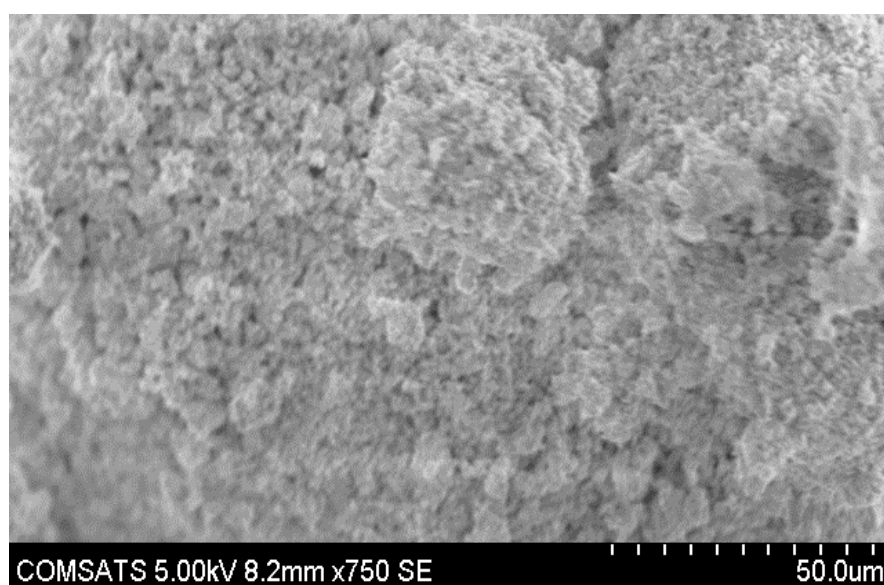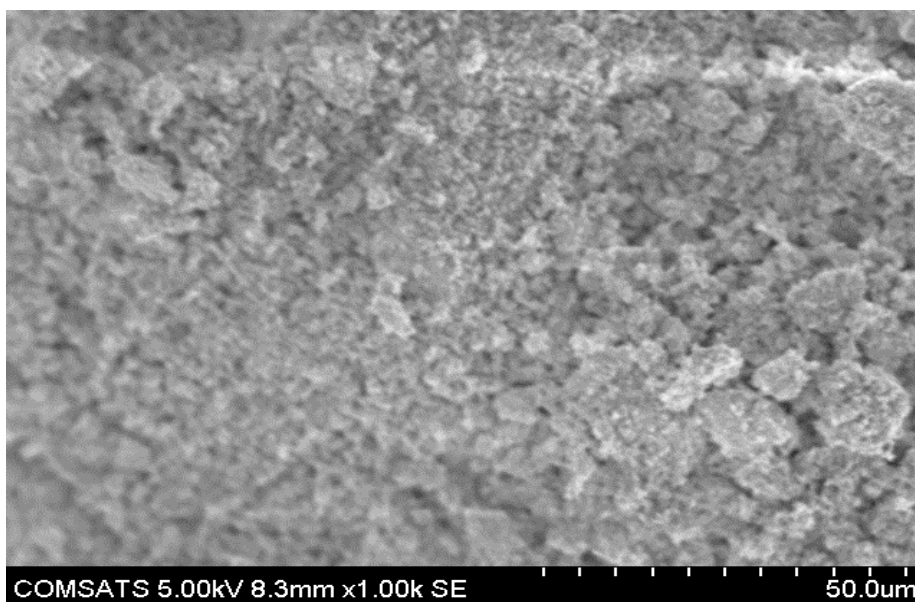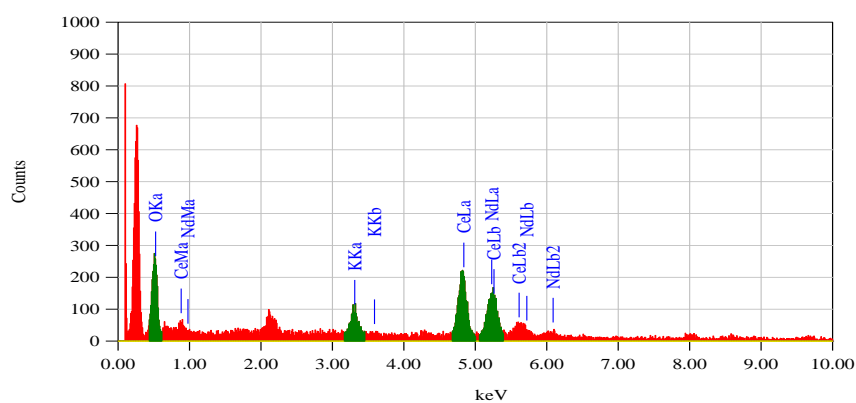
Element	Atomic %	
	KNDC10	**KNDC20**
O	67.63	75.38
K	4.82	13.32
Ce	20.11	6.43
Nd	7.44	4.87

5.5.3 Effects of Carbonates on DC conductivity

Fig. 5.15 shows the Arrhenius plots of DC electrical conductivity of NDC25, KNDC10 and KNDC20 respectively. Two probe DC conductivity method was implemented to measure the DC electrical conductivity of pellets. For this purpose, pellets with thickness of 2 mm and diameter 10mm were fabricated and their resistances were measured at different temperatures ranging from 200-700°C using WAYNEKERR 6440B LCR meter. The maximum conductivity of NDC25 at 650 °C was found to be 7.97×10^{-5} S/cm. To further improve the conductivity value of NDC25, we slightly introduced K_2CO_3. As it is clear from Table 5.4, carbonates brought very small change in lattice strain. smaller value of lattice strain also contributed in better ionic conductivity [13,15]. Reduced value of lattice strain helped to improve the ionic flow and hence increased the ionic conductivity [16]. KNDC10 and KNDC20 greatly improved the conduction properties of NDC25. The values of conductivity for KNDC10 and KNDC20 were found to be 3.46×10^{-4} S/cm and 1.05×10^{-3} S/cm respectively. These results showed that carbonates can greatly increase the conduction properties of NDC based electrolyte materials. Equations 4.1 and 4.2 were used to calculate the DC electrical conductivity of the samples. Carbonates remains in amorphous phase when slight quantity is added into doped ceria ceramics. This second phase helped to improve the conduction mechanism by making an extra layer and also contributed into introduction of disordered regions which enhance ionic conductivity [9]. Inclusion of carbonates caused multi ionic effect that greatly increased the intrinsic and extrinsic charge carriers and ultimately helped to enhance the conduction process. Carbonates increases the densification of electrolytes and improves cell efficiency [18]. Co-doping with carbonates increases the concentration of oxide ions and forms common pathways between doped ceria

and carbonates [19]. These pathways facilitate ionic flow. The ionic conductivity shows a remarkable difference between the electrolytes without inclusion of carbonates and with small addition of carbonates.
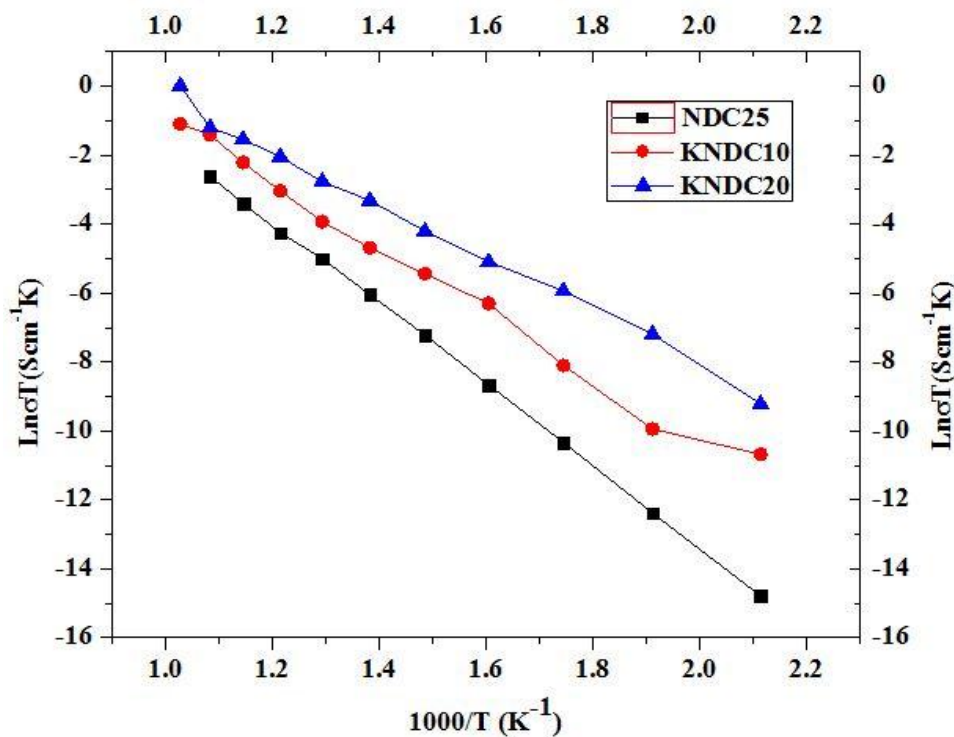
Fig. 5.15 DC electrical conductivity graph of NDC25, KNDC10 and KNDC20

In order to observe better ionic conductor, we have combined all the conductivity curves in one single graph. Fig. 5.16 shows the combined DC electrical conductivity curves of all the synthesized electrolyte materials. It is also clear from this figure that KNDC10 and KNDC20 exhibit higher ionic conductivity as compared to the other synthesized electrolytes. Table 5.6 gives information about the DC conductivity results of NDC20, NDC25, NYDC, SNDC, KNDC10 and KNDC20. This is clear from this table that addition of carbonates greatly improves the conductivity of NDC electrolyte.

5.6 Chemical stability of NDC with NiO-SDC Anode

As NDC electrolyte has recently evolved and there is not enough data available, that's why we carried out chemical stability test of NDC electrolyte material with

Nickel oxide samarium doped ceria (NiOSDC) anode to investigate whether both the compounds remain stable at elevated temperature.
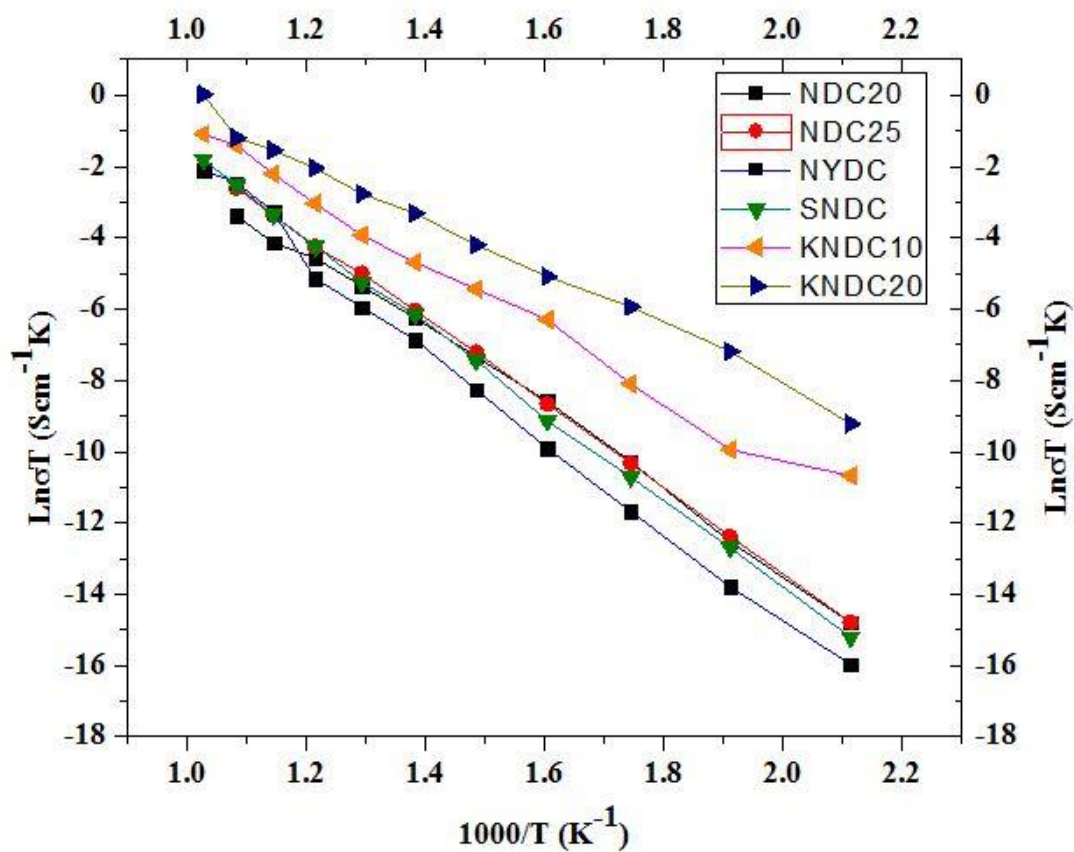
Fig. 5.16 Combined DC conductivity curves of NDC20, NDC25, NYDC, SNDC, KNDC10 and KNDC20

Table 5.6: Summary of DC Conductivity results of all synthesized electrolytes

Sample Name	DC conductivity at 700°C (S/cm)
NDC20	3.67×10^{-5}
NDC25	7.97×10^{-5}
NYDC	1.26×10^{-4}
SNDC	1.69×10^{-4}
KNDC10	3.46×10^{-4}
KNDC20	1.05×10^{-3}

The experimentation is already described in section 4.5. After mixing of both the powders, sintering was carried out at 800°C. Fig. shows the XRD analysis of prepared composite material. It is clear from the XRD pattern that both the compounds remained separate at this elevated temperature and no mixed phase was formed between them. That's why it can be depicted that both of these materials can be used in SOFC.
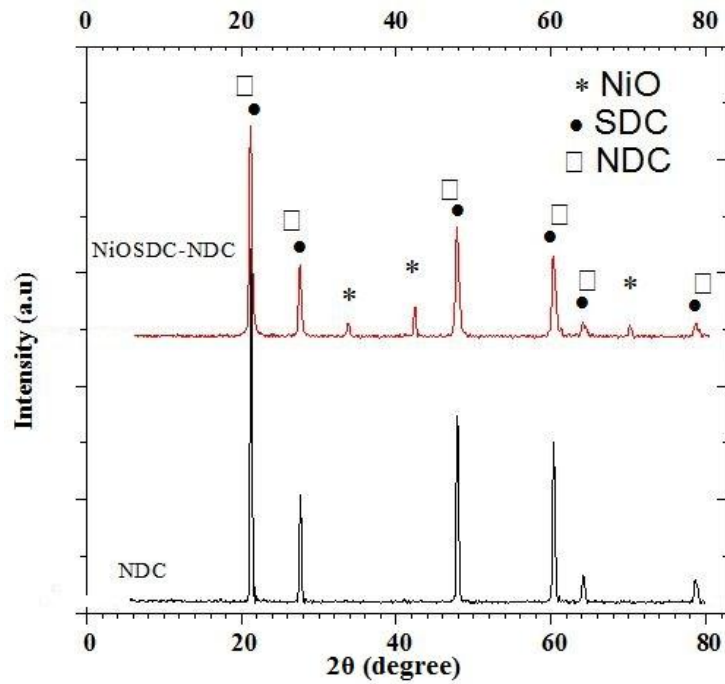
Fig. 5.17 XRD patterns of NDC25 and NiOSDC-NDC

Summary

The influence of the reaction conditions on the mechanism and kinetics of the reactions forms a key issue in understanding the structural evolution. The cross-linking between the polymer chains is much higher at high pH and high H2O: Ce ratio so that highly branched clusters are formed under these conditions, whereas more weakly branched clusters are formed at low pH. Therefore, particles were formed in both acidic and basic medium. Structural analysis was carried out after successful formation of the desired powders. XRD patterns showed that powders were free from impurities and all samples exhibited cubic fluorite structure that is highly desirable in order to get better ionic conductivity. Particle size analysis showed that particles with an average particle size of 1 μm were formed at pH10. It was depicted from the SEM analysis that spherical shaped homogeneous particles were formed using sol-gel route. Effects of co-doping were also carried out using Sm and Y as co-dopants. Conductivity results showed that Nd and Sm are best co-dopants for ceria system. Carbonates helped to improve the densification of powders with crystallite size of 13nm. Amorphous phase of carbonates form an extra layer that forms super-ionic pathways which greatly enhance the conduction properties of NDC electrolyte. DC conductivity results showed that addition of K_2CO_3 with 20% by volume increased the conductivity of pure NDC electrolyte from 7.97×10^{-5} S/cm to 1.05×10^{-3} S/cm. The sequence in the conductivity values at 700°C was found to be KNDC20>KNDC10>SNDC>YNDC>NDC25>NDC20

References

[1]   S. (Rob) Hui, J. Roller, S. Yick, X. Zhang, C. Decès-Petit, Y. Xie, et al., A brief review of the ionic conductivity enhancement for selected oxide electrolytes, J. Power Sources. 172 (2007) 493–502.

[2]   C. Ion, C. Membrane, Appraisal of Ce 12y Gd y O 22y / 2 electrolytes for IT-SOFC operation at, 129 (2000) 95–110.

[3]   W. Zając, J. Molenda, Electrical conductivity of doubly doped ceria, 179 (2008) 154–158.

[4]   H. Yoshida, H. Deguchi, K. Miura, M. Horiuchi, Investigation of the relationship between the ionic conductivity and the local structures of singly and doubly doped ceria compounds using EXAFS measurement, (2001) 191–199.

[5]   Y.-P. Fu, S.-H. Chen, Preparation and characterization of neodymium-doped ceria electrolyte materials for solid oxide fuel cells, Ceram. Int. 36 (2010) 483–490.

[6]   Ceramic processing and engineering, M.A. Rahaman

[7]   X. Wang, Y. Ma, R. Raza, M. Muhammed, B. Zhu, Electrochemistry Communications Novel core − shell SDC / amorphous Na 2 CO 3 nanocomposite electrolyte for low-temperature SOFCs, 10 (2008) 1617–1620.

[8]   S.-S. Baek, N. Lee, B.-K. Kim, H. Chang, S.-J. Song, J.-Y. Park, Addition effects of erbia-stabilized bismuth oxide on ceria-based carbonate composite electrolytes for intermediate temperature-−solid oxide fuel cells, Int. J. Hydrogen Energy. 37 (2012) 16823–16834.

[9]   R. Raza, M.A. Ahmad, J. Iqbal, N. Akram, Z. Gao, S. Javed, et al., for solid oxide fuel cell, 8 (2014).

[10]   B. Zhu, R. Raza, H. Qin, L. Fan, Single-component and three-component fuel cells, J. Power Sources. 196 (2011) 6362–6365.

[11]   E. of X-ray diffraction, B.D Cullity.

[12]   P. Constants, G. Accelerationeous.

[13]   D. a Andersson, S.I. Simak, N. V Skorodumova, I. a Abrikosov, B. Johansson, Optimization of ionic conductivity in doped ceria., Proc. Natl. Acad. Sci. U. S. A. 103 (2006) 3518–21.

[14]   S. Omar, E. Wachsman, J. Nino, Higher conductivity Sm3+ and Nd3+ co-doped ceria-based electrolyte materials, Solid State Ionics. 178 (2008) 1890–1897.

[15]   S. Buyukkilic, T. Shvareva, A. Navrotsky, Enthalpies of formation and insights into defect association in ceria singly and doubly doped with neodymia and samaria, Solid State Ionics. 227 (2012) 17–22.

[16]   K.C. Anjaneya, G.P. Nayaka, J. Manjanna, G. Govindaraj, K.N. Ganesha, Studies on structural , morphological and electrical properties prepared by citrate complexation method, J. Alloys Compd. 585 (2014) 594–601.

[17]   P. Taylor, Catalytic Properties of Ceria, (2006) 37–41.

[18]   M. Benamira, a. Ringuedé, V. Albin, R.-N. Vannier, L. Hildebrandt, C. Lagergren, et al., Gadolinia-doped ceria mixed with alkali carbonates for solid oxide fuel cell applications: I. A thermal, structural and morphological insight, J. Power Sources. 196 (2011) 5546–5554.

[19]   J. Patakangas, Y. Ma, Y. Jing, P. Lund, Review and analysis of characterization methods and ionic conductivities for low-temperature solid oxide fuel cells (LT-SOFC), J. Power Sources. 263 (2014) 315–331.

Chapter 6
Conclusions and Future Recommendations

6.1 Conclusions

➢ Neodymium Doped Ceria (NDC) electrolyte materials were successfully fabricated with cubic fluorite structure using highly versatile sol-gel method using nitrate based precursors.

➢ The DC conductivity values for NDC20 and NDC25 were found to be 3.67×10^{-5} S/cm and 7.97×10^{-5} S/cm respectively. Therefore it is concluded that NDC25 is better electrolyte as compared to NDC20.

➢ pH of medium did not affect the phase or structure of NDC25. Particle size as a function of various pH values was found to be increasing with increasing pH values.

➢ DC electrical conductivity values using Y and Sm as co-dopants were found to be 1.26×10^{-4} S/cm and 1.69×10^{-4} S/cm at 700^0C respectively. This increase in conductivity was due to the smaller mismatch in ionic radii between Sm and host ions.

➢ Effects of addition of carbonates were studied on microstructure and electrical transport properties. It was found that carbonates reduced the crystallite size of NDC. However, no new phases were found. Meanwhile the DC electrical conductivity was found enhanced which may be associated with super-ionic pathways. It is concluded that increasing the K_2CO_3 concentration from 10-20% by volume in NDC25, the value of conductivity increased and reached up-to 1.05×10^{-3} S/cm.

➢ Chemical compatibility test of NDC25 electrolyte and NiO-SDC anode revealed that both the materials remained stable and did not react with each other and no new phase was found at 800^0C.

6.2 Future Recommendations

Neodymium has opened new ways to explore Doped Ceria based electrolyte materials for SOFC as there is very limited data available on NDC based electrolytes. Though we have improved the conduction properties of NDC electrolyte material but there is still a need to further improve the conductivity of Neodymium doped ceria based electrolyte material and bring down the operating temperature of SOFC. Process parameters like hydrolysis ratio, gelation and ageing time can be further investigated. As it is also clear from the literature and our results that doubly doped ceria is more ionic conductor as compared to singly doped ceria, so there is a need to find suitable rare earth based co-dopants for ceria system. Addition of K_2CO_3 greatly increased the conduction of NDC, but there is still a need to explore the impacts of carbonates with increasing the concentration and even mixed carbonates on conduction properties of NDC electrolyte.

ICSSP, University of Punjab Lahore. December 1-6, 2013

Sol-gel fabrication of novel electrolytes based on Neodymium doped Ceria for application in low temperature solid oxide fuel cells

Muhammad Akmal Rana[a], M.N Akbar[a], Mustafa Anwar[a], Kamal Mustafa[a], Sahar shakir[a], Zuhair S. khan[a*]

[a]Advanced Energy Materials and Fuel Cells Lab, Centre for Energy Systems, National University of Sciences and Technology, Islamabad, Pakistan.

Email: zskhan@ces.nust.edu.pk

ABSTRACT

Neodymium doped ceria "$Ce_{1-x}Nd_xO_{2-x/2}$" (where x was kept 0.2 & 0.25) powders were synthesized by sol-gel technique using Cerium nitrate hexahydrate and Neodymium nitrate hexahydrate as precursors. Sintering of the powdered samples were done at 1300°C and then characterized by using X-ray diffraction, optical microscope and an impedance spectroscopy. Sintering effects were studied by using optical microscope and found that particle size was increased from 6.5 μm to 10.8 μm. The crystallite size of 35.9 nm was obtained and the value of ionic conductivity at room temperature was found to be $1.19*10^{-7}$ Scm^{-1}.

Key words SOFC, Sol-gel, Doped Ceria electrolytes, XRD

1. INTRODUCTION

As one of the major type of fuel cell, Solid Oxide Fuel cells (SOFCs) are the electrochemical devices that convert chemical energy of the fuel directly into the electrical energy with prominent conversion efficiency, very low pollutant emissions and fuel flexibility [1]. Electrolytes play a very important role in the ionic conduction mechanism. Ionic conduction can be enhanced by using thin electrolytes or choosing the materials with high ionic conductivity [2]. To date Yttria Stabilized zirconia (YSZ) electrolytes are widely in use but in order to provide sufficient oxide ions conductivity they must be operated at much higher temperature (1000°C) [3]. To operate the cell at such a high temperature; offers many design concerns, material degradation and high cost of the cell which are the major hurdles in the commercialization of the fuel cells [4-5]. To lower the fabrication cost of the cell we must reduce its working temperature. To address this issue; electrolyte materials that can provide the sufficient ionic conductivity

Annexure I

ICSSP, University of Punjab Lahore. December 1-6, 2013

at intermediate range of temperature i.e. 500-800 °C are highly desired. Doped ceria is considered as one of the alternate solution for this because its activation energy for oxygen ion diffusion is less than YSZ [6]. Doped ceria electrolytes offer higher ionic conductivity as compared to conventional YSZ based electrolytes. Ionic conductivity strongly depends on type of dopant and its concentration. Introducing dopant creates point defects. It is highly desirable that crystal lattice must not be disturbed. Therefore the best dopants are those which are highly close to the size of host ions. [7]. Presently gadolinium doped ceria (GDC) and Samarium doped ceria (SDC) electrolytes are also being studied but based on ionic size the current study utilized the introduction of neodymium because its ionic size is close to the host ions of ceria.

2. EXPERIMENTAL

2.1. POWDER PREPARATION
Powders of $Ce_{1-x}Nd_xO_{2-x/2}$ (where x was kept 0.2 & 0.25) through sol-gel route were fabricated by using $Ce(NO_3)_3.6H_2O$ (Sigma Aldrich Purity 99.99%) and $Nd(NO_3)_3.6H_2O$ (Sigma Aldrich Purity 99.99%) as precursors. 1M solution of both the precursors was prepared with the desired molar ratios using distilled water as a solvent and then drop-wise addition was done with continuous stirring. Ammonia solution was used as a complexing agent as well as to control the pH up-to 7.0. Prepared gels were dried in an oven at 110°C for several hours. Sintering was done at 1300°C for 5 hours using muffle furnace with the programmed heating and cooling rate of 10°C/min and 5°C/min respectively.

2.2. CHARACTERIZATION MEASUREMENT

 X-ray powder diffractometer with computer interface (STOE Germany) with Cu Kα at λ =1.5418 Å was used to predict the crystalline phase and crystallite size. Scan angle was kept ranging from 10°- 80° with Step size 0.04/sec. Lattice parameters were calculated using six main reflections (111), (200) (220), (311), (222) and (400) with fcc cell. Lattice parameter (a) of doped ceria cubic solid was calculated using the following mathematical relations:

$$n*\lambda = 2d*\sin(\theta) \qquad (1)$$

$$a = d\sqrt{h^2 + k^2 + l^2} \qquad (2)$$

Where d is the planar spacing, θ is the diffraction angle and h, k, l are the corresponding peak miller indices values. The crystallite size was calculated using Scherer formula and was calibrated using MDI Jade version 5.0 with the help of full width at half maximum of (111) plane reflection. The theoretical densities of sintered powders were calculated using following equation

$$\rho_{th} = (4M_r)/(N_A\, a^3) \qquad (3)$$

where M_r is the molecular formula mass of $Ce_{1-x}\,Nd_xO_{2-x/2}$ and N_A is the Avogadro's number with the value of $6.023*10^{23}$/mol. Conductivity of pellet was calculated using AC impedance spectroscopy using Agilent LCR meter by applying 1V signal with varying the frequency range of 100Hz to 5MHz.

2.3. Pellet formation

Sintered powders were ground utilizing pestle with mortar. Pellets with 13mm diameter and 3mm thickness were formed using hydraulic press under pressure of $4.88kg/cm^2$ for 5 minutes.

3. RESULTS AND DISCUSSION

Fig. 1 shows the XRD patterns of Neodymium doped Ceria ceramics sintered at 1300°C and after analyzing the obtained peaks in MDI- Jade version 5.0, which clearly showed that the synthesized powders were of cubic fluorite structure with space group of Fm3m (JCPDS powder diffraction files No. 075-0153 for $Ce_{0.8}\,Nd_{0.2}O_{1.9}$ and 028-0266 for $Ce_{0.75}\,Nd_{0.25}O_{1.875}$). No secondary phases were observed and the material was free from impurities. Decreasing trend in the inter-planar spacing was observed with decrease in the dopant concentration which can be observed by comparing the peaks obtained from XRD plots. By analyzing the peaks at x=0.2 and 0.25, it is clear that peaks shifted towards the lower value of 2θ which is the indication of increase in the inter-planar spacing value.

Annexure I

ICSSP, University of Punjab Lahore. December 1-6, 2013
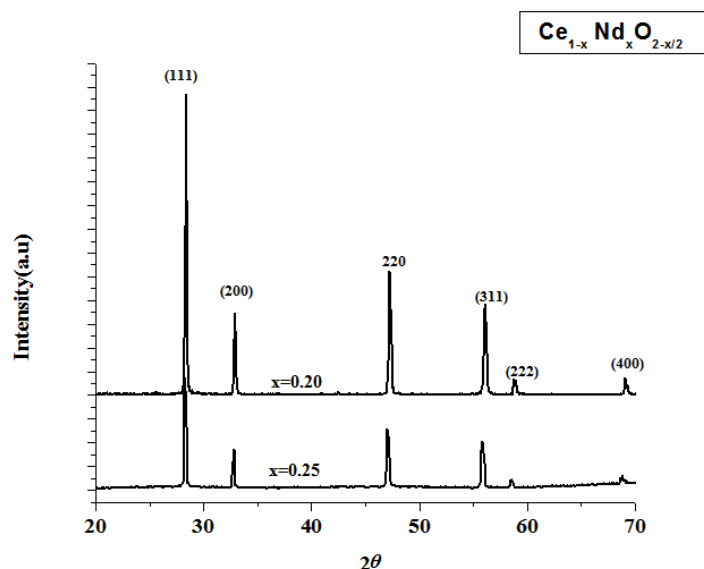
Figure 1: XRD pattern of NDC Sintered at 1300^0C

Table 1 shows the dopant concentration effects on lattice parameters and the crystallite size. Crystallite size reduced with increasing neodymium content. A difference of 0.02 Å can be seen between the lattice parameters at these two different concentrations. Also, it obeys Vegard's rule [8].

Table:1 Effects of dopant concentration on lattice parameters and the crystallite size

Composition	Lattice parameter(Å)	Theoretical density(g/cm^3)	Crystallite size(nm)
0.2	5.44	6.38	44.3
0.25	5.46	6.97	35.9

Fig. 2 shows the optical microscope images of before and after sintering of powder. The agglomerates of powder particles before sintering showed that some moisture is incorporated with them but after the heat treatment at 1300°C, no accumulation of particles was observed. The powder particle size was 6.5 μm before sinter and it increased to 10.8 μm after sintering.
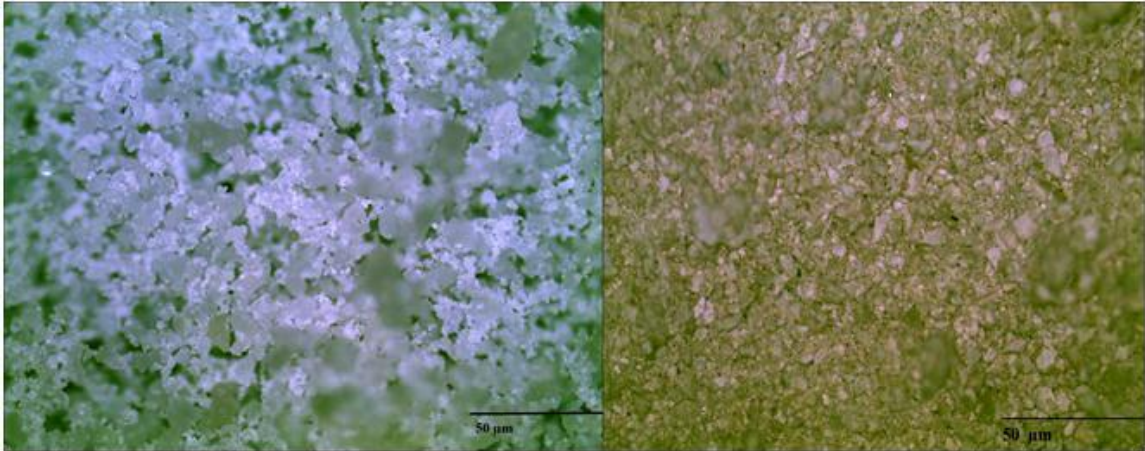
Figure 2: Sintering Effects on powder particle Size

Fig. 3 indicates the ionic conductivity curve in response to 1V signal at varying frequency range. It was observed that in start impedance value was very high but as frequency increased the impedance started to decrease and conductivity increased and maximum conductivity measured at 4.25 MHz with the value of $1.19*10^{-7}$ Scm^{-1} at room temperature.

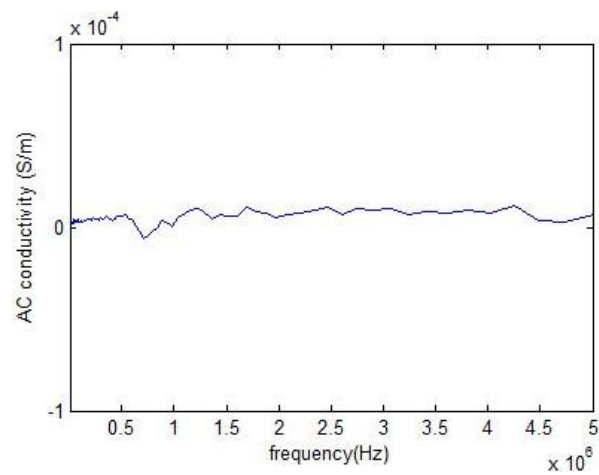Figure3: AC conductivity Vs. Voltage frequency

Annexure I

ICSSP, University of Punjab Lahore. December 1-6, 2013

CONCLUSION

Promising results were obtained by using sol-gel route and at the sintering temperature of 1300°C. Crystallite size is reduced with the increase in the dopant concentration. Ionic conductivity was measured for both of the synthesized powders and it was found that $Ce_{0.75}Nd_{0.25}O_{1.875}$ has high conductivity at room temperature. Further studies will include optimizing the dopant concentration, decrease in the crystallite size and the measurement of the ionic conductivity at elevated temperatures, which may result in even better performance.

References:

[1] Ryan O'Hayre, Suk-Won Cha, Whitney Colella, Fritz

 B. Prinz (2009) Fuel Cell Fundamentals California

[2] Qiu-An Huang, Rob Hui Bingwen et al (2007)

Electrochim. Acta. 52 8144–8164.

[3]] Hideaki Inaba et al (1996) Solid State Ionics. 83

1- 16

[4] Xin-Tai Su, Qing-Zhi Yan et al (2006) Solid State

Ionics.177.11: 1041-1045.

[5] Xin-Tai Su, Qing-Zhi Yan et al (2006) Solid State Ionics. 177.11: 1041-1045

[6] Wei Liu, Yanyi Liu et al (2010) Composite Science and technology. 70.1 181-185

[7] Ryan O'Hayre, Suk-Won Cha, Whitney Colella, Fritz

B. Prinz (2009) Fuel Cell Fundamentals California

[8] Yen-Pei Fu et al (2010) Ceramics. International.362 483-49

Investigations on doped Ceria electrolytes and their structural and electrical properties for applications in low temperature solid oxide fuel cells

Muhammad Akmal Rana[a], M.N Akbar[a], Mustafa Anwar[a], Kamal Mustafa[a], Sehar Shakir [a] Zuhair S. Khan[a]*

[a]Advanced Energy Materials and Fuel Cells Lab, Centre for Energy Systems, National University of Sciences and Technology, Sector H-12 Islamabad 44000, Pakistan.
e-mail: zskhan@ces.nust.edu.pk

As one of the clean and efficient energy conversion devices, Solid Oxide fuel cells (SOFCs) have attracted much of the attention during last few years. Electrolyte is one of the most important parts of SOFCs. Electrolytes made up of Yttria stabilized zirconia (YSZ) are currently in use but due to their high operating temperature various challenges occur in operating the cell smoothly. Tremendous studies have been made to improve the efficiency of electrolytes and reduce their operating temperature. Doped Ceria electrolytes are now being focused due to their better ionic conductivity at low temperature. Electrolytes based on Gadolinium doped ceria (GDC), Samarium doped ceria (SDC) have been extensively studied using different synthesis routes. Sol-gel method was applied to synthesize neodymium doped ceria (NDC) with general formula of $Ce_{1-x} Nd_x O_{2-x/2}$ (x represents the dopant concentration). Powders with two compositions, NDC20(x=0.2) and NDC25(x =0.25) were fabricated using nitrate based precursors and ammonia solution used as a complexing agent. Results based on X-Ray Diffraction (XRD) and Scanning Electron Microscope (SEM) showed that highly pure material was synthesized with cubic fluorite structure with spherical shaped powder particles. Structural changes in doped ceria such as lattice strain of 0.02 Å is being reported by varying the concentrations of dopant. Effects of pH on powder particle size were also studied and at pH10 average powder particle size of 0.17μm to 3.41μm was achieved. DC conductivity results showed that NDC25 is a better ionic conductor as compared to NDC20 at various temperatures ranging from 200 °C – 650 °C.

Keywords: SOFC, Sol-gel, Doped Ceria, Conductivity, Lattice strain, XRD

1. Introduction

Solid oxide fuel cells (SOFCs) are attractive because they are clean, energy efficient and almost nonpolluting. Among the other fuel cell types, SOFCs are considered best candidates for large scale power production applications [1]. Electrolyte is considered one of the most important parts of SOFC because it allows oxide ions to pass and reach at anode to complete the electrochemical reaction. YZS is conventionally available electrolyte material that offers better ionic conductivity but it works more effectively at high temperature i.e., 1000°C that arises some serious issues regarding selection of costly gaskets and inter-connects materials to operate the cell at such a high temperature [2]. Aiming to lower the operating temperature of the cell various oxide ion conductors were developed[3]. Doped ceria is considered a potential candidate in this regard as it provides the same ionic conduction at lower temperature [4]. Pure ceria is poor ionic conductor but its conductivity can be greatly enhanced by doping it with some trivalent atoms [5]. To increase the transport properties of the ceria various combinations of materials have been studied like Yttria doped ceria (YDC) [6–9], Gadolinium doped Ceria (GDC)[10–19], Samarium Doped Ceria (SDC) [3,15,18,20–22] and Neodymium doped Ceria (NDC) [5,7,18,23–29]. The main focus in developing new solid electrolyte materials is to improve the oxide ions conductivity. Conduction mechanism in doped ceria depends on several complex factors like dopant ion and its concentration, lattice parameters, oxide ion vacancy concentration and association enthalpy between dopant and oxide ion vacancy [5]. Increasing the dopant ions increases the conductivity but there is an upper limit of dopant addition above which the conductivity drops because defects star to interact with each other [1]. In this present work, effects of Neodymium contents were studied along with little inclusion of K_2CO_3 as a function of conductivity. Sol-gel method was used to develop powder with spherical shaped particles in nanometric scale. Structural changes like lattice strain also studied.

2. Experimentation

Sol-gel method was applied to fabricate powders of $Ce_{1-x}Nd_xO_{2-x/2}$ (x=0.2 & 0.25) using $Ce(NO_3)_3.6H_2O$ and $Nd(NO_3)_3.6H_2O$ as starting materials. sols of both the precursors were prepared in separate beakers with the desired molar ratios using distilled water as solvent and then drop-wise addition of dopant sol was done with continuous stirring. Ammonia solution was used as a complexing agent as well as to control the pH. Prepared gels were dried in an oven at 110°C for several hours. Sintering was done at 1300°C for 5 hours using box furnace. Samples with K_2CO_3 inclusion were also prepared via already described sol-gel route. Three main compositions were prepared by adding potassium carbonate solution into NDC25 with 10,20 and 30% v/v named as KNDC10, KNDC20 and KNDC30. Pellets with carbonates inclusion were sintered at 700°C for 5 hours keeping in view the melting point of carbonates.

2.1 Characterization measurement

X-ray powder diffractometer with computer interface (STOE Germany) with Cu Kα at λ =1.5418 Å was used to predict the crystalline phase and purity of the powders. Scan angle was kept ranging from 10°- 80° with Step size 0.04/sec. Lattice parameters were calculated using six main reflections (111), (200) (220), (311), (222) and (400). The crystallite size was calculated using Scherer formula and was calibrated using MDI Jade version 5.0 with the help of full width at half maximum of (111) plane reflection. Morphology and size of the particles was studied using Scanning Electron Microscope and particle size analyzer.

2.2 Pellet formation and Electrical Conductivity measurement

Calcined powders were ground utilizing pestle with mortar. Pellets with 10mm diameter and 2mm thickness were formed using hydraulic press under pressure of 4.88kg/cm^2 for 10 minutes. Pellets were then sintered at 1300°C for 5 hours in a muffle furnace. Conductivity of pellets was calculated using two probe method with the help of Wayne Kerr 6440B LCR meter.

3. Results and Discussions

Fig. 1 shows the XRD patterns of NDC20 and NDC25. It can be seen clearly that synthesized powders were free from impurities. Both the samples exhibited cubic fluorite structure. It can also be noticed that the peaks shifted towards the lower value of 2θ when dopant concentration increased from 0.2 to 0.25. This effect of dopant concentration was later confirmed by analyzing the larger value of inter-planar spacing "d" for NDC25 as compared to NDC20.
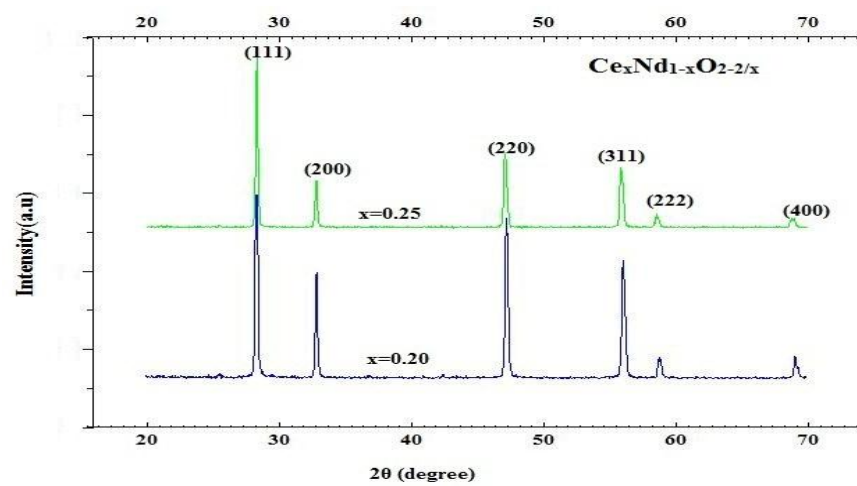
Fig. 1 XRD patterns of $Ce_xNd_{1-x}O_{2-2/x}$ at various compositions of dopant

Table 1 shows the lattice parameters, volumetric strain, theoretical density and crystallite sizes of NDC20 and NDC25. It can be seen that with increase in dopant concentration the lattice parameters were also increased which follows the Vegard's rule[5]. Theoretical density was also increased by increasing the concentration of neodymium from 20% to 25% showing that the grain density increases with addition of small amount of Neodymium that helps in lowering the sintering temperature as well increases the densification process. Fig.2 shows the XRD patterns of KNDC10, KNDC20 and KNDC30. Here the inclusion with carbonates did not appear in XRD peaks because of the amorphous nature of $K_2CO_3.$

Table 1 Results obtained from XRD analysis

Composition	Lattice Parameter(Å)	Lattice Strain (%)	Crystallite size(nm)
NDC20	5.44	0.05	53
NDC25	5.47	0.06	41

Scanning electron microscope was used to further analyze the morphology of prepared powders. Fig. 2 shows clearly that the particles are well dispersed and homogeneous with spherical shape. This shape is highly desirable in sol-gel processing to improve the sintering mechanism.
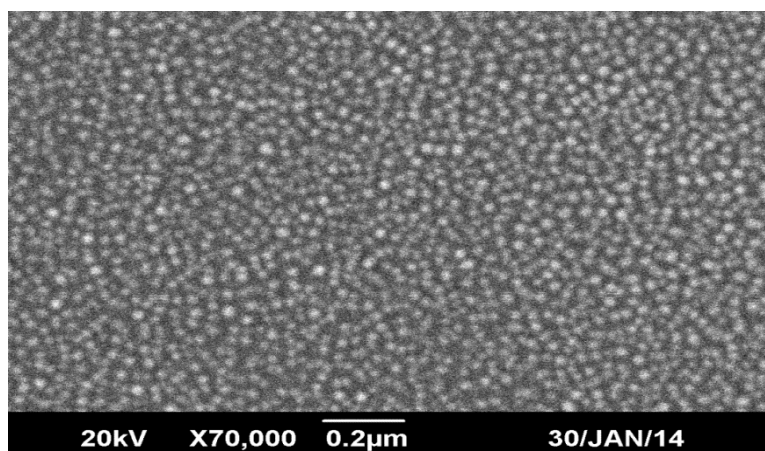
Fig. 2 SEM Image showing the morphology of particles

Changes in size of prepared powder particles were observed using HORIBA Particle size analyzer. Fig.3 shows a comparison of powder particle sizes before and after calcination. It is clear from the figure 3a that average particles ranging from 1.15 to 10.09 μm were formed with maximum particle size distribution of 14.5% at 3.91 μm before calcination. Average particle size ranging from 0.17-3.41 μm obtained after calcination. This reduction in particle size occurred due to the removal of nitrates from the particles.
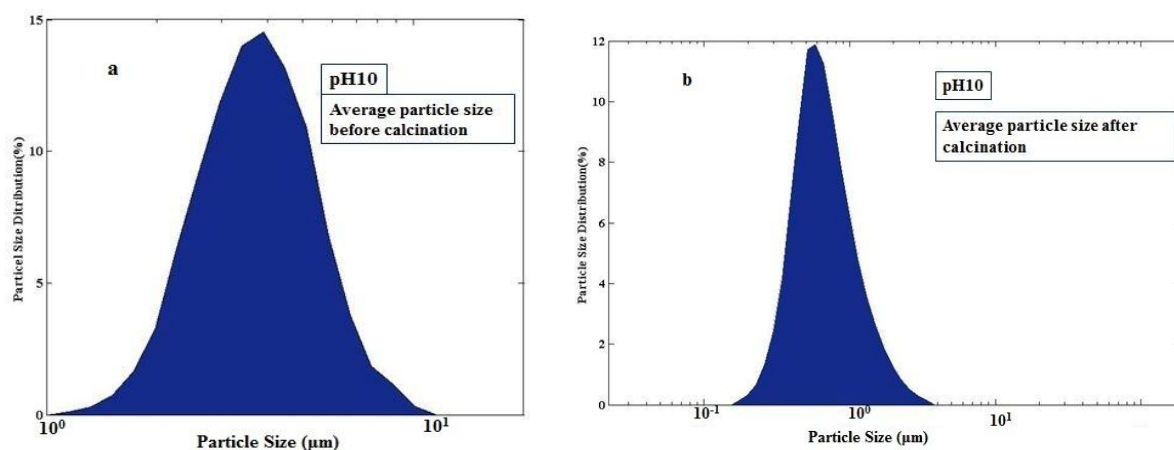
Fig. 3 Particle Size distribution before and after calcination at pH10

Two probe method was implemented to measure the DC electrical conductivity of pellets. For this purpose, pellets of thickness 2 mm and diameter 10mm were fabricated and their resistances were measured at different temperatures ranging from 20-650 °C using WAYNEKERR LCR meter.   Fig.4 clearly shows the difference in conductivity curves of NDC20 and NDC25. The maximum conductivity of NDC20 at 650 °C reached up-to a value of $3.67*10^{-5}$ S/cm and for NDC25 the maximum conductivity at this temperature was found to be $7.97*10^{-5}$ S/cm. The difference in these values may be affected mainly due to the changes in dopant concentration and increase in lattice strain. The more the lattice strain there will be more space for oxide ions to pass with less resistance.

Fig.4 Conductivity of NDC20 and NDC25

4. Conclusions

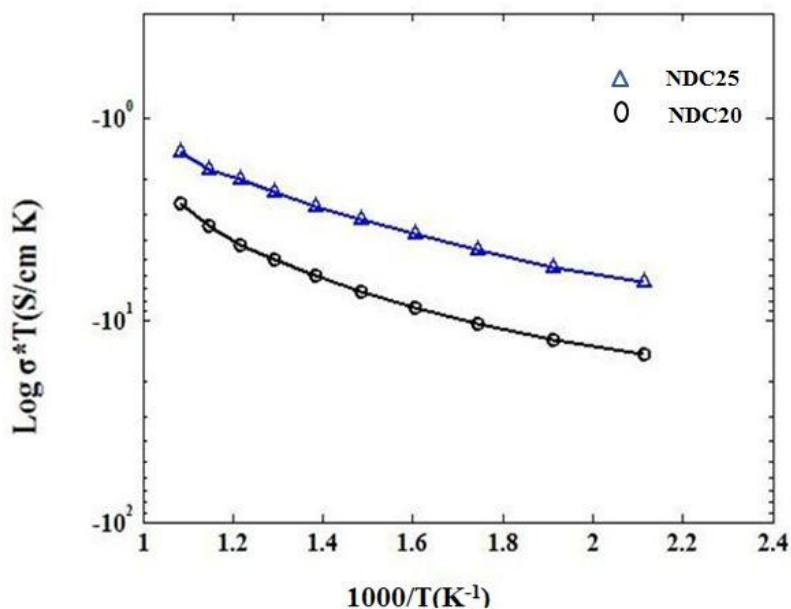Promising results were obtained using sol-gel route. Spherical shaped particles ranging from 0.17-3.14 μm were formed successfully using nitrate based precursors. XRD analysis showed that both the synthesized materials exhibited cubic fluorite structure. DC conductivity was measured for both of the synthesized powders and it was found that NDC25 has high conductivity at 650°C with a value of $7.97*10^{-5}$ S/cm. we recommend that NDC25 may be a better ionic conductor for low temperature solid oxide fuel cells.

References

[1]   Ryan P. O Hyre, Fuel Cell Fundamentals, John Willey & Sons, INC, 2009.

[2]   X. Wang, Y. Ma, B. Zhu, State of the art ceria-carbonate composites (3C) electrolyte for advanced low temperature ceramic fuel cells (LTCFCs), Int. J. Hydrogen Energy. 37 (2011) 19417–19425.

[3]   C.M. Lapa, F.M.L. Figueiredo, D.P.F. de Souza, L. Song, B. Zhu, F.M.B. Marques, Synthesis and characterization of composite electrolytes based on samaria-doped ceria and Na/Li carbonates, Int. J. Hydrogen Energy. 35 (2010) 2953–2957.

[4]   V. Kharton, F. Marques, a Atkinson, Transport properties of solid oxide electrolyte ceramics: a brief review, Solid State Ionics. 174 (2004) 135–149.

[5]   Y.-P. Fu, S.-H. Chen, Preparation and characterization of neodymium-doped ceria electrolyte materials for solid oxide fuel cells, Ceram. Int. 36 (2010) 483–490.

[6]   D.R. Ou, Microstructures and electrolytic properties of yttrium-doped ceria electrolytes : Dopant concentration and grain size dependences, 54 (2006) 3737–3746.

[7]   M. Kahlaoui, S. Chefi, A. Inoubli, A. Madani, C. Chefi, Synthesis and electrical properties of co-doping with La3+, Nd3+, Y3+, and Eu3+ citric acid-nitrate prepared samarium-doped ceria ceramics, Ceram. Int. 39 (2013) 3873–3879.

[8]   M. Coduri, M. Scavini, M. Allieta, M. Brunelli, C. Ferrero, I. Unit, et al., Defect Structure of Y - Doped Ceria on Different Length Scales, (2013).

[9]   T.S. Zhang, J. Ma, H.T. Huang, P. Hing, Z.T. Xia, S.H. Chan, et al., Effects of dopant concentration and aging on the electrical properties of Y-doped ceria electrolytes, 5 (2003) 1505–1511.

[10]   A. Arabac, M. Faruk, Preparation and characterization of 10 mol % Gd doped CeO 2 (GDC) electrolyte for SOFC applications, 38 (2012) 6509–6515.

[11]   L. Hildebrandt, C. Lagergren, R. Vannier, M. Cassir, Gadolinia-doped ceria mixed with alkali carbonates for SOFC applications : II e An electrochemical insight, 7 (2011).

[12]   H. Yokokawa, N. Sakai, T. Horita, K. Yamaji, M.E. Brito, E lectrolytes for Solid-Oxide Fuel Cells, 30 (2005) 591–595.

[13]   K. Muthukkumaran, P. Kuppusami, E. Mohandas, V.S. Raghunathan, IONIC CONDUCTIVITY MEASUREMENTS IN GADOLINIA DOPED CERIA, (2004).

[14]   P.N.O.Ţ. Ingher, N.P. Pogrion, INFLUENCE OF SINTERING TEMPERATURE ON THE STRUCTURAL AND ELECTRICAL PROPERTIES OF CERIA-BASED COMPOSITES, 75 (2013).

[15]   S. (Rob) Hui, J. Roller, S. Yick, X. Zhang, C. Decès-Petit, Y. Xie, et al., A brief review of the ionic conductivity enhancement for selected oxide electrolytes, J. Power Sources. 172 (2007) 493–502.

[16]   Z. Gao, Advanced Functional Materials for Intermediate-Temperature Ceramic Fuel Cells, 2011.

[17]   M. Benamira, a. Ringuedé, V. Albin, R.-N. Vannier, L. Hildebrandt, C. Lagergren, et al., Gadolinia-doped ceria mixed with alkali carbonates for solid

oxide fuel cell applications: I. A thermal, structural and morphological insight, J. Power Sources. 196 (2011) 5546–5554.

[18]   Recent advances in high temperature electrolysis using solid oxide fuel cells : A review, J. Power Sources. 203 (2012) 4–16.

[19]   P.P. Dholabhai, S. Anwar, J.B. Adams, P. a Crozier, R. Sharma, Predicting the optimal dopant concentration in gadolinium doped ceria: a kinetic lattice Monte Carlo approach, Model. Simul. Mater. Sci. Eng. 20 (2012) 015004.

[20]   X. Wang, Y. Ma, R. Raza, M. Muhammed, B. Zhu, Electrochemistry Communications Novel core – shell SDC / amorphous Na 2 CO 3 nanocomposite electrolyte for low-temperature SOFCs, 10 (2008) 1617–1620.

[21]   Y. Ma, X. Wang, R. Raza, M. Muhammed, B. Zhu, Thermal stability study of SDC / Na 2 CO 3 nanocomposite electrolyte for low-temperature SOFCs, Int. J. Hydrogen Energy. 35 (2010) 2580–2585.

[22]   R. Raza, X. Wang, Y. Ma, B. Zhu, Study on calcium and samarium co-doped ceria based nanocomposite electrolytes, J. Power Sources. 195 (2010) 6491–6495.

[23]   G. Kim, N. Lee, K. Kim, B. Kim, H. Chang, S. Song, et al., Various synthesis methods of aliovalent-doped ceria and their electrical properties for intermediate temperature solid oxide electrolytes, Int. J. Hydrogen Energy. 38 (2012) 1571–1587.

[24]   Y. Zheng, H. Gu, H. Chen, L. Gao, X. Zhu, L. Guo, Effect of Sm and Mg co-doping on the properties of ceria-based electrolyte materials for IT-SOFCs, 44 (2009) 775–779.

[25]   M.A. Khan, R. Raza, R.B. Lima, M.A. Chaudhry, E. Ahmed, G. Abbas, Comparative study of the nano-composite electrolytes based on samaria-doped ceria for low temperature solid oxide fuel cells (LT-SOFCs), Int. J. Hydrogen Energy. 38 (2013) 16524–16531.

[26]   G. Zhao, D. Zhou, J. Zhu, M. Yang, J. Meng, Effect of MoO3 concentration on sintering and electrical properties of SiO2-containing neodymium-doped ceria electrolytes, Solid State Sci. 13 (2011) 1072–1075.

[27]   J.X. Zhu, D.F. Zhou, S.R. Guo, J.F. Ye, X.F. Hao, X.Q. Cao, et al., Grain boundary conductivity of high purity neodymium-doped ceria nanosystem with and without the doping of molybdenum oxide, J. Power Sources. 174 (2007) 114–123.

[28]   V. Gil, J. Tartaj, C. Moure, Chemical and thermomechanical compatibility between neodymium manganites and electrolytes based on ceria, J. Eur. Ceram. Soc. 29 (2009) 1763–1770.

[29]   İ. Uslu, A. Aytimur, M.K. Öztürk, S. Koçyiğit, Synthesis and characterization of neodymium doped ceria nanocrystalline ceramic structures, Ceram. Int. 38 (2012) 4943–4951.

[30]   L. Science, Effects of MoO 3 Amounts on Sintering and Electrical Properties of Ce 0 . 8 Nd 0 . 2 O 1 . 9, 28 (2012) 9–13.

[31]   M. Biswas, S. Bandyopadhyay, Tight binding approximation in Nd3+ doped nano ceria prepared via gel combustion method, Ceram. Int. 39 (2013) 9699–9701.

[32]   B. Choudhury, A. Choudhury, Lattice distortion and corresponding changes in optical properties of CeO 2 nanoparticles on Nd doping, Curr. Appl. Phys. 13 (2013) 217–223.

[33]   S. Omar, E. Wachsman, J. Nino, Higher conductivity Sm3+ and Nd3+ co-doped ceria-based electrolyte materials, Solid State Ionics. 178 (2008) 1890–1897.

[34]   H. Okkay, M. Bayramoğlu, M.F. Öksüzömer, Ultrasound assisted synthesis of Gd and Nd doped ceria electrolyte for solid oxide fuel cells, Ceram. Int. 39 (2013) 5219–5225.

Electrical properties of ceramic electrolyte materials based on stabilized zirconia and doped ceria for applications in solid oxide fuel cells (SOFCs): a brief review

Muhammad Akmal Rana [a], Zuhair S. Khan [a]*

[a]Advanced Energy Materials and Fuel Cells Lab, Centre for Energy Systems, National University of Sciences and Technology, Sector H-12 Islamabad 44000, Pakistan.

E-mail: zskhan@ces.nust.edu.pk

Phone: +92-51-90855276

Abstract

Electrolyte plays a vital role in ionic conduction. So far many electrolyte materials have been explored to attain better ionic conductivity in Solid oxide fuel cells. Stabilized zirconia is considered better ionic conductor but various problems like material degradation, gasket issues and thermal stability occur due to its higher operating temperature. Such drawbacks bring an opportunity to explore alternative materials that offer better ionic conductivity at low temperature. Doped ceria is considered better option in this regard. This work is concerned on the comparative analysis of various electrolytes based on conventional stabilized zirconia and rare earth doped ceria along with inclusion of alkali carbonates. The mechanism for improving conduction properties has been discussed in detail. A brief analysis of the effects of dopant concentrations, oxide ions conductivity and their electron transport properties is presented at different ranges of temperature. The compositions containing the highest ionic conductivity have been discussed briefly.

Keywords: Solid oxide fuel cells, Ionic Conductivity, Doped ceria, Sintering additives, Alkali carbonates

1. Introduction

Sustainability is the major concern in present era. Due to massive use of fossil fuels by the mankind various challenges have risen. These challenges include depletion of fossil fuel reserves as well as environmental concerns which needs to be addressed. Different renewable resources to get useful energy have been explored. Fuel cells are one of these resources which provide useful energy and create very less environmental effects by converting chemical energy of the fuel directly into electrical energy. Solid Oxide fuel cells (SOFCs) are one of the major types of fuel cells which have the potential to be

used for large scale power production applications [1] . It has three main parts; anode, cathode and electrolyte. Hydrogen based fuel enters from Anode where it gets oxidized and produces a pair of electrons and these electrons pass through an external circuit and produce useful power. Air as an oxygen source enters from cathode and is reduced. Electrolyte plays an important role in this mechanism because it helps oxygen ions to pass through solid electrolyte and reach at anode where the reaction gets completed. The completion of the reaction depends on how efficiently ions are allowed to pass through the electrolyte. To increase the transport properties of the electrolyte various combinations of materials have been studied like Yttria Stabilized Zirconia, Gadolinium doped Ceria (GDC) [2], Samarium Doped Ceria (SDC) [3], Neodymium doped Ceria (NDC) [4]. To tailor the transport properties, dopant identity and its concentration play a vital role. Herein we will highlight the effects of dopant concentration on conventional used SZ and the recently evolved electrolyte materials based on doped ceria such as gadolinium doped ceria (GDC), Samarium doped ceria (SDC) and neodymium doped ceria (NDC).

2. Stabilized Zirconia (SZ)

SZ is one of the most commonly used electrolyte material in Solid Oxide fuel cells. The cubic fluorite structure of Zirconia makes it good oxide ions conductor but it can't remain stable [5]. For this purpose, it is doped with Yttria (Y_2O_3). Inclusion with Y_2O_3 makes it stable and even more conductive [1]. By the addition of Yttria into Zirconia creates oxygen vacancies which are caused by charge compensation effects. Yttrium ions disturb the charge balance when they enter into lattice of Zirconia. By the addition of 8 mol% of dopant, 4% of oxide ions sites become vacant. Fig. 1 [1] shows the oxide ion conductivity graph with respect to concentration of dopant in ZrO_2. Conductivity value increases up to 8%, but when dopant concentration increase to a certain upper limit, conductivity starts to decrease. By further inclusion of dopant reduces the ionic conduction behavior in the electrolyte as the defects start to interact with each other [1].
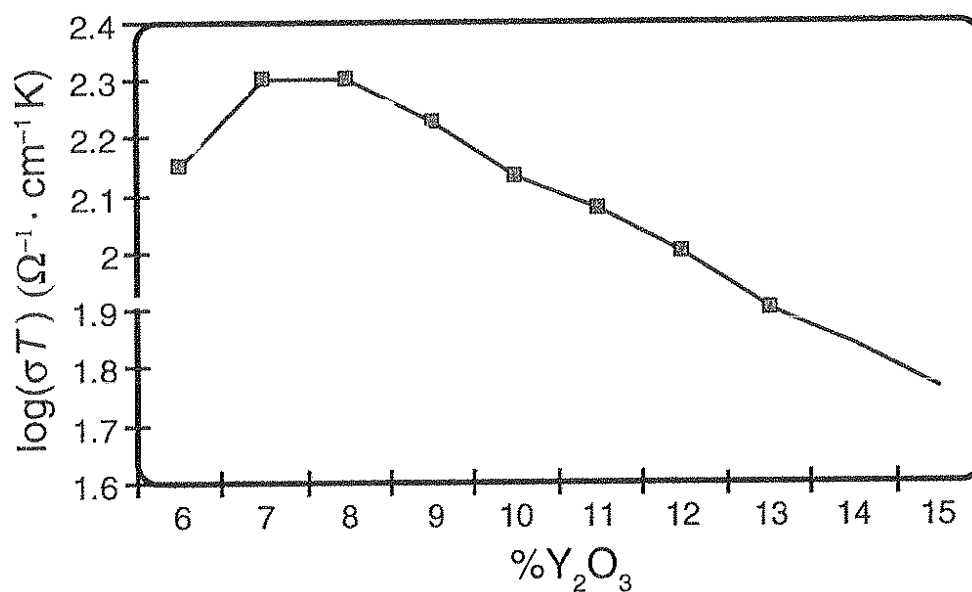
Fig. 1 Conductivity of YSZ with respect to Yttria content [1]

In addition to the fluorite structure, the effect of grain boundaries on overall behavior of ionic conductivity of the electrolyte is important. Grain boundaries offer less resistance at high temperature i.e. 1000 °C for YSZ system. Scandia stabilized zirconia (ScSz) have also been studies widely. Fig. 2 [6] shows ionic conductivity of 8mol% YSZ and 10mol% ScSZ. This comparison graph clearly shows that ScSZ offers better ionic conduction than conventional YSZ. The 10mol% ScSZ offers less grain boundary resistance as compared to YSZ at low temperature which finally improves the ionic conduction mechanism at high temperature. Also the better ionic conductivity is mainly due to the minimum mismatch between the ionic sizes of host and the dopant ions which is less in ScSZ with respect to YSZ [5, 6].

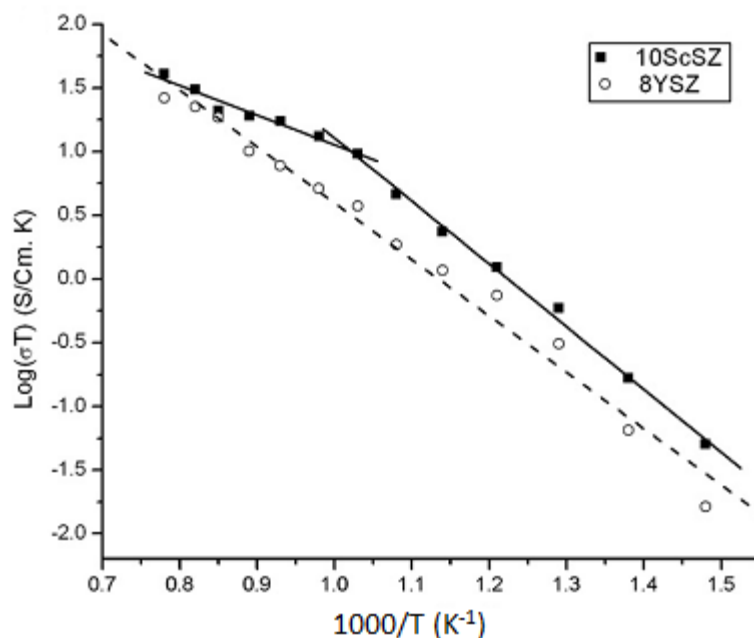Submitted in Journal of Fuel Cell Science and Technology

Fig. 2 Conductivity of YSZ and ScSZ [6]

Association of defects can also cause traps for vacancies which directly influence ions not to flow easily [6]. Defects ordering can be minimized by selecting dopants with closer ionic sizes to that of host ions [7]. One major issue with ScSZ system is that at higher dopant concentration more than 10mol%, the more conductive cubic phase transforms into less conductive rhombohedral phase at low operating temperature. This phase change can be eliminated by keeping the Sc content up-to 8mol% or inclusion with other oxides like bismuth and oxides [8]. As the temperature decreases the grain boundary resistance increases and impedes ionic flow which makes YSZ based electrolyte only suitable for high temperature applications. Conductivities of other dopants in SZ were also studied and ytterbium showed comparable results to ScSZ. Alumina on the other hand is used to improve the mechanical properties and it also affects the conductivity of YSZ depending on the doping level. Improvement effect is attributed to alumina scavenging silica [9]. The effects which cause alumina to reduce the conductivity are considered due to increase in defects association. Alumina forms a three phase boundary which increases Schottky defects and contributes into more grain boundary resistance [10]. Niobium contents also increased grain boundary resistance and hence reduced conductivity by defects association [11].

Doped ceria electrolytes offer more ionic conductivity than SZ at low temperature range. Operating the cell at such a high temperature causes many disorders in cell components. These challenges bring need to find new materials which are better ionic conductors as well as they can operate at low to intermediate temperature range. Ceria based electrolytes fulfills all these requirements.

3. Doped Ceria Electrolytes

Ceria has opened new ways to improve the ionic conductivity at low temperature range as compared with YSZ. The value of ionic conductivities for doped ceria at 750 °C is same for YSZ at 1000°C. Like zirconia ceria also exhibit cubic fluorite structure which has made this material more suitable in applications in low temperature Solid oxide fuel cells (SOFCs) [12]. Pure ceria is a poor ion conductor, for this reason it is doped with some trivalent ion which introduces charge compensation and enhances the oxide ions conduction [13]. Doped ceria electrolytes have been successfully synthesized and proven electrolyte materials for SOFCs applications with general formula of $Ce_{1-x}M_xO_{2-x/2}$ (where M= Gd, Sm and Nd, Er, Dy and Y etc.) and x represents the dopant concentration. Gadolinium doped ceria (GDC) [14,15,16,17,18,19] samarium doped ceria(SDC) [20,21,22,23,24,25] and neodymium doped ceria(NDC) [4,26,27,28,29,30,31] have been studied but there are upper limits 5-25mol% of all these dopants above which defects association increases and conductivity drops gradually. GDC offers higher ionic conductivity with maximum dopant concentration of 10-20mol% often abbreviated as GDC10 and GDC20 respectively. Fig. 3 [32] shows the ionic conduction of various GDC compositions, i. e., 10-20mol%. Ionic conduction mechanism depends on many factors in which grain and grain boundaries are also important parameters. Less resistance offered by grains and grain boundaries make electrolyte more suitable for ionic conduction. GDC10 has more lattice ionic conductivity with the value of 0.01S/cm at 500 °C [5,14] but GDC20 offers more total conductivity [33]. Zhang et al. divided grain boundary (gb) conduction into three regions. Fig. 4 [33] shows the effect of Gadolinium concentration on grain boundary conductivity. There is a sharp increase in conductivity in gb for gadolinium content less than 10mol%, for 10-20mol% there is no prominent change and as dopant concentration

increases from 20mol% value of gb decreases which is due to the increase in defects associations. GDC20 is considered better ionic conductor. This is due to GDC20 grain resistance is less sensitive to impurities [34].
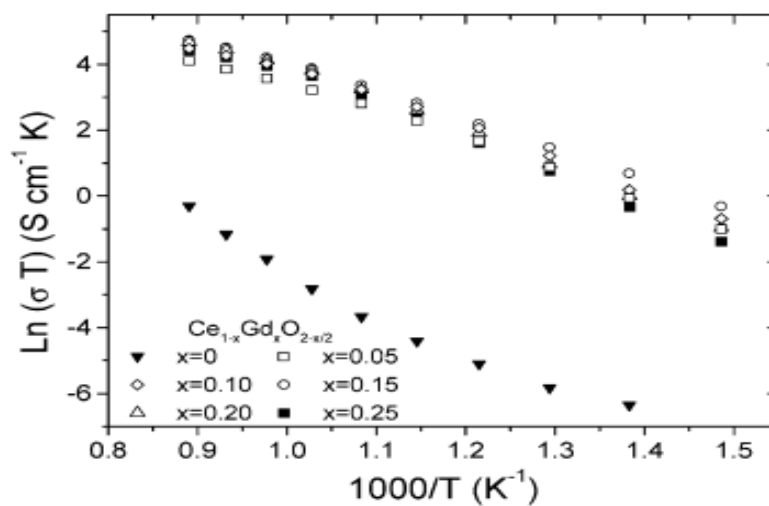

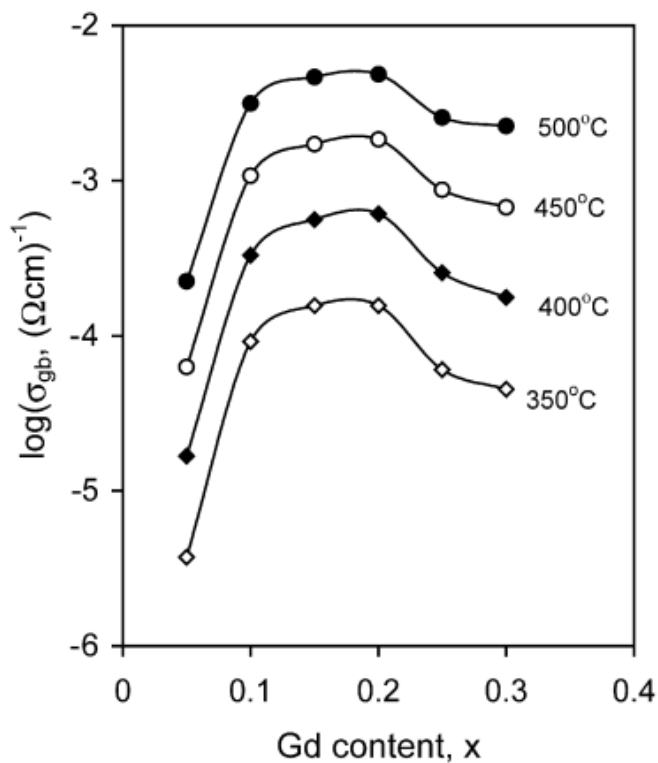Fig. 3 Conductivity of GDC at various concentrations [32]

Fig. 4 Effect of Gd content on grain boundary
conductivity[33]

The second candidate for doped ceria is samarium which is also considered good ionic conductor with promising results for SDC20(20mol% dopant) [35]. SDC20 is considered for its highest conductivity among other doped ceria electrolytes [36]. Fig. 5 [13] shows the conduction behavior of SDC with various concentrations of samarium.
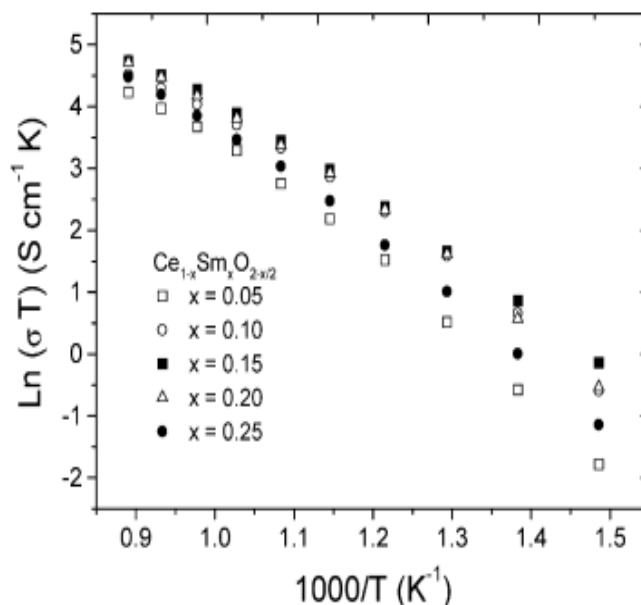

Fig. 5 Conductivity of SDC at various concentrations [13]

Fig. 6 [4] shows the ionic conductivity of Neodymium doped ceria (NDC) electrolytes ranging from 5mol% to 25mol% of neodymium as dopant. NDC exhibit higher ionic conductivity than YSZ at 800 °C which makes it suitable for SOFCs applications [26]. For NDC based electrolytes the activation energy ranges from 0.79-1.09 ev which are promising with GDC and SDC. Synthesis routes also contribute in conduction properties of electrolyte materials. Hikmet et.al [26] improved the conduction properties of NDC15 by implying ultrasound assisted co-precipitation method which are in good agreement with already reported NDC15(15mol% dopant) with slightly better results but for NDC system higher ionic conductivity is reported for NDC25(25mol% dopant) with activation energy of 0.794 ev [4].
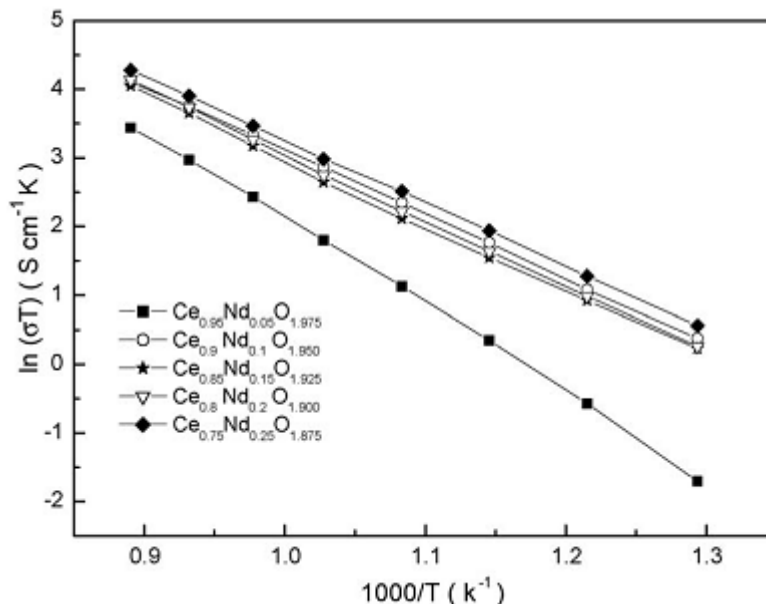
Fig.6 Conductivity of Neodymium doped ceria [4]

One of the relevant hurdle for doped ceria materials is that they need high sintering temperature for getting relative density more than 95% [27]. Addition of small amount of sintering additives improves densification at less temperature and also increases the conductivity [20-23]. Minute amount of Molybdenum oxide (MoO_3) and Tungsten oxide (WO_3) was studied for Neodymium doped ceria (NDC) system and were sintered at 1300°C [29] as compared to conventionally sintered at 1500°C [4]. Along with the increased densification the ionic conductivity of NDC electrolyte was greatly enhanced. Fig. 7 [29] shows the effect of these sintering additives on better electrical conductivity of NDC and WO_3 brought much better effects than MoO_3. This effect is due to liquid phase formed between the doped ceria additives used. SDC20 have also been studied using lithium oxide as sintering additives. Only 2mol% lithium oxide improved relative density of 99.5% only at 900 °C as compared to previously attained relative density of 88% at 1250 °C [36].To further improve the ionic conductivity mechanism of doped ceria, addition of small amounts of alkali carbonates have been incorporated in already synthesized electrolyte materials.
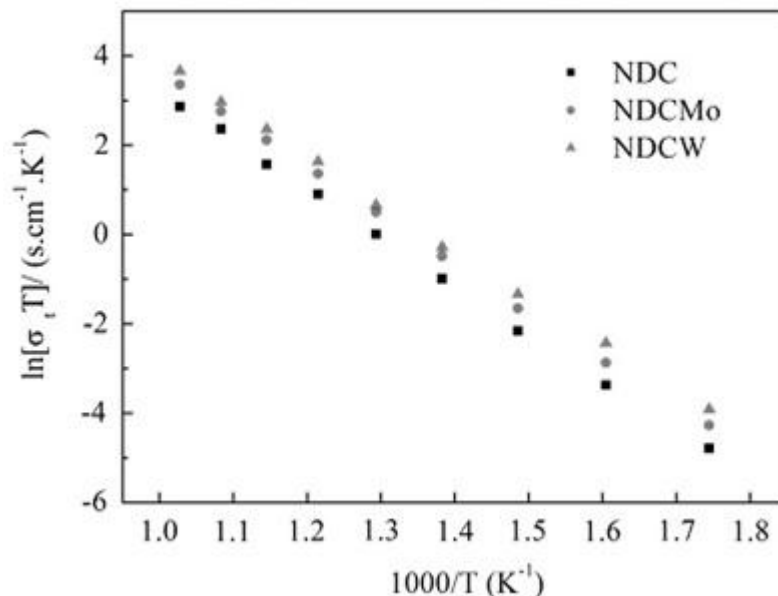
Fig. 7 Effects of sintering aids on NDC[29]

4.   Effects of Alkali Carbonates on Doped Ceria Electrolytes

To further increase the conductivity of doped Ceria electrolytes addition of small amount of alkali carbonates offers better results even at low temperatures [18-19]. Carbonates remains in amorphous phase when slight quantity is added into doped ceria ceramics. This second phase helps to improve the conduction mechanism by making an extra layer and also contributes into introduction of disordered regions which enhance ionic conductivity [38]. Inclusion of carbonates causes multi ions effect which increases the intrinsic and extrinsic charge carriers and ultimately helps to enhance the conduction process [37]. SDC when doped with alkali carbonates showed better results than pure SDC electrolytes in the range of 600°C. Addition of Na_2CO_3 into pure SDC increases the disordered patterns in SDC regions and upon increasing the temperature these irregular layers take part in increased ionic flow. Carbonates increases the densification of electrolytes and improves cell efficiency [38]. It is also stated that at increased temperature carbonates form super ionic conduction phase which promotes the ionic flow [24-25]. Sodium carbonate also resolves the problem of ceria based electrolytes which is the transformation of Ce^{+4} into Ce^{+3} [38]. Co-doping with carbonates increases the concentration of oxide ions and forms common pathways between doped ceria and carbonates. These pathways facilitate ionic flow. The ionic conductivity shows a

remarkable difference between the electrolytes without inclusion of carbonates and with small addition of carbonates [39].

5. Summary and Conclusions

YSZ and Doped Ceria offer better ionic conductivity among the various electrolytes for solid oxide fuel cells. YSZ exhibits better conductivity at 1000 °C but Doped Ceria electrolytes like GDC, SDC and NDC offer same ionic conductivity at much lower temperature as compared to conventionally used YSZ. Sintering additives also help to sinter materials at much lower temperature and help to improve the conduction behavior of doped ceria electrolytes. Alkali carbonates improve conduction process by providing super ionic pathways for ionic flow and also help to control the transitional change of Ce^{+4} into Ce^{+3}. This shows great potential for doped ceria electrolytes for future applications in ceramic fuel cells.

Acknowledgement

References

[1]   Ryan P. O Hyre, Fuel Cell Fundamentals, John Willey & Sons, INC, 2009.

[2]   J.P.P. Huijsmans: 'Ceramics in solid oxide fuel cells' , 5 (2001) 317–323.

[3]   N. Shehata, K. Meehan, M. Hudait, N. Jain: 'Control of oxygen vacancies and Ce+3 concentrations in doped ceria nanoparticles via the selection of lanthanide element' , J. Nanoparticle Res. 14 (2012) 1173.

[4]   Y.-P. Fu, S.-H. Chen: 'Preparation and characterization of neodymium-doped ceria electrolyte materials for solid oxide fuel cells' , Ceram. Int. 36 (2010) 483–490.

[5]   V. Kharton, F. Marques, a Atkinson: 'Transport properties of solid oxide electrolyte ceramics: a brief review' , Solid State Ionics. 174 (2004) 135–149.

[6]   V.V. Lakshmi, R. Bauri, A.S. Gandhi, S. Paul: 'Synthesis and characterization of nanocrystalline ScSZ electrolyte for SOFCs' , Int. J. Hydrogen Energy. 36 (2011) 14936–14942.

[7]   S.K. Zacate MO, Minervini L, Bradfield DJ, Grimes RW: 'Defect cluster formation in M2O3-doped cubic Zr2O3' , Solid State Ionics. 128 (2000) 243–54.

Submitted in Journal of Fuel Cell Science and Technology

[8]   Y.M. O, Yamamoto, Y. Arati, Y.Takeda, N. Imanishi: , Solid State Ionics. 124 (1995) 137–142.

[9]   S.L. D. Lybe, Y.L Liu, M.Mogensen:, Electrochem. Soc. Proc. (2005) 954–963.

[10]   M. Engineering: 'Effects of the addition of minute amounts of alumina on the microstructure and sintering behavior of yttria stabilized tetragonal zirconia polycrystals ceramic via a co-precipitation process' , 9 (2008) 1–6.

[11]   X.G. Z. Wang, Z.Q. Chen, S.J Wang: , J. Mater. Lett. 19 (2000) 1275–1278.

[12]   S. Kuharuangrong: 'Ionic conductivity of Sm , Gd , Dy and Er-doped ceria' , J. Power Sources 171 (2007) 506–510.

13]   D. Bucevac, A. Radojkovic, M. Miljkovic, B. Babic, B. Matovic: 'Effect of preparation route on the microstructure and electrical conductivity of co-doped ceria' , Ceram. Int. 39 (2013) 3603–3611.

[14]   C.J. Fu, Q.L. Liu, S.H. Chan, X.M. Ge, G. Pasciak: 'Effects of transition metal oxides on the densification of thin-film GDC electrolyte and on the performance of intermediate-temperature SOFC' , Int. J. Hydrogen Energy 5 (2010) 1–8.

[15]   A. Arabac, M. Faruk: 'Preparation and characterization of 10 mol % Gd doped CeO 2 (GDC) electrolyte for SOFC applications' , Ceram. Int. 38 (2012) 6509–6515.

[16]   Y. Ma, M. Singh, X. Wang, F. Yang, Q. Huang, B. Zhu: 'ScienceDirect Study on GDC-KZnAl composite electrolytes for low-temperature solid oxide fuel cells' , Int. J. Hydrogen Energy. (2014) 4–9.

[17]   A. Gondolini, E. Mercadelli, A. Sanson, S. Albonetti, L. Doubova, S. Boldrini: 'Microwave-assisted synthesis of gadolinia-doped ceria powders for solid oxide fuel cells' , Ceram. Int. 37 (2011) 1423–1426.

[18]   M. Benamira, a. Ringuedé, V. Albin, R.-N. Vannier, L. Hildebrandt, C. Lagergren, et al: 'Gadolinia-doped ceria mixed with alkali carbonates for solid oxide fuel cell applications I. A thermal, structural and morphological insight' , J. Power Sources. 196 (2011) 5546–5554.

[19]   Y.J. Kang, G.M. Choi: 'The effect of alumina and Cu addition on the electrical properties and the SOFC performance of Gd-doped CeO 2 electrolyte' , Solid State Ionics. 180 (2009) 886–890.

[20]   R. V Mangalaraja, S. Ananthakumar, K. Uma, R.M. Jiménez, S. Uthayakumar, M. López: 'Processing Research Synthesis and characterization of Gd 3 + and Sm

3 + ion doped ceria electrolytes through an in-situ sulphated combustion technique' , 13 (2012) 15–22.

[21]   C.M. Lapa, F.M.L. Figueiredo, D.P.F. de Souza, L. Song, B. Zhu, F.M.B. Marques: 'Synthesis and characterization of composite electrolytes based on samaria-doped ceria and Na/Li carbonates' , Int. J. Hydrogen Energy. 35 (2010) 2953–2957.

[22]   X. Wang, Y. Ma, R. Raza, M. Muhammed, B. Zhu: 'Electrochemistry Communications Novel core – shell SDC / amorphous Na 2 CO 3 nanocomposite electrolyte for low-temperature SOFCs' , 10 (2008) 1617–1620.

[23]   M.A. Khan, R. Raza, R.B. Lima, M.A. Chaudhry, E. Ahmed, G. Abbas: 'Comparative study of the nano-composite electrolytes based on samaria-doped ceria for low temperature solid oxide fuel cells (LT-SOFCs)' , Int. J. Hydrogen Energy. 38 (2013) 16524–16531.

[24]   M. Chen, H. Zhang, L. Fan, C. Wang, B. Zhu: 'Ceria-carbonate composite for low temperature solid oxide fuel cell Sintering aid and composite effect' , Int. J. Hydrogen Energy. (2014) 1–8. doi:10.1016/j.ijhydene.2014.04.004.

[25]   M. Kahlaoui, S. Chefi, A. Inoubli, A. Madani, C. Chefi: 'Synthesis and electrical properties of co-doping with La3+, Nd3+, Y3+, and Eu3+ citric acid-nitrate prepared samarium-doped ceria ceramics' , Ceram. Int. 39 (2013) 3873–3879.

[26]   H. Okkay, M. Bayramoğlu, M.F. Öksüzömer: 'Ultrasound assisted synthesis of Gd and Nd doped ceria electrolyte for solid oxide fuel cells' , Ceram. Int. 39 (2013) 5219–5225.

[27]   L. Science, 'Effects of MoO 3 Amounts on Sintering and Electrical Properties of Ce 0 . 8 Nd 0 . 2 O 1 . 9' , 28 (2012) 9–13.

[28]   H. Okkay, M. Bayramoğlu, M.F. Öksüzömer: 'Ultrasound assisted synthesis of Gd and Nd doped ceria electrolyte for solid oxide fuel cells' , Ceram. Int. 39 (2013) 5219–5225. doi:10.1016/j.ceramint.2012.12.021.

[29]   Y. Xia, Y. Bai, X. Wu, D. Zhou, Z. Wang, X. Liu, et al: 'Effect of sintering aids on the electrical properties of Ce0.9Nd0.1O2−δ' , Solid State Sci. 14 (2012) 805–808.

[30]   X. Zhou, P. Wang, L. Liu, K. Sun, Z. Gao, N. Zhang: 'Improved electrical performance and sintering ability of the composite interconnect La0.7Ca0.3CrO3−δ/Ce0.8Nd0.2O1.9 for solid oxide fuel cells' , J. Power Sources. 191 (2009) 377–383.

Submitted in Journal of Fuel Cell Science and Technology

[31] H. Yoshida, H. Deguchi, K. Miura, M. Horiuchi: 'Investigation of the relationship between the ionic conductivity and the local structures of singly and doubly doped ceria compounds using EXAFS measurement; , (2001) 191–199.

[32] S. Zha, C. Xia, G. Meng: 'Effect of Gd (Sm) doping on properties of ceria electrolyte for solid oxide fuel cells' , 115 (2003) 44–48.

[33] Z. Tianshu, P. Hing, H. Huang, J. Kilner: 'Ionic conductivity in the CeO 2 – Gd 2 O 3 system (0 . 05 V Gd / Ce V 0 . 4) prepared by oxalate coprecipitation' , 148 (2002) 567–573.

[34] B.C.H. Steele: , Solid State Ionics 2. 129 (2000) 95–110.

[35] M. Dokiya, T. Horita, T. Kawada, N. Sakai, H. Yokokawa: , Low temperature, 2738 (1996) 0–3.

[36] S. Le, S. Zhu, X. Zhu, K. Sun: 'Densification of Sm0.2Ce0.8O1.9 with the addition of lithium oxide as sintering aid' , J. Power Sources. 222 (2013) 367–372.

[37] X. Wang, Y. Ma, B. Zhu: 'State of the art ceria-carbonate composites (3C) electrolyte for advanced low temperature ceramic fuel cells (LTCFCs)' , Int. J. Hydrogen Energy. 37 (2011) 19417–19425.

[38] R. Raza, X. Wang, Y. Ma, X. Liu, B. Zhu: 'Improved ceria – carbonate composite electrolytes' , Int. J. Hydrogen Energy. 35 (2010) 2684–2688.

[39] R. Raza, H. Qin, L. Fan, K. Takeda, M. Mizuhata, B. Zhu: 'Electrochemical study on co-doped ceria – carbonate composite electrolyte' , J. Power Sources. 201 (2012) 121–127.

1550624X

Effect of Sm, Y and K_2CO_3 on structural and electrical properties of Neodymium doped Ceria electrolytes for applications in low temperature solid oxide fuel cells

Muhammad Akmal Rana[a], M.N Akbar[a], Mustafa Anwar[a], Kamal Mustafa[a], Sehar Shakir [a] Zuhair S. Khan[a]*

[a]*Advanced Energy Materials and Fuel Cells Lab, Centre for Energy Systems, National University of Sciences and Technology, Sector H-12 Islamabad 44000, Pakistan.*

email: zskhan@ces.nust.edu.pk

Abstract:

A comparative study based on structural and electrical properties of Neodymium doped ceria electrolyte with two main compositions of $Ce_{0.80}Nd_{0.20}O_{1.90}$ (NDC20) and $Ce_{0.75}Nd_{0.25}O_{1.875}$ (NDC25) using sol-gel route has been investigated. X-ray diffraction (XRD) and scanning electron microscope (SEM) results showed that powder particles containing cubic fluorite structure with homogenous and spherical shape with an average size of 1.11 μm were formed at pH10. DC conductivity values for NDC25 and NDC20 were found to be 7.9×10^{-5} S/cm and 3.67×10^{-5} S/cm respectively at 650°C. We further enquired the effect of small amount of Sm, Y and K_2CO_3 to improve the conduction mechanism in NDC25. Conductivity of NDC25 greatly improved by adding small amount of Sm with composition of $Ce_{0.75}Sm_{0.15}Nd_{0.10}O_{1.875}$ (SNDC) and Y with composition of $Ce_{0.75}Y_{0.15}Nd_{0.10}O_{1.875}$ (YNDC) at 700°C . It was also depicted that Sm and Nd are best co-dopants for Ceria. K_2CO_3 was added into NDC25 with 10 and 20% by volume and the compounds were named as KNDC10 and KNDC20 respectively. It was observed that the amorphous phase of carbonates greatly increased the conductivity values of NDC25 from 7.9×10^{-5} S/cm to 1.03×10^{-3} S/cm. The sequence in the conductivity values at 700°C found to be KNDC20>KNDC10>SNDC>YNDC>NDC25>NDC20.

Keywords: SOFC, Sol-gel, Neodymium doped Ceria, Conductivity, Co-doping

5. Introduction

Solid oxide fuel cells (SOFCs) are attractive because they are clean, energy efficient and almost nonpolluting. Among the other fuel cell types, SOFCs are considered best candidates for large scale power production applications [1]. Solid electrolyte is considered one of the most important parts of SOFC because it allows oxide ions to pass and reach at anode to complete the electrochemical reaction. YZS is conventionally available electrolyte material that offers better ionic conductivity but it works more effectively at high temperature i.e., 1000°C that arises some serious issues regarding selection of costly gaskets and inter-connects materials to operate the cell at such a high temperature [2]. Aiming to lower the operating temperature of the cell various oxide ion conductors were developed[3]. Doped ceria is considered a potential candidate in this regard as it provides the same ionic conduction at lower temperature [4]. Pure ceria is poor ionic conductor but its conductivity can be greatly enhanced by doping it with some trivalent atoms [5]. To increase the transport properties of the ceria various combinations of materials have been studied like Yttria doped ceria (YDC) [6–9], Gadolinium doped Ceria (GDC)[10–19], Samarium Doped Ceria (SDC) [3,15,18,20–22] and Neodymium doped Ceria (NDC) [5,7,18,23–29]. The main focus in developing new solid electrolyte materials is to improve the oxide ions conductivity. Conduction mechanism in doped ceria depends on several complex factors like dopant ion and its concentration, lattice parameters, oxide ion vacancy concentration and association enthalpy between dopant and oxide ion vacancy [5]. Increasing the dopant ions increases the conductivity but there is an upper limit of dopant addition above which the conductivity drops because defects star to interact with each other [1]. In this present work, effects of Neodymium contents along with Yttrium and Samarium as co-dopants into Ceria and inclusion of K_2CO_3 as a function of conductivity were studied. To the best of our knowledge, the study based on co-doping and carbonates inclusion into Neodymium doped ceria electrolyte has not been reported yet. Sol-gel method was used to develop powder with spherical shaped particles in nanometric range.

6. Experimentation

2.1 Synthesis of Neodymium doped Ceria (NDC)

Sol-gel method was applied to fabricate neodymium doped ceria solid electrolyte with two main compositions $Ce_{0.80}Nd_{0.20}O_{1.90}$ (NDC20) and $Ce_{0.75}Nd_{0.25}O_{1.875}$ (NDC25) using $Ce(NO_3)_3.6H_2O$ (Purity 99.99%) and $Nd(NO_3)_3.6H_2O$ (Purity 99.99%) as starting materials. 1M solutions of both precursors were prepared in separate beakers using distilled water as solvent and then dopant sol was added drop-wise with continuous stirring. Ammonia solution was used as a complexing agent as well as to control the pH. Prepared gels were dried in an oven at 110°C for several hours. Sintering was done at 1300°C for 5 hours.

2.2 Co-doping of Ceria using Neodymium, Yttrium and Samarium

To observe the effects of Yttrium and Samarium as co-dopants, we prepared further two compositions $Ce_{0.75}Y_{0.15}Nd_{0.10}O_{1.875}$ (NYDC) and $Ce_{0.75}Sm_{0.15}Nd_{0.10}O_{1.875}$ (SNDC). Same molar ratios were used as mentioned above. $Y(NO_3)_3.6H_2O$ (Purity 99.99%) and $Sm(NO_3)_3.6H_2O$ (Purity 99.99%) were used as precursors in co-doping experiment. Drying of gels was done in an oven at same temperature as kept during synthesis of NDC20 and NDC25.

2.3 Synthesis of NDC-carbonate composite electrolyte

Powders with K_2CO_3 inclusion were also prepared via already described sol-gel route. For this purpose 1M solution of K_2CO_3 was prepared and drop-wise added into NDC25 solution with 10 and 20 v/v% and finally obtained compounds were names as KNDC10 and KNDC20. Pellets with carbonates inclusion were sintered at 700°C for 3 hours keeping in view the melting point of potassium carbonate [17].

2.4 Characterization Measurement

X-ray powder diffractometer with computer interface (STOE Germany) with Cu Kα at λ =1.5418 Å was used to predict the crystalline phase and purity of the powders. Scan angle was kept ranging from 10°- 70° with step size 0.04/sec. Lattice parameters were calculated using six main reflections (111), (200) (220), (311), (222) and (400). The crystallite size was calculated using Scherer formula and was calibrated using MDI Jade version 5.0 with the help of full width at half maximum (FWHM) of (111) plane reflection. Morphology and size of the particles was studied using Scanning Electron Microscope (HITACHI SU-1500) and particle size analyzer (HORIBA LA-950).

2.5 Pellet formation and Conductivity measurement

Prepared powders were ground utilizing pestle with mortar in acetone environment to make fine powders. Pellets with 10mm diameter and 2mm thickness were formed using uniaxial hydraulic press under pressure of 4.88kg/cm^2 for 10 minutes. Detail of sintering the pellets of all samples is summarized in Table 1. Conductivity of pellets was measured using two probe method with the help of Wayne Kerr 6440B LCR meter. Following equations were used to calculate the conductivity.

$$\rho = (Ravg * A)/L \qquad (1.1)$$
$$\sigma = 1/\rho \qquad (1.2)$$

where; ρ, σ, R_{avg}, A and L Resistivity, conductivity, Average resistance at various temperatures, Area and thickness of pellet respectively.

3 Results and Discussions

3.1 Phase composition

Fig. 1 shows the XRD patterns of NDC20 and NDC25. It can be seen clearly that synthesized powders were free from impurities. Both the samples exhibited cubic fluorite structure. It can also be noticed that the peaks shifted towards the lower value of 2θ when dopant concentration increased from 0.2 to 0.25. This effect of dopant concentration was later confirmed by analyzing the larger value of inter-planar spacing "d" that resulted into increase of lattice parameters as well for NDC25 as compared to NDC20. Fig.2 shows the XRD patterns of NDC25, NYDC and SNDC. It is evident from these patterns that all the samples are free from impurities. It was also noticed that addition of Y and Sm did not affect the cubic fluorite structure of NDC. However, Co-doping reduced the crystallite size. This could have happened due to the heterogeneous nucleation due to the addition of co-dopants. Fig. 3 shows the XRD patterns of samples prepared by adding K_2CO_3. Here the inclusion with carbonates did not appear in XRD peaks because of the amorphous nature of K_2CO_3. Broader peaks obtained for KNDC10 and KNDC20 that is an indication that the crystallites formed using K_2CO_3 were smaller in size. This was also confirmed by analyzing these X-ray diffraction peaks using
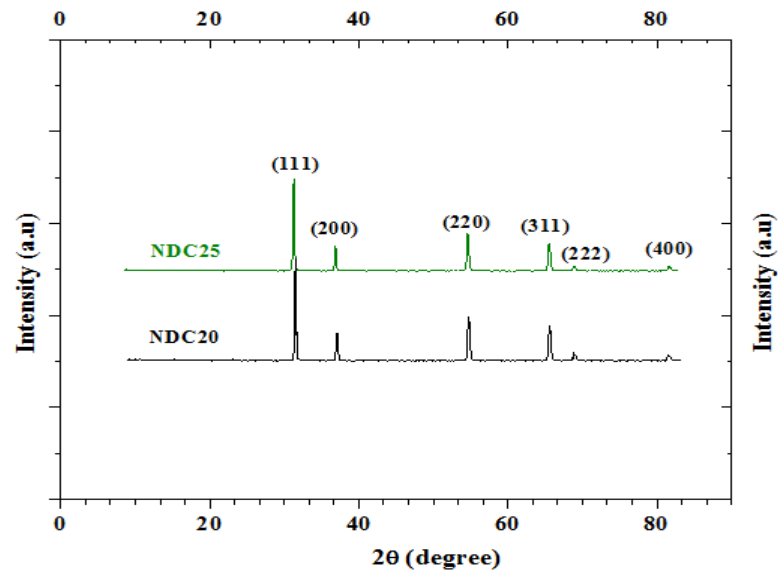
Submitted in Journal of Electroceramics

Fig. 1 XRD patterns of NDC20 and NDC25

FWHM values of corresponding higher intensity peaks the samples. Table 1 summarizes the results obtained by XRD patterns of all the samples prepared. It can be seen that with increase in dopant concentration the lattice parameters were also increased that follows the Vegard's rule[5].
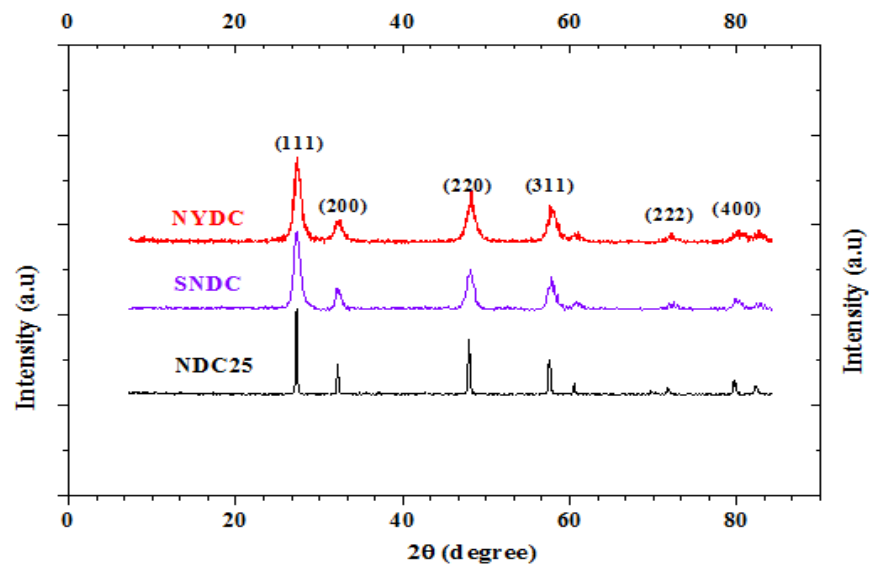

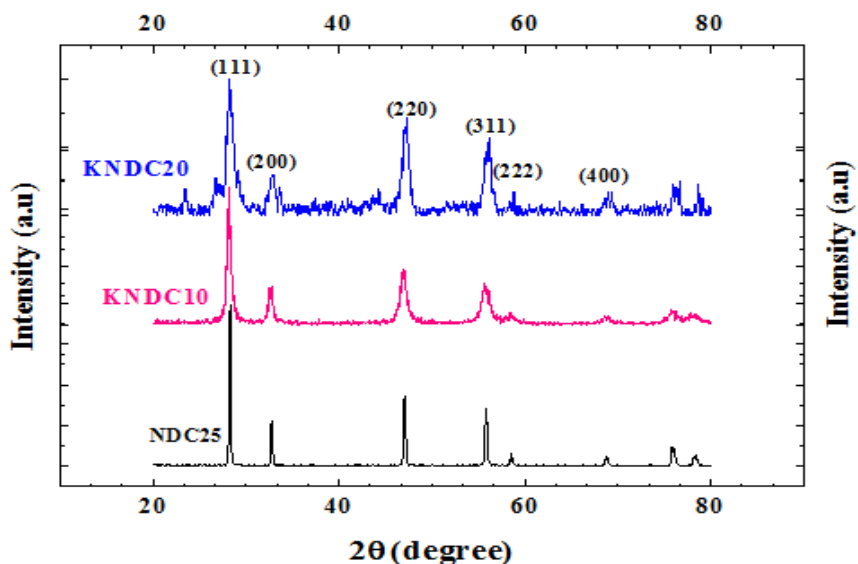Fig.2 XRD patterns of NDC25, NYDC and SNDC

Fig.3 XRD patterns of NDC25, KNDC10 and KNDC20

Table 1: Results obtained from XRD analysis

Composition	Lattice Parameter (Å)	Lattice Strain (%)	Crystallite size(nm)
NDC20	5.44	0.05	53
NDC25	5.47	0.06	41
NYDC	5.47	0.06	13
SNDC	5.46	0.06	15
KNDC10	5.48	0.06	15
KNDC20	5.46	0.06	13

3.2 Microstructure Analysis

As the carbonates didn't appear in XRD peaks therefore, presence of carbonates was confirmed by SEM/EDS. Figures 4a and 4b also show homogeneity and small grains can be seen. These small grains may have contributed into better densification and lowering the sintering temperature of NDC25. Therefore if the desired microstructure can be formed, the maximum value of conductivity can be achieved. Figures 5a and 5b show EDS analysis of KNDC10 and KNDC20 respectively. Presence of K, C and O can be seen on both samples that is an indication that carbonates have been successfully incorporated with NDC. As the powder particle size greatly improved the conduction

mechanism we prepared three samples of NDC25 at two different pH values because pH has great influence in nucleation and growth mechanisms.

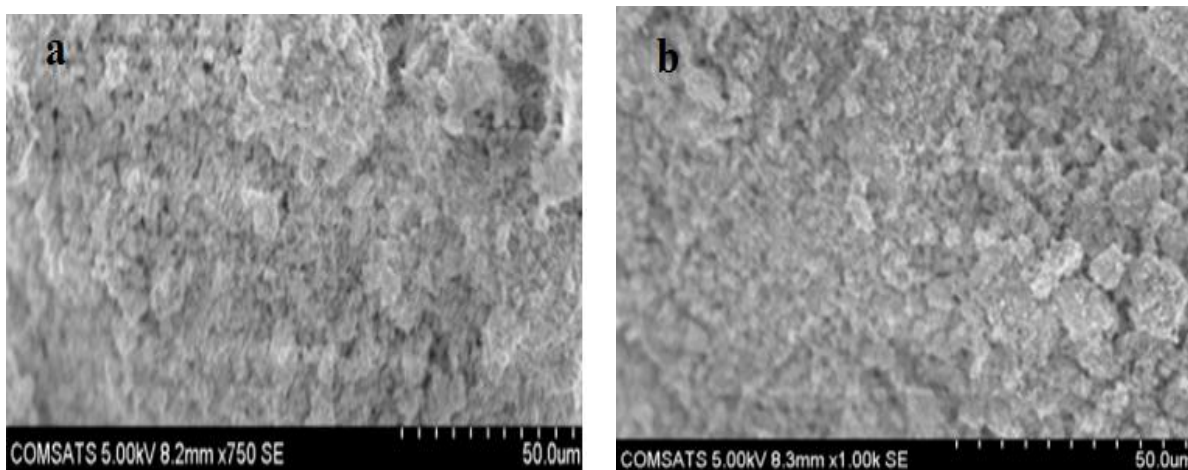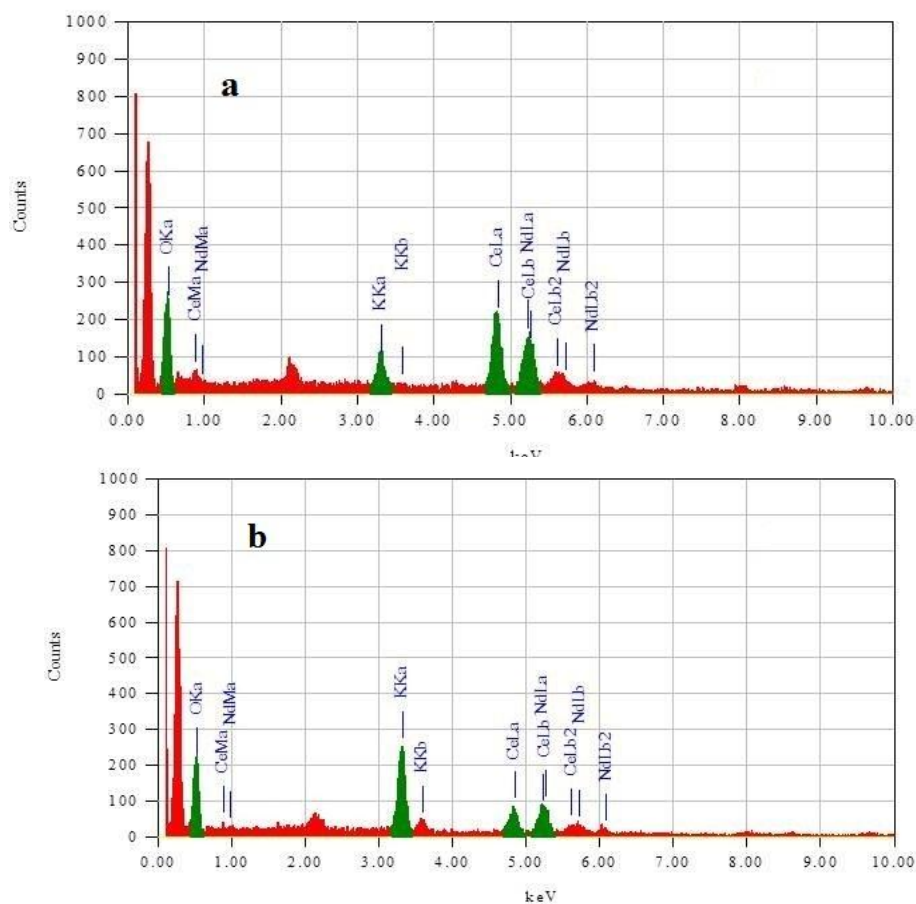Fig.4 SEM/EDS images of (a): KNDC10 and (b): KNDC20

Fig. 5 (a): EDS results of KNDC10 (b): EDS results of KNDC20

Fig. 6 Particle Size distribution before and after calcination at pH3
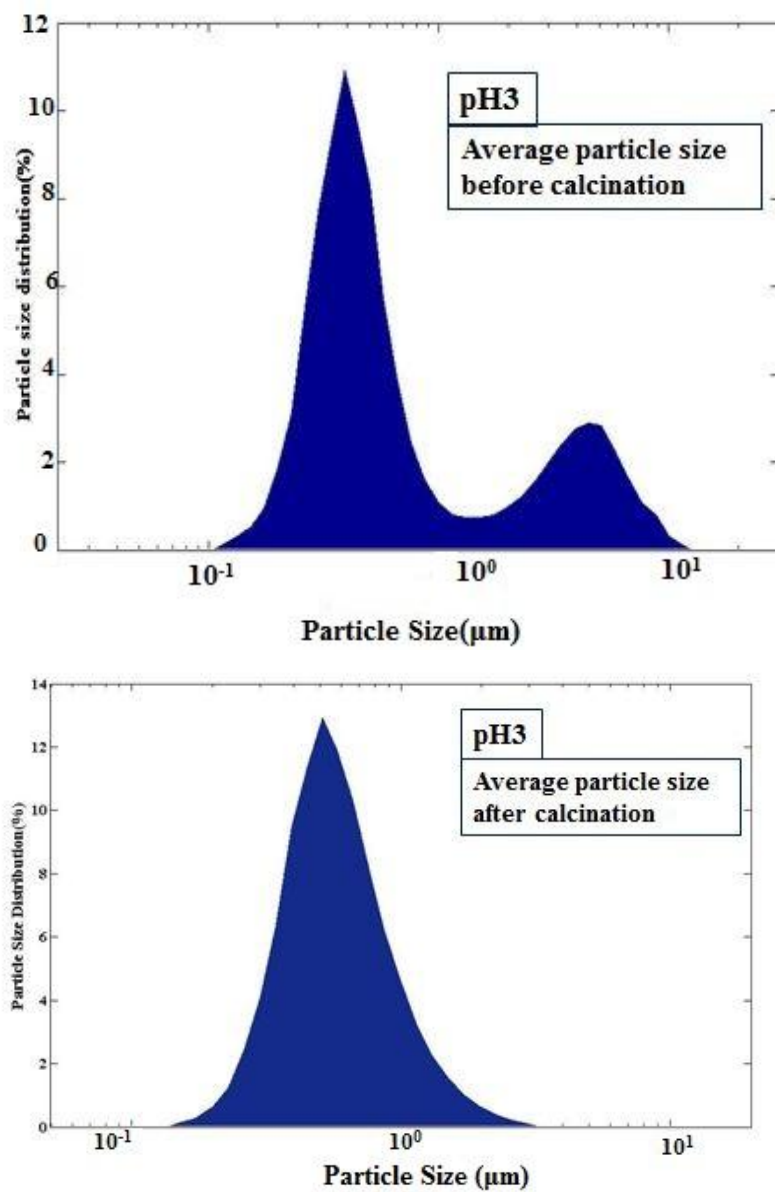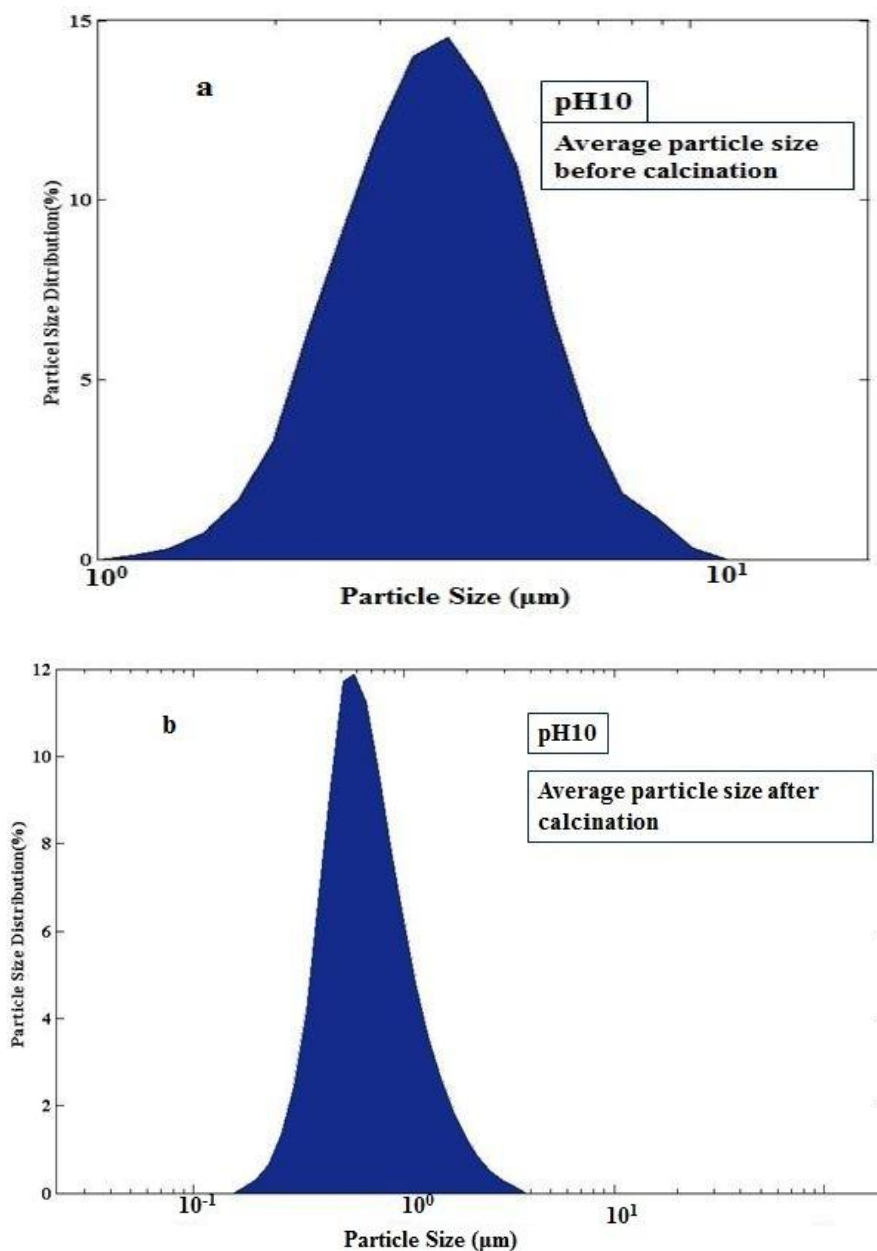
Fig. 7 Particle Size distribution before and after calcination at pH10

The comparison between particle sizes at pH3 and 10 is summarized in Table 2. Fig.6 and Fig.7 show a comparison of powder particle sizes before and after calcination at pH3 and pH10. Both the figures comprise of two parts which shows particle size distributions before and after calcination of prepared samples of NDC25. For pH3 it can be seen that particles with maximum particle size distribution of 11.08% with particle size of 0.389 μm and the average particle size obtained before calcination was 2.58 μm.

When this powder was calcined at elevated temperature, the average particle size reduced from 2.58 μm to 0.97 μm.

As for pH10 it can be seen that particles with maximum particle size distribution of 14.53 % with particle size of 3.905 μm and the average particle size obtained before calcination was found to be 4.214μm. When this powder was calcined at elevated temperature, the average particle size reduced from 4.214 μm to 1.1 μm. Further the pellets were formed to check the electrical conductivity of all the prepared samples. This reduction in particle size helped to reduce the sintering temperature and increased the conductivity.

Table 2: Effect of pH on average particle size

pH	Average particle size before calcination (μm)	Average particle size after calcination (μm)
3	2.58	0.97
10	4.21	1.1

4 Electrical conductivity measurement

Fig.8 shows the Arrhenius plots of DC electrical conductivity of all the prepared samples. Two probe DC conductivity method was implemented to measure the DC electrical conductivity of pellets. For this purpose, pellets with thickness of 2 mm and diameter 10mm were fabricated and their resistances were measured at different temperatures ranging from 200-700°C using WAYNEKERR 6440B LCR meter. Fig.7 clearly shows the difference in conductivity curves of NDC20 and NDC25. The maximum conductivity of NDC20 at 650 °C reached up-to a value of $3.67*10^{-5}$ S/cm and for NDC25 the maximum conductivity at this temperature was found to be $7.97*10^{-5}$ S/cm. To further improve the conductivity value of NDC25, we slightly introduced Yttrium and Samarium as co-dopants. Both the co-dopants brought a reasonable increase in conductivity values but SNDC exhibited better conductivity as compared with NYDC. This showed that Samarium and Neodymium are better co-dopants for ceria [35]. Effect of carbonates on conductivity was also measured. KNDC10 and KNDC20 greatly improved the conduction properties of NDC25. Table 3 summarizes the DC electrical conductivity values of all prepared samples.
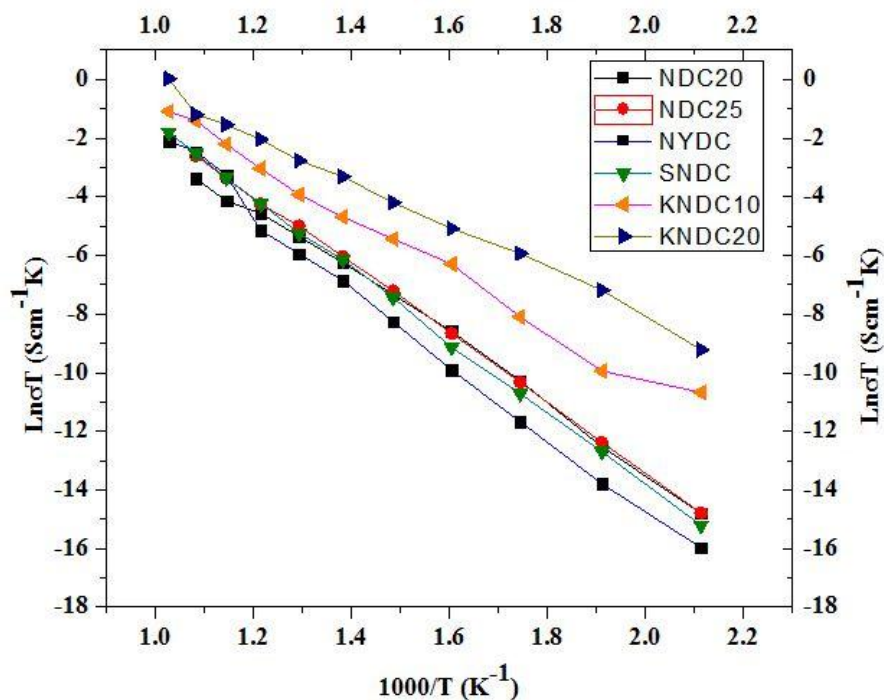
Fig.8 Combined DC conductivity curves of NDC20, NDC25, NYDC, SNDC, KNDC10 and KNDC20

Carbonates remains in amorphous phase when slight quantity is added into doped ceria ceramics. This second phase helped to improve the conduction mechanism by making an extra layer and also contributed into introduction of disordered regions which enhance ionic conductivity [36].

Table 3: DC conductivity values of all prepared samples

Sample Name	DC conductivity at 650-700°C(S/cm)
NDC20	3.67×10^{-5}
NDC25	7.97×10^{-5}
NYDC	1.26×10^{-4}
SNDC	1.69×10^{-4}
KNDC10	3.46×10^{-4}
KNDC20	1.05×10^{-3}

Inclusion of carbonates caused multi ions effect that greatly increased the intrinsic and extrinsic charge carriers and ultimately helped to enhance the conduction process [2].

Carbonates increases the densification of electrolytes and improves cell efficiency. Co-doping with carbonates increases the concentration of oxide ions and forms common pathways between doped ceria and carbonates. These pathways facilitate ionic flow. The ionic conductivity shows a remarkable difference between the electrolytes without inclusion of carbonates and with small addition of carbonates [37].

5 Conclusions

Promising results were obtained using sol-gel route. XRD analysis showed that all the synthesized materials exhibited cubic fluorite structure and particle size increased with increasing pH. Co-doping effect confirmed that Sm and Nd are better co-dopants for ceria as compared to Y. DC conductivity results proved that NDC25 is better ionic conductor than NDC20 at 650°C with a value of $7.97*10^{-5}$ S/cm. Addition of small amount of $K_2CO_3(20v\%)$ greatly enhanced the conductivity value upto 1.05×10^{-3} S/cm . We recommend that NDC25 with small amount of K_2CO_3 may be a better ionic conductor for low temperature solid oxide fuel cells.

Acknowledgment

References

[1]   Ryan P. O Hyre, Fuel Cell Fundamentals, John Willey & Sons, INC, 2009.

[2]   X. Wang, Y. Ma, B. Zhu, Int. J. Hydrogen Energy. 37 (2011)

[3]   C.M. Lapa, F.M.L. Figueiredo, D.P.F. de Souza, L. Song, B. Zhu, F.M.B. Marques, Int. J. Hydrogen Energy. 35 (2010)

[4]   V. Kharton, F. Marques, a Atkinson, Solid State Ionics. 174 (2004)

[5]   Y.-P. Fu, S.-H. Chen, Ceram. Int. 36 (2010)

[6]   D.R. Ou, Acta. Mater. 54 (2006)

[7]   M. Kahlaoui, S. Chefi, A. Inoubli, A. Madani, C. Chefi, Ceram. Int. 39 (2013)

[8]   M. Coduri, M. Scavini, M. Allieta, M. Brunelli, C. Ferrero, I. Unit, et al, Chem. Mater. (2013)

[9]   T.S. Zhang, J. Ma, H.T. Huang, P. Hing, Z.T. Xia, S.H. Chan, et al., Solid State Ionics 5 (2003)

[10]   A. Arabac, M. Faruk, Ceram. Int.38 (2012)

Submitted in Journal of Electroceramics

[11] L. Hildebrandt, C. Lagergren, R. Vannier, M. Cassir, Int. J. Hydrogen Energy 7 (2011).

[12] H. Yokokawa, N. Sakai, T. Horita, K. Yamaji, M.E. Brito, 30 (2005)

[13] K. Muthukkumaran, P. Kuppusami, E. Mohandas, V.S. Raghunathan, (2004).

[14] P.N.O.Ţ. Ingher, N.P. Pogrion, 75 (2013).

[15] S. (Rob) Hui, J. Roller, S. Yick, X. Zhang, C. Decès-Petit, Y. Xie, et al., J. Power Sources. 172 (2007)

[16] Z. Gao, Advanced Functional Materials for Intermediate-Temperature Ceramic Fuel Cells, 2011.

[17] M. Benamira, a. Ringuedé, V. Albin, R.-N. Vannier, L. Hildebrandt, C. Lagergren, et al., J. Power Sources. 196 (2011)

[18] M.A. Laguna-Bercero, J. Power Sources. 203 (2012)

[19] P.P. Dholabhai, S. Anwar, J.B. Adams, P. a Crozier, R. Sharma, Mater. Sci. Eng. 20 (2012)

[20] X. Wang, Y. Ma, R. Raza, M. Muhammed, B. Zhu, Electrochem. Commun., 10 (2008)

[21] Y. Ma, X. Wang, R. Raza, M. Muhammed, B. Zhu, Int. J. Hydrogen Energy. 35 (2010)

[22] R. Raza, X. Wang, Y. Ma, B. Zhu, J. Power Sources. 195 (2010)

[23] G. Kim, N. Lee, K. Kim, B. Kim, H. Chang, S. Song, et al., Int. J. Hydrogen Energy. 38 (2012)

[24] Y. Zheng, H. Gu, H. Chen, L. Gao, X. Zhu, L. Guo, Mater. Res. Bull. 44 (2009)

[25] M.A. Khan, R. Raza, R.B. Lima, M.A. Chaudhry, E. Ahmed, G. Abbas, Int. J. Hydrogen Energy. 38 (2013)

[26] G. Zhao, D. Zhou, J. Zhu, M. Yang, J. Meng, Solid State Sci. 13 (2011)

[27] J.X. Zhu, D.F. Zhou, S.R. Guo, J.F. Ye, X.F. Hao, X.Q. Cao, et al., J. Power Sources. 174 (2007)

[28] V. Gil, J. Tartaj, C. Moure, J. Eur. Ceram. Soc. 29 (2009)

[29] İ. Uslu, A. Aytimur, M.K. Öztürk, S. Koçyiğit, Ceram. Int. 38 (2012)

[30] L. Science, Chem. res. chinese universities (2012) 9–13.

[31] M. Biswas, S. Bandyopadhyay, Ceram. Int. 39 (2013)

Submitted in Journal of Electroceramics

[32]   B. Choudhury, A. Choudhury, Appl. Phys. 13 (2013)

[33]   S. Omar, E. Wachsman, J. Nino, Solid State Ionics. 178 (2008)

[34]   H. Okkay, M. Bayramoğlu, M.F. Öksüzömer, Ceram. Int. 39 (2013)

[35]   D. a Andersson, S.I. Simak, N. V Skorodumova, I. a Abrikosov, B. Johansson, Proc. Natl. Acad. Sci. U. S. A. 103 (2006)

[36]   R. Raza, M.A. Ahmad, J. Iqbal, N. Akram, Z. Gao, S. Javed, et al. 8 (2014)

[37]   J. Patakangas, Y. Ma, Y. Jing, P. Lund, J. Power Sources. 263 (2014)